A NON LINEAR THEORY OF ACOUSTOELECTRIC AMPLIFICATION IN PIEZOELECTRIC SEMICONDUCTORS

A thesis submitted by

N.R. OGG B.Sc.

for the Degree of Doctor of Philosophy

at the University of Warwick, Coventry.

April, 1969

TEXT BOUND INTO THE SPINE

TEXT
CUT OFF IN THE
ORIGINAL

Preface

This research was carried out during the period January 1967 to December 1968 at the Royal Radar Establishment, Malvern. During this time, the author was registered as an external student at the University of Warwick.

Throughout the course of the work, the task of supervision was shared jointly by Professor P.N. Butcher at the University of Warwick, and Dr. T.P. McLean at the Royal Radar Establishment. It is a pleasure for the author to record here his gratitude for their constant advice and encouragement.

Apart from the general supervision of the work, Professor P.N. Butcher collaborated closely with the author in the development of the theory of non-linear acoustic gain described in Chapter 3 and 4. Several of the ideas contained therein originally stemmed from this collaboration and the author is indebted to Professor Butcher for this.

The author also wishes to thank many of his colleagues at R.R.E. for useful discussions during the course of the research, and in particular, Dr. E.G.S. Paige, for making available the treatment of acoustic wave propagation in three-dimensions described in Chapter 2.

The results of the research will be published in the form of four papers. Two of these have already been published. They are: 'A non-linear theory of acoustoelectric gain and current in piezoelectric semiconductors', by P.N. Butcher and N.R. Ogg, Brit. J. Appl. Phys. 1968, Ser. 2, 1, 1271, and 'A non-linear theory of acoustoelectric gain and current in piezoelectric semiconductors II' by P.N. Butcher and N.R. Ogg, Brit. J. Appl. Phys. 1969, (March issue). The other two papers are at present being prepared for publication.

Finally, the author would like to thank the Ministry of Technology for financial support during the period of research, and Miss A. Smith for her careful and expert typing of the thesis.

Abstract

At the present time there is a great deal of interest in non-linear acoustoelectric phenomena in piezoelectric semiconductors. The behaviour of acoustic gain in the large signal regime is fundamental to an understanding of these phenomena. In this work we develop a non-linear theory of acoustoelectric gain.

General expressions are derived for the dependence of acoustoelectric gain and current on the electron density distribution associated with an acoustic wave propagating through a piezoelectric semiconductor. The results are valid for nearly periodic travelling waves with arbitrary harmonic content. It is shown that the frequency of peak gain and the magnitude of the peak gain both tend to zero as the acoustic wave amplitude increases and the electrons bunch more strongly. These features agree qualitatively with experimental observations. A quantitative comparison of the predicted frequency shift at a given flux level agrees to within an order of magnitude with available experimental data.

A theory for the dependence of acoustic gain on the electric potential accompanying the acoustic wave is also given. Numerical computations using the theory again produce a reduction in the acoustic gain and the frequency of peak acoustic gain. These results are also in reasonable agreement with experimental data.

Index

Chapter 1

INTRODUCTION

1.1 The Interaction of Acoustic Waves with Conduction Electrons

The interaction of acoustic waves with conduction electrons has been of considerable interest for some time. This interaction produces most of the electrical resistance in normal metals, and gives rise to an important contribution to the scattering of electrons in most semiconductors[1].

The effects of the interaction on the propagation of an acoustic wave in a conducting solid are threefold. First, the wave is attenuated[2]; second, the velocity of propagation, (the 'sound' velocity), is altered[3], and third, the interaction gives rise to an 'acoustoelectric' field or current in the material[4]. These effects will all be discussed in detail in a subsequent chapter. For the moment only simple qualitative explanations will be given.

The attenuation of the acoustic wave arises simply because of the fact that energy may be exchanged between the acoustic wave and the electron system via the mechanism of interaction. The direction of energy flow will be governed by the average velocity of the electrons relative to the sound velocity. If the electrons on average drift more slowly than the sound velocity, the acoustic wave will tend to drag the electrons along with it, and in doing so will lose energy and hence experience attenuation. On the other hand however, if by application of a suitable d.c. electric field the electrons are caused to drift through the material at a mean velocity which exceeds that of sound, then the situation will be reversed, and energy will be fed from the electron system into the acoustic wave with its consequent amplification[5]. It is this possibility of amplification which has brought about a great upsurge of interest and activity, both theoretical and experimental, in the field of acoustic wave propagation in conducting solids in recent years. A great deal more will be said about this presently.

The coupling between the acoustic wave and the electron can be regarded, quite generally, as giving rise to a modification in the effective elastic constants of the material. From this point of view, the attenuation (or gain), is due to the introduction of an imaginary contribution to the elastic constants. The associated modification of the real parts of the elastic constants is responsible for the alteration of the sound velocity.

In addition to providing a mechanism for energy interchange between the acoustic wave and the electron system, the coupling also allows momentum to be exchanged. This momentum exchange produces an effective force acting on the electrons which manifests itself as an 'acoustoelectric' field or current.

1.2 Mechanisms of Interaction

The mechanisms by which acoustic waves interact with conduction electrons can be divided into several types, each of which is important in different classes of materials or in differing ranges of frequency or conductivity. These have recently been discussed in detail in a review article by Spector[6]. We shall briefly summarise the different types of interaction here.

The passage of an acoustic wave through a solid will give rise to an oscillatory motion of the atoms which constitute the solid. This motion will modify the effective potential field which a conduction electron will experience in the lattice, and hence produce interaction. The form that this effective change of potential takes depends on the nature of the material considered.

For substances containing a large number of free electrons such as metals, it is important to take account of the screening effect of the electrons on the motion of the metal ions. This has been done[7] by visualising the acoustic wave as giving rise to ionic currents which produce electric fields which in turn produce electron currents. The self-consistent field which results from this process may be calculated using Maxwell's equations with the ion and electron currents as sources. This self consistent field, which turns out to be proportional to the electron density, provides the so-called 'electro-

magnetic' interaction which is responsible for the major part of acoustic attenuation in metals, where the electron density is large $\sim 10^{23}$ cm^{-3}. This interaction is independent of the frequency of the acoustic wave.

For semiconductors, the screening effects of free electrons are not so important in normal ranges of conductivity. In this case, the motion of the atoms induced by the passage of the acoustic wave changes the electrostatic potential in the lattice. In an ionic material, this potential will consist of two parts; a long range Coulomb part produced by the effective ionic charges, and a short range part arising from multipole and other sources within the neutral part of the atoms. The change in potential associated with the motion of the ionic charges may be represented by a polarisation wave in the material. For acoustic waves of reasonably long wavelengths, this polarisation may be expanded as a series in the strain produced by the acoustic wave, and its derivatives. For materials which lack inversion symmetry, the term proportional to the strain itself is in general non-vanishing and the coefficient of the strain is the piezoelectric tensor for the material. The polarisation field produced by this term gives rise to 'piezoelectric' scattering[8], and the polarisation, being proportional to strain, can be shown to give rise to a potential which is independent of the acoustic wave frequency.

For ionic materials which are centro-symmetric however, the piezoelectric contribution to the polarisation vanishes, and the lowest order non-vanishing term in the series is the one proportional to the 1st derivative of the strain. The interaction produced by this type of term, (or indeed higher terms), has not as far as the author knows, been discussed in detail or given a name anywhere in the literature. The potential produced by it will vary as the 1st power of the acoustic wave frequency.

The effects produced by the change in the short range part of the potential are of primary importance in non-ionic materials. In this case, it is found that the change of potential itself may be expanded in the strain and its derivatives. The term proportional to the strain gives rise to 'deformation-potential' coupling, so called because the coefficient of this term may be related to the change in electronic band structure with strain[9]. Because of this proportionality to strain, the deformation potential interaction varies as the frequency of the acoustic wave. It is this dependence on frequency which makes deformation potential coupling the most important mechanism at high frequencies in most materials.

Besides the interaction mechanisms outlined above, there is an additional coupling known as magnetoelastic coupling which is present in magnetic materials. This mechanism will not concern us here.

1.3 Acoustic Wave Amplification

We shall now return to a qualitative consideration of the possibility of obtaining acoustic wave amplification by interaction with supersonic electrons in the light of the various coupling mechanisms outlined above.

The particular feature of semiconductors which distinguishes them from metals in this connection is their relatively low conductivity, which is typically in the order of a few $(\text{ohm-cm})^{-1}$. Because of this, the dielectric relaxation time in a typical semiconductor is $\lesssim 10^{-12}$ sec compared with $\sim 10^{-18}$ sec in a metal. This means that in a semiconductor it is possible to produce appreciable spatial 'bunching' of electrons by the propagation of an acoustic wave at presently attainable ultrasonic frequencies. (The limit of attainability is set by the fact the lattice loss (see Chap. 2), increases with increasing frequency. The present maximum frequency possible is $\sim$ 10 GHz). As will be seen in Chapter 2, acoustoelectric amplification depends on the existence of such bunching, so that any amplification in metals would be

extremely small at ultrasonic frequencies where dielectric relaxation would be extremely rapid. In addition, the passage of supersonic electrons through a metal would dissipate sufficient power as Joule heating (at 1 kV/cm this is typically $\sim 10^{12}$ watts/cm^3 in a metal), to certainly melt and probably vaporise the metal! It was those two features which focussed attention on semiconductors as the most likely candidates for the observation of acoustic amplification in practice.

The first discussion of the acoustoelectric effect with special reference to semiconductors was given by G. Weinreich in 1956[10]. Prior to this a number of authors had studied the theory of acoustic attenuation in metals[11]-[15]. In his original paper Weinreich was primarily concerned with the theory of the 'acoustoelectric' effect in non-polar semiconductors such as Germanium and Silicon. In these materials, as mentioned in 1.2, the coupling between the acoustic wave and the conduction electrons arises through deformation potential interaction. Because of the linear frequency dependence of this effect, it has been found subsequently that at present ultrasonic frequencies, this coupling gives rise to only a small effect. However, in the course of his discussion, Weinreich noted that if the electrons were subjected to a d.c. electric field which caused them to drift faster than sound in the material, then the sign of the acoustic attenuation became reversed, and energy and momentum were transferred to the acoustic wave with its consequent amplification. Also, Weinreich showed that the momentum transfer to the acoustic wave was reflected in the current through the material by the appearance of an 'acoustoelectric' current in addition to the ohmic current. He developed a formula for this acoustoelectric current in terms of the acoustic flux and attenuation per unit length which has subsequently become known as the 'Weinreich relation'. This formula showed that the sign of the acoustoelectric current reversed when amplification of the acoustic wave was achieved. It was these two discoveries by Weinreich which laid the foundations for modern studies of acoustoelectric effects.

The next crucial step in the development of the subject came in 1961 when Hutson, McFee and White[16] reported the first observed amplification of 15 and 45 MHz acoustic waves in the piezoelectric semiconductor cadmium sulphide (CdS). Strong amplification of the waves was observed when the electrons were drifted through the material at a velocity in excess of that of sound, in agreement with Weinreich's prediction. The strength of the interaction was due to the fact that at ultrasonic frequencies (up to a few GHz), piezoelectric coupling is very much more pronounced than is deformation potential coupling. It was this demonstration of the feasibility of acoustic amplification by Hutson, McFee and White, which has been responsible for the rapid growth of interest in acoustoelectrics since 1961, not only because of the technological significance of the amplification process itself, but because of the discovery of various related phenomena in its wake. Some of these will be discussed in 1.4.

The experimental arrangement used by Hutson et al. is illustrated diagramatically below.

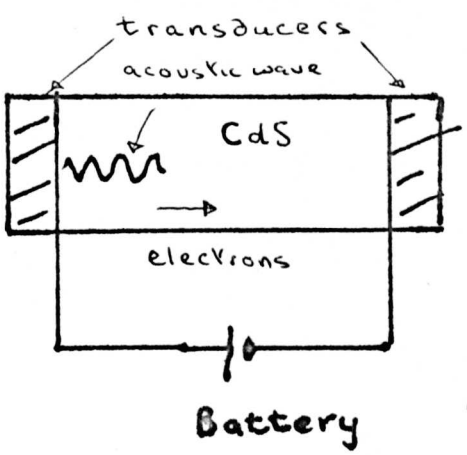

In 1962, D.L. White[17] gave the small signal theory of the amplification process in a piezoelectric semiconductor. A detailed account of this will be given in chapter 2. For acoustic waves of small amplitude, the predictions of White's theory agreed well with the experimental results of Hutson et al. The major result of White's work

was the derivation of a formula for the gain per unit length of an acoustic wave of a small amplitude propagating in a piezoelectric semiconductor. The formula gave the variation of the gain with applied d.c. electric field, (i.e. electron drift velocity), with the frequency of the acoustic wave, and with the conductivity of the material.

Since 1962, most interest, both theoretical and experimental, has been centred around the discovery of nonlinear acoustoelectric phenomena which occur when large amplitude acoustic waves propagate in piezoelectric semiconductors. These effects which are the primary concern of present work, and indeed the primary concern of present day experimental investigations will be described in the next section.

1.4 Non-Linear Acoustoelectric Effects in Piezoelectric Semiconductors

In 1963, R.W. Smith[18] measured the current-voltage characteristic of a sample of CdS and found that the current exhibited saturation above a certain voltage. This observation was confirmed and further investigated by other workers[19]-[22]. Current saturation of apparently similar origin has been subsequently observed in other piezoelectric semiconductors, CdSe[23], GaSb[24], and ZnO[25].

The evidence that the saturation is acoustoelectric in origin is threefold. First, the estimated electron drift velocity at the field where saturation begins is close to the velocity of acoustic waves in the direction of the current. Second, if the current is plotted against the time after the application of the voltage, then it is found that the current initially reaches the ohmic value and then decays to an equilibrium value. This is illustrated below.

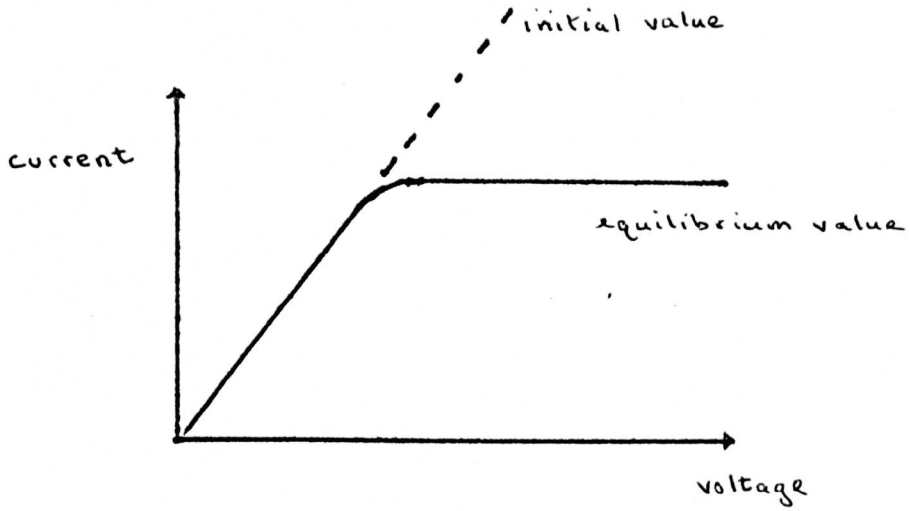

The time required to establish equilibrium was found to be characteristic of the rate of growth of acoustic waves from thermal noise by acoustoelectric amplification. Third, the rate of decay of current after the voltage pulse was removed, was typical of the rate of loss of energy of acoustic waves to electrons and other phonons[26].

Explanations of current saturation have been given by several authors[27]-[31]. In most cases the explanations depend on the existence of the acoustoelectric current predicted by Weinreich. As we shall see later this acoustoelectric current arises from a non-linearity in the conduction current associated with the acoustic wave. When the voltage across the sample is increased, the ohmic current rises, but so also does the acoustoelectric current due to the additional growth of acoustic waves. Under conditions of acoustic gain, the acoustoelectric current represents a loss of momentum from the electron system and hence will be in opposition to the ohmic current. If the ohmic and acoustoelectric currents increase at roughly the same rate with applied voltage, then the difference between them will be approximately constant, i.e. the total current will exhibit saturation.

When the electric field is examined in a sample of CdS under conditions of current saturation, it is found[32] that it exhibits strong non-uniformity. The distribution of d.c. field along a sample is found to be of the form indicated in the diagram below.

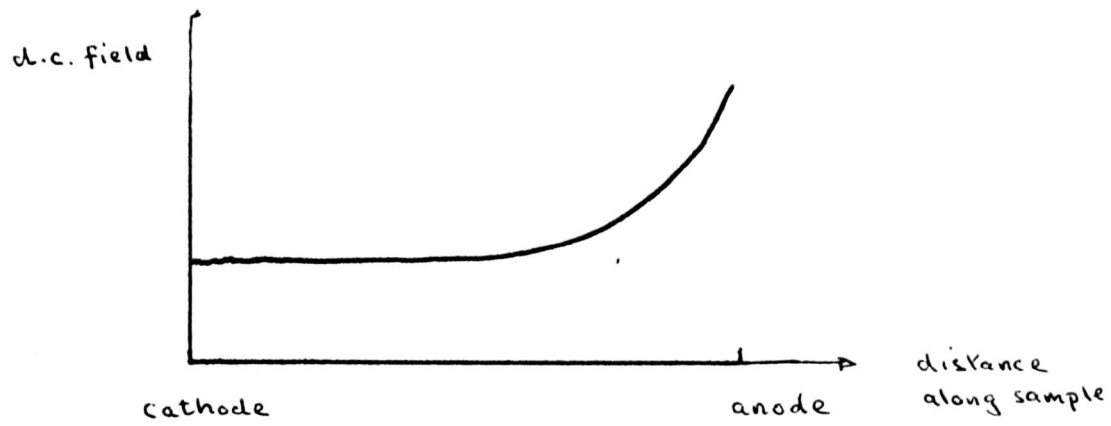

Again, one can give plausible arguments for this observation based on the concept of acoustoelectric current. At the cathode end of the sample, the acoustic flux will be small and therefore so will the acoustoelectric current. At the anode the opposite will be true owing to the gain experienced by acoustic waves along the sample, i.e. the acoustic flux and the acoustoelectric current will both be large. Since the total current (i.e. ohmic-acoustoelectric), must be constant along the sample due to current continuity, it follows that the conduction current, and hence the d.c. electric field, must be large where the acoustoelectric current is large as is the case indicated in the diagram.

The current saturation described above occurs in fairly low conductivity CdS typically $\sim 10^4$ ohm cm. Since 1965 many authors have observed a different phenomenon in high conductivity (typically 10 ohm cm) CdS[33]-[38] and several other piezoelectric semiconductors. On application of a voltage greater than that required to produce acoustic gain, oscillations were found in the current passing through the material. Studies of these current oscillations indicate that they are produced by the periodic propagation of domains of high acoustic flux and d.c. electric field. The current oscillates between the ohmic value when the domain is absent and the saturated value when the domain is present. The domains propagate at a velocity close to that of sound. Once formed, the domains are found to travel with approximately stable size and shape, although the details of the shape of the domain seem to depend to some extent on the

excitation conditions[39]. This would seem to indicate that the total acoustic gain in a fully formed domain is zero. Brillouin scattering experiments[40] have revealed that the domains contain a large spread in acoustic wave frequencies. The predominant frequency is found to be substantially below that which should be maximally amplified on the basis of White's small signal theory (see Chap. 2), the reduction being up to an order of magnitude.

So far, only plausibility arguments have been given for the existence of these domains. Essentially these arguments run as follows. As we shall see in Chap. 2, the acoustic gain increases as the conductivity of the material increases. It is conjected therefore, that in high conductivity CdS because of the high acoustic gain, the acoustoelectric current may increase so rapidly with applied voltage as to produce a negative resistance region in the current-voltage characteristic. This negative resistance will then lead to instability and domain propagation in much the same way as in the Gunn effect[41]-[42]. While this argument is plausible, it is not very satisfactory since it does not allow one to develop a detailed theory of domain shapes, sizes etc. The calculation of these features will require the development of a realistic non-linear theory.

Another form of instability has recently been observed in thin platelets of CdS[43]. These platelets are several hundred microns long with polished parallel end faces. On application of a voltage greater than that required to produce acoustic gain, current oscillations are observed in the external circuit. These oscillations are found to be at frequencies which are integral multiples of the fundamental mode frequency of the platelet. A simple analysis[44] based on White's small-signal theory of acoustoelectric gain has indicated that the instability may be expected when conditions of 'round trip gain' in the resonant platelet are achieved. This means that the gain of an acoustic wave travelling with the electron stream must be greater than the loss entailed by reflection at the end faces and by the

journey in opposition to the electron stream. For a voltage just in excess of the threshold which produces round trip gain, it is found that the modes which are present in the current spectrum are those closest to the frequency which would have the largest gain on the basis of the simple linear theory. For voltages well in excess of threshold however, it is found that the mode spectrum shifts to lower frequencies. Again it seems that for large acoustic wave amplitudes, the total acoustic gain reduces to zero (in order to yield a stable amplitude), and the frequency at which peak gain occurs shifts towards lower frèquencies.

A realistic non-linear theory which accounts for all of the observed features in the phenomena outlined above has not yet been developed. In the present work, the author has concentrated on what seems to be the most tractable, and at the same time most fundamental aspect of large signal acoustoelectric phenomena, namely the study of acoustoelectric gain in the non-linear regime. It is hoped that ultimately this will provide some insight and guidance as to how to tackle the various non-linear effects described above.

There are two distinct features which emerge from the experiments already mentioned. First, it seems clear that the acoustic gain decreases as the amplitude of the acoustic wave increases, and second the frequency at which maximum acoustic gain occurs seems to shift to lower frequencies as the acoustic wave amplitude rises. Any non-linear theory of the acoustoelectric gain process will therefore have to incorporate these two effects. The object of this work is to produce such a theory. The results of this study are given in Chapters 3-5. As an introduction to this however, the small-signal linear theory of the amplification process is described in the next chapter.

Generation of the 2nd harmonic of an injected sound wave is clearly feasible in the non-linear regime and has been observed by several authors[45]-[47]. This again is a consequence of the non-linearity in the conduction current mentioned above. Theories of this effect have also be given[45],[47].

Another phenomenon of interest observed under large signal condition in amplifying CdS is that of collective wave or 'second sound' propagation. It has been reported[48] that when a pulse of sound was injected into a piece of amplifying CdS, two pulses emerged, one having travelled at a velocity less than that of sound in the direction of propagation. It has been proposed[49]-[50] that the trailing pulse is not a single sound wave, but rather a distribution of sound waves amplified from the thermal background which have a coherent amplitude modulation. This amplitude modulation would propagate at some average velocity of the participating sound waves. Because it is only the component of sound velocity in the direction of propagation which is of importance, the velocity of the collective wave is lower than the sound velocity. The non-linearity is responsible for the collective nature of the wave since it provides the coupling between waves of differing frequency.

References Chapter 1

1. Ziman, J.M., (1960), Electron and Phonons (Clarendon Press, Oxford).
2. Blount E.I., (1959) Phys. Rev. 114, 418.
3. Bohm D and Staver T., (1952), Phys. Rev., 84, 836.
4. Parmenter, R.H., (1953), Phys. Rev. 89, 990.
5. Hutson, A.R., McFee, J.H., and White, D.L., (1961), Phys. Rev. Letts. 7, 237.
6. Spector, H.N., (1966), Solid State Phys. Vol. 19, 291.
7. Cohen, M.H., Harrison, M.J., and Harrison, W.A., (1960), Phys. Rev. 117, 937.
8. Meijer, H.J.G. and Polder, D., (1953), Physica, 19, 255.
9. Bardeen, J and Shockley, W., (1950), Phys. Rev. 80, 72.
10. Weinreich, G., (1956), Phys. Rev. 104, 321.
11. Akhieser, A., (1939), J. Phys. (U.S.S.R), 1, 289.
12. Mason, W.P., (1955), Phys. Rev. 97, 557.
13. Morse, R.W., (1955), Phys. Rev. 97, 1716.
14. Kittel, C., (1955), Acta Metallurgica 3, 295.
15. Pippard, A.B., (1955), Phil. Mag. 46, 1104.
16. See Ref. (5).
17. White, D.L., (1962), J. Appl. Phys. 33, 2547.
18. Smith, R.W., (1963), Phys. Rev. Letts. 9, 87.
19. McFee, J.H., (1963), J. Appl. Phys. 34, 1548.
20. Moore, A.R., (1964), Phys. Rev. Letts. 12, 47.
21. Wang, W.C., and Pua, J., (1965), Proc. IEEE 53, 330.
22. Spear, W.E., and P.G. Lecomber, (1964), Phys. Rev. Letts. 13, 434.
23. Kikuchi, M., (1963), J. Appl. Phys. (Japan), 2, 807.
24. Sliva, P.O. and Bray, R., (1965), Phys. Rev. Letts. 14, 372.
25. See ref. (19).
26. Maines, J.D., and Paige, E.G.S. (1965), Phys. Letts., 17, 14.
27. Prohofsky, E.W., (1964), Phys. Rev. 134 A, 1302.

28. Hutson, A.R., (1962), Phys. Rev. Letts. 9, 296.

29. Grinberg, A.A., (1964), Soviet Phys. Doklady 9, 301.

30. Gurevich, V.L. and Kagan, V.D., (1965), Sov. Phys. Solid State 6, 1752.

31. Quentin, G., and Thullier, J.M., (1966), Phys. Letts., 23, 42.

32. Maines, J.D., 1966, Appl. Phys. Letts., 8, 67.

33. Haydl, W.H. and Quate, C.F., (1966), Phys. Letts, 20, 443.

34. See ref. (24).

35. Bray, R., Kumar, C.S., Ross, J.B., and Sliva, P.O., (1966), Proc. Int. Conf. Phys. of Semiconductors, Kyoto, 483.

36. Yamashita, I., Ishiguro, T., and Tanaka,T., (1965), J. Appl. Phys. (Japan), 4, 470.

37. Ishida, A., Hamaguchi, C., and Inuishi, Y., (1966), Proc. Int. Conf. Phys. of Semiconductors, Kyoto, 469.

38. Many, A., and Balberg, I., (1966), Proc. Int. Conf. Phys. of Semiconductors, Kyoto, 474.

39. Butler, M.B.N. Private Communication.

40. Zucker, J. and Zemon, S.A., (1966), Appl. Phys. Letts., 9, 398.

41. Gunn, J.B., (1963), Solid State Comm., 1, 88.

42. Butcher, P.N., Fawcett, W., and Hilsum, C., (1966), Brit. J. Appl. Phys., 17, 1425.

43. Maines, J.D., and Paige, E.G.S., (1968), Proc. Int. Conf. Phys. Semiconductors, Moscow, 928.

44. Maines, J.D., (1967), Solid State Comm., 5, 271.

45. Kroger, H., (1964), Appl. Phys. Letts., 4, 190.

46. Elbaum, C., and Truell, R., (1964), Appl. Phys. Letts., 4, 212.

47. Tell, B., (1964), Phys. Rev. 136, A772.

48. Kroger, H., Prohofsky, E.W., and Damon, R.W., (1964)
Phys. Rev. Letts., 11, 246.

49. Kroger, H., Prohofsky, E.W., and Damon, R.W., (1964), Proc. IEEE,
52, 912.

50. Prohofsky, E.W., (1964), Phys. Rev., 136, A1731.

Chapter 2

THE LINEAR SMALL SIGNAL THEORY OF ACOUSTOELECTRIC AMPLIFICATION IN PIEZOELECTRIC SEMICONDUCTORS

2.1 Classical and Quantum Theories of Acoustic Amplification

Two distinct approaches have been used in developing theories of acoustic amplification in piezoelectric semiconductors. One is the classical or phenomenological approach which is valid at reasonably low frequencies. The other is the so-called quantum approach which is correct at high frequencies. The transition between the two approaches occurs at frequencies such that the acoustic wavelength is in the order of the mean free path of the electrons.

In the language of the classical theory, one speaks of electric currents and space charges which interact with the piezoelectric field produced by the propagation of an acoustic wave[1]. Both the electrons and the acoustic wave are treated phenomenologically. If k is the wave vector of the acoustic wave and ω its angular frequency and ℓ and τ are the averaged electron mean free path and relaxation time respectively, then the classical description will hold provided $k\ell \ll 1$ and $\omega\tau \ll 1$. The second inequality may be rewritten as $k\ell v_s/v_{th} \ll 1$ where v_s and v_{th} are the sound and thermal velocities respectively. We have used here the relations $\omega = kv_s$ and $\tau = \ell/v_{th}$. Since v_s is typically of order 10^5 cm/sec and v_{th} is at room temperature of order 10^7 cm/sec, we see that the inequality $k\ell \ll 1$ is the more stringent requirement for the validity of a classical description. If $k\ell > 1$ this picture breaks down. It is not possible to speak of an electron distribution which is in equilibrium with a local electric field wave when the electron mean free path is larger than the wavelength.

In the regime where $k\ell \gg 1$, $\omega\tau \gg 1$, one must use the quantum picture. Here one speaks of electrons interacting with acoustic phonons of well defined energy and momentum and the interaction process is described in terms of the emission and absorption of phonons[2]. In this case the $\omega\tau \gg 1$ inequality is the more stringent. As $k\ell$ and $\omega\tau$ diminish towards unity this picture fails. When the mean free path of the electrons decreases, the uncertainty in their energy and momentum increases. If this

uncertainty becomes roughly equal to the energy and momentum of the acoustic phonons, then the interaction can no longer be meaningfully described in terms of phonon absorption and emission.

A more unified approach to the problem of reconciling the two descriptions has recently been given by Nakamura and Yamashita[3]. These authors have developed a microscopic theory of the interaction process starting from a Hamiltonian, which reduces naturally to both pictures in the correct limits. Their treatment is however, extremely complex and will not be discussed further here.

Typically, at room temperature the mean free path for electrons in CdS, (and zinc oxide, ZnO), which we shall primarily be concerned with is $\sim 10^{-7}$ cm[4]. This means that a classical description of acoustoelectric interaction will be valid for frequencies up to about 100 GHz, (since the sound velocity $\sim 10^5$ cm/sec). This is an order of magnitude above presently attainable ultrasonic frequencies, and so a classical description will be used throughout the present work.

2.2 The General Classical Small-Signal Theory of Acoustoelectric Amplification in Piezoelectric Semiconductors

As is customary in this subject we shall henceforth use rationalised m.k.s. units throughout. Notation will be defined as required and a table of all symbols used is provided at the end of the work.

In this section, we shall be concerned with the propagation of mechanical strain waves in an elastic solid, and their coupling to electromagnetic and space charge waves. Because we shall be limited to frequencies < 100 GHz by the use of a classical theory, this means that the smallest wavelength we shall need to consider will be $\sim 10^{-8}$ metre. In view of the fact that this dimension is very much larger than a typical crystal lattice spacing, we can treat the solid as an elastic continuum.

The general equation of motion[5] for an elastic solid is obtained by equating the internal stress force $\partial T_{ij}/\partial x_j$ to the product of the local acceleration $\partial^2 u_i/\partial t^2$ and the density ρ of the material, i.e.

$$\rho \frac{\partial^2 u_i}{\partial t^2} = \frac{\partial T_{ij}}{\partial x_j} \qquad (2.1)$$

T_{ij} is the stress tensor at a point in the body, u_i is the local mechanical displacement in the medium, the suffices refer to Cartesian components along the coordinate directions x_j, and the summation convention over repeated suffices is employed.

In a piezoelectric material, the stress will be a functional of the strain and the electric field. If the wavelength of the disturbance produced by the presence of an acoustic wave in the material is large compared to the crystal lattice spacing, which we established above is the case for ultrasonic frequencies, then the relation will be a local one. Approximately the same requirement will ensure that the relation is instantaneous. In this case we may expand the stress tensor in powers of the strain tensor and the electric field. Provided that the strains are not too large, ($\ll 1$), i.e. that the change in length of a unit cell is a small fraction of the lattice spacing a, and that the electric fields developed are small compared to typical atomic fields, ($\sim$ electron charge/a^2), then the expansion may be curtailed at the linear terms. The coefficients of these linear terms may be taken to be functions of temperature provided that the angular frequency ω of the acoustic wave is small compared to the relaxation time governing the approach to local equilibrium of the phonon distribution function. In a period of the acoustic wave, heat will be transmitted over a distance $\sqrt{\kappa/\omega}$ [6], (κ is the thermal conductivity), which will be small compared to the wavelength $\lambda = 2\pi v_s/\omega$

provided $\omega << 4\pi^2 v_s^2/\kappa$. For a typical semiconductor, this means that if $\omega << 1000$ GHz, then the passage of an acoustic wave may be regarded as adiabatic and the coefficients in the expansion may be taken to have their adiabatic values.

Under these conditions then, we may finally write down the desired constitutive relation[7]:

$$T_{ij} = c_{ijk\ell} S_{k\ell} - e_{kij} E_k \tag{2.2}$$

where

$$S_{k\ell} = \frac{1}{2} \left(\frac{\partial u_k}{\partial x_\ell} + \frac{\partial u_\ell}{\partial x_k} \right) \tag{2.3}$$

is the strain tensor, $c_{ijk\ell}$ the elastic tensor of the material, e_{kij} the piezoelectric tensor of the material and E_k is the electric field vector. It can be shown that

$$c_{ijk\ell} = c_{ij\ell k} = c_{jik\ell} = c_{k\ell ij} \text{ and } e_{kij} = e_{kji} \tag{8}$$

In equation (2.2) we have, in writing the constitutive relation as a function of the local thermodynamic variables, neglected irreversible effect which occur when an elastic wave propagates in a solid. These irreversible processes convert mechanical energy into heat and give rise to the so-called 'lattice loss'. We show in Appendix 2.1 that these effects may be taken account of, (as far as wave propagation is concerned), by the addition of an imaginary part to the elastic constants.

Equation (2.2), when used in conjunction with equation (2.1), couples the mechanical strain to the electric field. The equations governing the electromagnetic properties of an n-type semiconductor with which we shall be concerned are Maxwell's equations:

$$\nabla \times \underline{E} = - \frac{\partial \underline{B}}{\partial t} \tag{2.4}$$

$$\nabla \times \underline{H} = \underline{j} + \frac{\partial \underline{D}}{\partial t} \tag{2.5}$$

$$\nabla \cdot \underline{B} = 0 \tag{2.6}$$

$$\nabla \cdot \underline{D} = \rho = - q(n-n_o) \tag{2.7}$$

where $\underline{B}$ is the magnetic induction, $\underline{H}$ the magnetic field, $\underline{D}$ the electric displacement, ρ the space charge density and $\underline{j}$ the conduction current density. q is the magnitude of the electronic charge, n the electron density and n_o the equilibrium electron density.

To complete the set of equations, we require additional constitutive relations determining $\underline{B}$, $\underline{D}$, and $\underline{j}$, in terms of the other variables. If we make similar assumptions to these used in writing down the constitutive relation for stress, then we may write

$$\underline{B} = \mu^M \underline{H} \tag{2.8}$$

$$D_i = \epsilon_{ij} E_j + e_{ijk} S_{jk} \tag{2.9}$$

where μ^M is the magnetic permability, which will be assumed isotropic for simplicity, and ϵ_{ij} is the dielectric permittivity tensor. These will be taken to have their low frequency values since ultrasonic frequencies are well below resonances causing optical dispersion. The fact that the piezoelectric tensor e_{ijk} appears in (2.9) is a consequence of the thermodynamic relation,[9] $\left(\frac{\partial D_k}{\partial S_{ij}}\right)_E = -\left(\frac{\partial T_{ij}}{\partial E_k}\right)_S$. Strictly speaking, the thermodynamic reasoning employed in deriving this relation is only valid for reversible processes. The propagation of an acoustic wave in a

conducting piezoelectric is not reversible. However, provided the decay (or growth) of the acoustic wave is small over a wavelength, the processes involved may be treated as very nearly reversible so that serious deviations from the above relation should not occur.

The constitutive relation determining the conduction current $\underline{j}$ is derived from the Boltzmann transport equation. Provided $\omega\tau \ll 1$ and $k\ell \ll 1$ this relation may be written

$$j_i = nq\mu_{ij}E_j + q D^n_{ij} \frac{\partial n}{\partial x_j} \qquad (2.10)$$

where μ_{ij} and D^n_{ij} are the electronic mobility and diffusion tensors, assumed to be independent of the electric field. This neglects possible hot electron effects which can become important at fields $\sim 10^6$ kV/m in CdS[10].

The equation (2.10) contains the only non-linearity in the system of equations (2.1)-(2.10), the nonlinearity appearing in the product nE in the conduction current.

We shall be interested in the propagation of small amplitude waves in a piezoelectric semiconductor subjected to an applied d.c. electric field $\underline{E}_o$, with an equilibrium electron density equal to n_o. To obtain an equation valid for small a.c. perturbations about this d.c. state, we linearise equation (2.10) to obtain.

$$j_i = \sigma_{ij}(E_{oj} + E'_j) + n'q\mu_{ij}E_{oj} + qD^n_{ij}\frac{\partial n'}{\partial x_j} \qquad (2.11)$$

where $\sigma_{ij} = n_o q\mu_{ij}$ is the conductivity tensor for the material and we have denoted d.c. variables by the subscript o; a.c. perturbations will for the moment be denoted by primed variables. The equations (2.1)-(2.9) and (2.11) constitute a complete set of equations for the study of the propagation of acousto-electromagnetic waves in piezoelectric materials[11]-[12].

Since we are interested in wave propagation in an infinite medium, we shall take all a.c. quantities to have the space-time dependence of a travelling wave with wave vector $\underline{k}$, (which we allow to be complex to take account of spatial growth), and real frequency ω. For example we write

$$\underline{E}'(x,t) = \underline{E}' e^{i(\underline{k}.\underline{x}-\omega t)} + c.c \qquad (2,12)$$

where c.c. denotes complex conjugate.

Substitution of the travelling wave form in the equations leads, after some manipulation, to a secular equation determining the complex dispersion relation of the coupled acousto-electromagnetic waves. In general, this is extremely complicated. However, since we are only interested in the acoustic like part of the dispersion relation, a large degree of simplification may be achieved by noting that at ultrasonic frequencies, the electromagnetic field accompanying an acoustic wave will be predominantly electrostatic in nature. This means that the a.c. electric field $\underline{E}'$ may be derived solely from a scalar potential ϕ' and so is purely longitudinal. This means that equation (2.4) may be replaced by $\nabla \times \underline{E}' = 0$ i.e.

$$\underline{E}' = -\nabla\phi' \qquad (2.13)$$

The rigorous justification for this procedure is complex and will be relegated to Appendix 2.2. It is shown there, that the corrections introduced by retaining the transverse electric field, result in additional terms in the acoustic dispersion relation of order $(v_s/c)^2$, where v_s is the sound velocity, and c is the velocity of light in vacuum. These corrections will therefore be small.

Taking the divergence of equation (2.5) yields the equation of current continuity:

$$\nabla.\underline{j}' + \frac{\partial \rho'}{\partial t} = 0 \qquad (2.14)$$

where the d.c. parts vanish.

Because of the condition $\nabla \times \underline{E}' = 0$, equation (2.14) may be seen to replace equations (2.4)-(2.6). From (2.1) and (2.2) together with (2.13) we have, on using the travelling wave form (2.12).

$$-\omega^2 \rho u_i = ik_j [ic_{ijk\ell} k_\ell u_k + ie_{qik} k_q \phi'] \qquad (2.15)$$

Substitution of (2.9) and (2.11) into (2.14) gives on using (2.7):

$$\phi' = \frac{u_k k_p e_{pk\ell} k_\ell [\omega + k_n \mu_{nm} E_{om} + ik_n k_m D^n_{nm}]}{k_p \epsilon_{pm} k_m [\omega + k_n \mu_{nm} E_{om} + ik_n k_m D^n_{nm}] + ik_n k_m \sigma_{nm}} \qquad (2.16)$$

Combining (2.15) and (2.16) then shows that

$$[-\omega^2 \rho \, \delta_{ik} + c'_{ijk\ell} k_j k_\ell] u_k = 0 \qquad (2.17)$$

where

$$c'_{ijk\ell} = c_{ijk\ell} + e_{qij} e_{pk\ell} k_q k_p \chi \qquad (2.18)$$

is a modified complex elastic constant and

$$\chi = \frac{[\omega + k_n \mu_{nm} E_{om} + ik_n k_m D^n_{nm}]}{k_p \epsilon_{pm} k_m [\omega + k_n \mu_{nm} E_{om} + ik_n k_m D^n_{nm}] + ik_n k_m \sigma_{nm}} \qquad (2.19)$$

Equation (2.17) determines the form of the acoustic modes of propagation. The complex dispersion relation for acoustic waves follows immediately from the consistency condition on (2.17), i.e.

$$\left| -\omega^2 \rho\delta_{ik} + c'_{ijk\ell}\, k_j k_\ell \right| = 0 \qquad (2.20)$$

2.3 White's One-Dimensional Theory of Acoustic Amplification in Piezoelectric Semiconductors

While the three-dimensional theory given in 2.2 is instructive, much of the physics is obscured by the complexity of the tensor notation. In this section therefore, the theory is briefly presented in a 1-dimensional form as given originally by White[13], and the results are discussed in detail. The general 3-dimensional results will be given in sections 2.4 and 2.5.

We shall consider the one-dimensional situation in which the electric field E, the electric displacement D and the strain S each have only one component which is a function of the position coordinate x, and time t. In one-dimension it is expedient to employ the following sign convention. Electric fields, electric displacements, and currents which point in the negative x-direction will be measured positive. With this convention, acoustic waves will amplify in the positive x-direction at high positive applied d.c. field strengths. All other vector quantities will be measured positive along the positive x axis. In one-dimension, equations (2.2), (2.3), (2.4), (2.7), (2.9) and (2.11) yield the following equations

Wave Equation

$$\frac{\partial^2 S'}{\partial t^2} - v_s^2 \frac{\partial^2 S'}{\partial x^2} = \frac{e}{\rho} \frac{\partial^2 E'}{\partial x^2} \tag{2.21}$$

Current Continuity

$$\frac{\partial}{\partial x}\left(\sigma E' + n' q \mu E_o - q D_n \frac{\partial n'}{\partial x}\right) + q \frac{\partial n'}{\partial t} = 0 \tag{2.22}$$

Poisson's Equation

$$\frac{\partial D'}{\partial x} = q n' \tag{2.23}$$

Constitutive Relation

$$D' = \epsilon E' - e S' \tag{2.24}$$

where $v_s^2 = c/\rho$ is the velocity of sound in the absence of piezoelectric coupling. Insertion of the travelling wave form $e^{i(kx-\omega t)}$ into these equations and eliminating n' and D' from (2.22)-(2.24) gives two equations in E' and S' which yield the complex dispersion equation

$$\left(\frac{\omega^2}{v_s^2} - k^2\right)\left(1 - \frac{\mu E_o k}{\omega} + i\left(\frac{\omega_c}{\omega} + \frac{k^2 D_n}{\omega}\right)\right)$$

$$= K^2 k^2 \left(1 - \frac{\mu E_o k}{\omega} + \frac{i k^2 D_n}{\omega}\right) \tag{2.25}$$

where $\omega_c = \sigma/\epsilon$ is the inverse of the dielectric relaxation time and the dimensionless parameter $K^2 = e^2/\epsilon c$ is known as the electromechanical coupling constant. If the piezoelectric coupling is reduced to zero, i.e. $K^2 = 0$, then equation (2.25) has two roots. The first, $\frac{\omega}{k} = v_s$, is the acoustic root, while the 2nd root given by

$\omega = \mu E_o k - i(\omega_c + k^2 D_n)$ describes the propagation of damped space charge waves. We shall not be concerned with these space charge waves since normally they are very heavily damped and do not play a part in acoustoelectric phenomena. However, we note in passing that under some circumstances[14] they require more careful consideration.

Since the electromechanical coupling constant K^2 is small, (typically $\sim 10^{-2}$), we may solve (2.25) by a perturbation treatment. We have for the perturbed acoustic root

$$\left(\frac{\omega^2}{v_s^2} - k^2\right) \approx \frac{K^2 \frac{\omega^2}{v_s^2}\left(\gamma + \frac{i\omega}{\omega_D}\right)}{\gamma + i\left(\frac{\omega_c}{\omega} + \frac{\omega}{\omega_D}\right)} \qquad (2.26)$$

where we have replaced ω/k by v_s in the right hand side, since corrections to this will be of a higher order in K^2. $\gamma = 1 - E_o/E_s$, where $E_s = v_s/\mu$ is the synchronous field at which the electron drift velocity is equal to v_s and $\omega_D = v_s^2/D_n$ is a frequency characteristic of electronic diffusion. Solving (2.26) for $k = k_r + ik_i$ we find, to 1st order in K^2, that the real and imaginary parts of the wave vector k are given by

$$k_r = \frac{\omega}{v_s}\left[1 - \frac{K^2\left(\gamma^2 + \frac{\omega}{\omega_D}\left(\frac{\omega_c}{\omega} + \frac{\omega}{\omega_D}\right)\right)}{2\left[\gamma^2 + \left(\frac{\omega_c}{\omega} + \frac{\omega}{\omega_D}\right)^2\right]}\right] \qquad (2.27)$$

$$k_i = \frac{K^2 \omega_c \gamma}{2 v_s \left[\gamma^2 + \left(\frac{\omega_c}{\omega} + \frac{\omega}{\omega_D}\right)^2\right]} \qquad (2.28)$$

Equation (2.28) gives the attenuation or growth of the acoustic wave due to piezoelectric coupling. The perturbed velocity of sound $v_s' = \frac{\omega}{k_r}$ follows from (2.27) as

$$v_s' = v_s \left[1 + \frac{K^2}{2} \frac{\left(\gamma^2 + \frac{\omega}{\omega_D} \left(\frac{\omega_c}{\omega} + \frac{\omega}{\omega_D} \right) \right)}{\gamma^2 + \left(\frac{\omega_c}{\omega} + \frac{\omega}{\omega_D} \right)^2} \right] \qquad (2.29)$$

Using equation (2.26) together with equations (2.21)-(2.24) we may relate the complex amplitudes of the various waves. We find for example that

$$E' = \frac{e}{\epsilon} \frac{\left(\gamma + \frac{i\omega}{\omega_D} \right) S'}{\left(\gamma + i \left(\frac{\omega_c}{\omega} + \frac{\omega}{\omega_D} \right) \right)} \qquad (2.30)$$

and

$$n' = \frac{\epsilon \omega_c}{q v_s} \frac{E'}{\left(\gamma + \frac{i\omega}{\omega_D} \right)} \qquad (2.31)$$

It is of interest to plot the dispersion and attenuation curves given by (2.27) and (2.28) as functions of applied d.c. electric field and frequency. We do this below

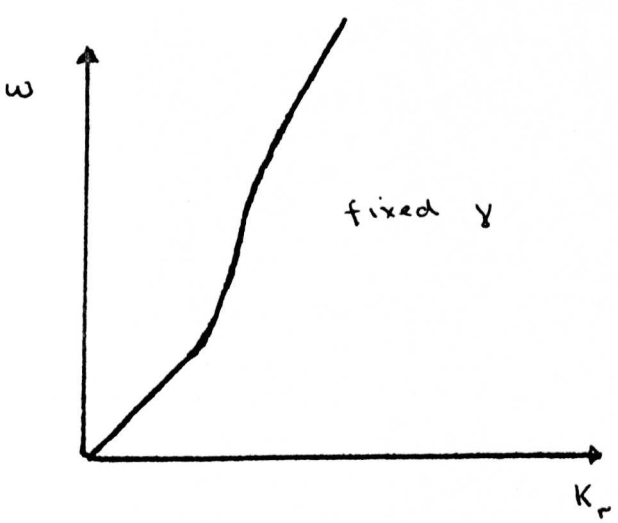

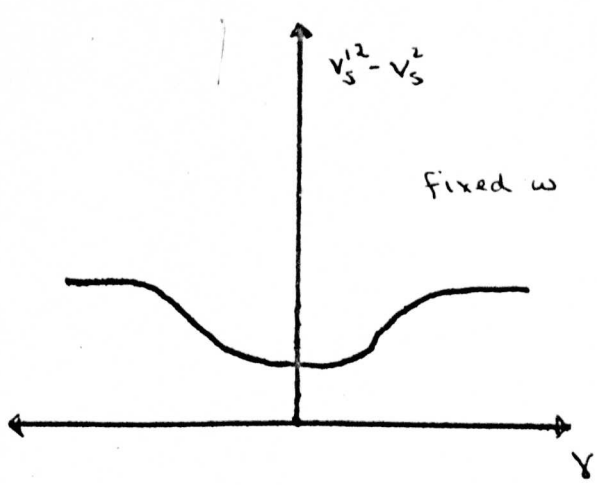

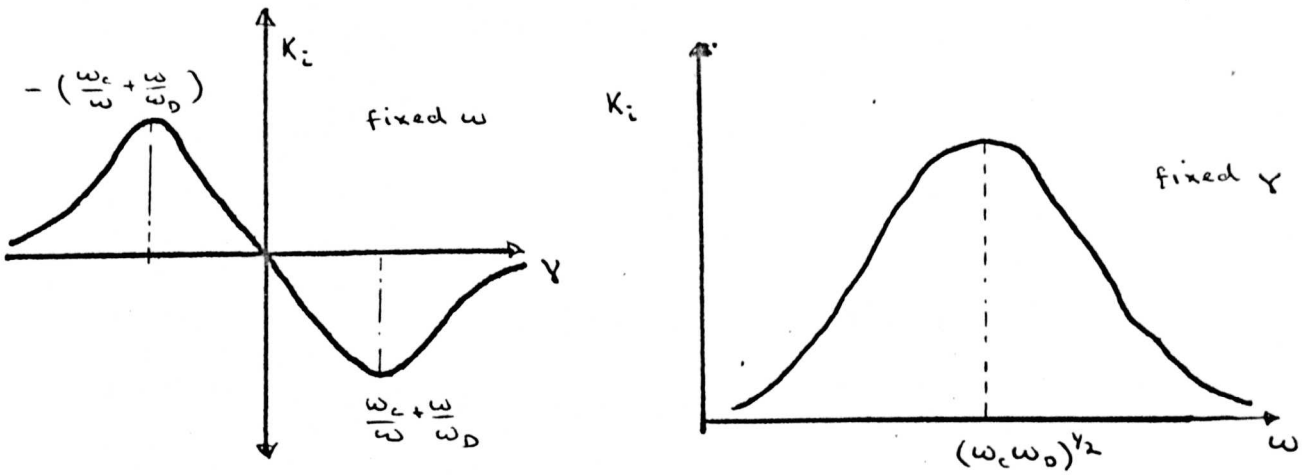

It is clear from (2.29) that for small ω, $v_s' \to v_s$. This is a consequence of the fact that at low frequencies the space charge always has time to adjust itself in such a way as to short out the alternating piezoelectric field. For large ω, we see that $v_s' \to v_s\left[1 + \frac{1}{2}K^2\right]$. In this limit, the space charge has no time to redistribute itself and the material behaves like a piezoelectric insulator. For large $|\gamma|$ i.e. large applied d.c. field in either direction $v_s' \to v_s\left[1 + \frac{1}{2}K^2\right]$.

From (2.28) we find the behaviour of k_i as indicated above. The curve of k_i against γ may be understood as follows. The attenuation k_i is essentially the product of two factors. First, the factor γ which determines the direction of energy transfer. For γ positive i.e. $E_o < E_s$ the sound wave is attenuated; for γ negative, $E_o > E_s$ the sound wave is amplified i.e. $k_i < 0$. The other factor in equation (2.28) determines the degree of synchronism which exists between the electrons and the acoustic wave. This is a maximum for $E_o = E_s$ (i.e. $\gamma = 0$), and falls off as γ departs from this value.

The k_i versus frequency curve also has a simple interpretation. It is clear from physical considerations that the growth of the acoustic wave will depend on the number of electrons in regions of decelerative a.c. electric field relative to the number of electrons in regions of accelerative, (along positive x-direction) a.c. electric field. The electrons in the decelerative (negative) a.c. electric fields will transfer energy to the acoustic wave, while those in the accelerative, (positive) a.c. electric

fields will absorb energy from the acoustic wave. Equation (2.31) determines the phase of n' relative to E'. For $\omega << \omega_D$ and $\gamma < 0$, (i.e. $E_o > E_s$), we see that n' is in antiphase to E' so that energy is transferred to the acoustic wave and gain occurs. For $\gamma > 0$ the opposite is true and attenuation occurs. As ω increases the peak of n' moves backwards relative to E' until at large frequencies, $(\frac{\omega}{\omega_D} >> |\gamma|)$, the electrons are symmetrically disposed with respect to region of positive and negative a.c. electric fields. In this case the acoustic gain will clearly be zero. The two situations are illustrated below.

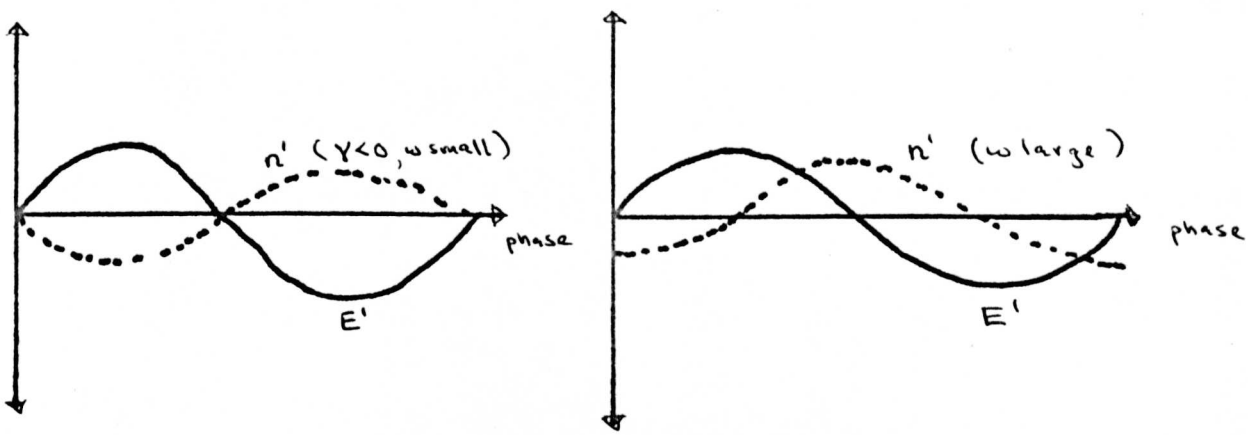

The number of electrons n' is given by (2.31). From (2.30) we see that E' and therefore n' is small when $\omega << \omega_c$. n' is also clearly small when $\omega >> \omega_D$. We therefore only expect significant acoustic gain when the frequency ω is in the ranges $\omega_c \lesssim \omega \lesssim \omega_D$. n' is small when $\omega << \omega_c$ due to the fact that at low frequencies, the electrons have time to redistribute themselves due to dielectric relaxation in a period of the acoustic wave. At high frequencies, electronic diffusion acts in a similar fashion to reduce n'.

It is not difficult to show (by differentiation of (2.28)), that the peaks on the attenuation (or gain) versus γ curve occur at $\gamma = \pm \left(\frac{\omega_c}{\omega} + \frac{\omega}{\omega_D} \right)$ and that the peak on the attenuation (or gain) curve versus frequency occurs at $\omega = (\omega_c \omega_D)^{\frac{1}{2}}$. Also, we find that the gain or attenuation increases with

ω_c (or conductivity), if $\gamma^2 + \frac{\omega^2}{\omega_D^2} > \frac{\omega_c^2}{\omega^2}$.

These features described above are the main results of the small signal one-dimensional theory of acoustoelectric amplification. In the next two sections we shall outline the theory in three dimensions applied to a crystal of the wurtzite structure (e.g. CdS).

2.4 Propagation in a Non-Conducting Hexagonal Crystal of the 6 mm Class in Zero d.c. Electric Field

The materials of most interest in connection with the acoustoelectric effect at the present time are the piezoelectric semiconductors CdS and ZnO. Both of these belong to the crystal class 6 mm. We shall accordingly study the propagation of acoustic waves in a 6 mm crystal using the theory developed in section 2.2. We follow here and in the next section, some unpublished work of E.G.S. Paige.

Before studying propagation in a piezoelectric material it is instructive to look at the acoustic modes which propagate in the absence of piezoelectric coupling in a crystal belonging to the class 6 mm. We do this in this section. In writing down the secular equation (2.20), we shall use a contracted notation for the elastic constants, (and later for the piezoelectric constants). This notation together with the requirements imposed by hexagonal symmetry, is given in Appendix 2.3.

Since there is no piezoelectric coupling, $\underline{k} = (k_1, k_2, k_3)$ is purely real. We label our Cartesian axes 1, 2, 3 and these are chosen as in Appendix 2.3. The secular equation (2.20) becomes in this case.

$$\begin{vmatrix} -\omega^2\rho + c_{11}k_1^2 + c_{66}k_2^2 + c_{44}k_3^2 & (c_{66}+c_{12})k_1k_2 & (c_{44}+c_{13})k_1k_3 \\ (c_{12}+c_{66})k_1k_2 & -\omega^2\rho + c_{66}k_1^2 + c_{22}k_2^2 + c_{44}k_3^2 & (c_{44}+c_{23})k_2k_3 \\ (c_{13}+c_{44})k_1k_3 & (c_{23}+c_{44})k_2k_3 & -\omega^2\rho + c_{44}k_1^2 + c_{44}k_2^2 + c_{33}k_3^2 \end{vmatrix}$$

$$= 0 \qquad (2.32)$$

Equation (2.32) may be simplified by choosing the $\underline{k}$ vector to lie along particular symmetry directions. We list these as follows. The directions are defined in the Appendix 2.3. The polarisation of the modes follows after using the solutions of (2.32) in equation (2.17).

Propagation Parallel to c-axis: $\underline{k} = (0, 0, k_3)$

From (2.32) and (2.17) we find

$(\frac{\omega}{k})^2 = c_{44}/\rho$ polarised transverse to $\underline{k}$, (shear)

$(\frac{\omega}{k})^2 = c_{44}/\rho$ " " "

$(\frac{\omega}{k})^2 = c_{33}/\rho$ polarised along $\underline{k}$ (longitudinal)

Propagation in Basal Plane $\underline{k} = (k_1, k_2, 0)$

$$\left(\frac{\omega}{k}\right)^2 = c_{44}/\rho \qquad \text{shear} \qquad \text{(parallel to c-axis)}$$

$$\left(\frac{\omega}{k}\right)^2 = c_{66}/\rho \qquad \text{shear} \qquad \text{(in basal plane perp to } \underline{k}\text{)}$$

$$\left(\frac{\omega}{k}\right)^2 = c_{11}/\rho \qquad \text{longitudinal} \qquad \text{(in basal plane)}$$

Propagation in the 1-3 Plane $\underline{k} = (k_1, 0, k_3)$

This case is slightly more complicated since the waves do not now decouple simply as in the preceeding cases. The wave polarised normal to the 1-3 plane decouples however; for it we find

$$\left(\frac{\omega}{k}\right)^2 = \frac{1}{\rho}\left(c_{66}\left(\frac{k_1}{k}\right)^2 + c_{44}\left(\frac{k_3}{k}\right)^2\right) \qquad \text{- shear}$$

For the remaining modes the secular equation is

$$(\omega^2\rho - c_{11}k_1^2 - c_{44}k_3^2)(\omega^2\rho - c_{44}k_1^2 - c_{33}k_3^2) - (c_{44} + c_{13})^2 k_1^2 k_3^2 = 0 \qquad (2.33)$$

$$\text{i.e.} \quad \left(\frac{\omega}{k}\right)^2 = \frac{1}{2\rho}\left[(c_{11} + c_{44})\left(\frac{k_1}{k}\right)^2 + (c_{44} + c_{33})\left(\frac{k_3}{k}\right)^2 \pm \left[\left[(c_{44}-c_{11})\left(\frac{k_1}{k}\right)^2 + (c_{33}-c_{44})\left(\frac{k_3}{k}\right)^2\right]^2 + 4(c_{44}+c_{13})^2\left(\frac{k_1}{k}\right)^2\left(\frac{k_3}{k}\right)^2\right]^{\frac{1}{2}}\right] \qquad (2.34)$$

The modes associated with this are mixed shear and longitudinal. However, because of the small anisotropy usually found in 6 mm crystals these may be identified as quasi longitudinal and quasi shear.

Propagation in an Arbitrary Direction $\underline{k} = (k_1, k_2, k_3)$

By applying a rotation of axes about the c-axis, it is possible to transform this case into the preceeding one. This is because a hexagonal crystal is elastically isotropic as far as rotations about the c-axis are concerned. If we rotate axes through an angle α such that $k_2' = -k_1 \sin\alpha + k_2 \cos\alpha = 0$, then we find that the secular equation becomes identical with (2.22) except that k_1 is replaced by $(k_1^2 + k_2^2)^{\frac{1}{2}}$. This replacement in the results of the preceeding case yields the general formulae. Again the mode polarised normal to the k_1', k_3 plane is decoupled.

For CdS the values of the elastic constants are given in table 2.1 (15)

Table 2.1

c_{11}	9.14×10^{10} Nm^{-2}
c_{12}	5.88 .....
c_{13}	5.15 .....
c_{33}	9.48 .....
c_{44}	1.50 .....
c_{66}	1.63 .....

The velocity surfaces are sketched below

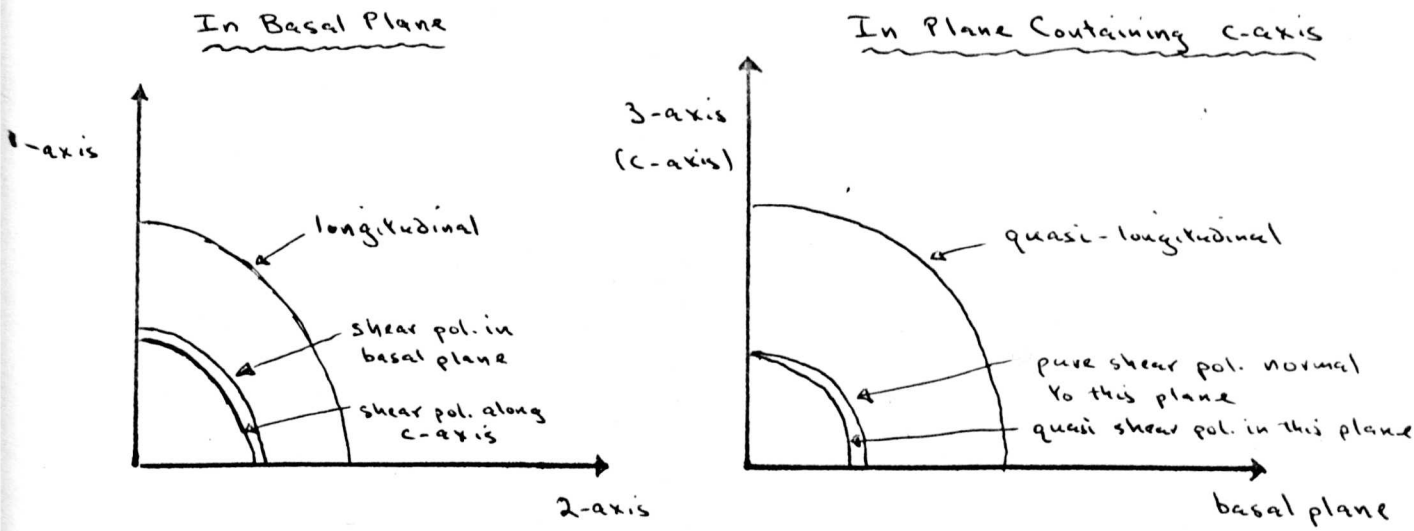

2.5 Propagation in a 6 mm Crystal with Piezoelectric Coupling in an Applied d.c. Electric Field

We shall now include the effects of piezoelectric coupling to the free carriers and the application of a d.c. electric field. Once again, the requirements imposed by hexagonal symmetry, together with the contracted notation are given in Appendix 2.3. All 2nd rank tensors, (conductivity etc), are now diagonal, e.g. $\sigma_{mn} = \sigma^{(m)} \delta_{mn}$ where the upper suffix is not summed. From (2.19), the quantity χ becomes

$$\chi = \frac{[\omega + k_n \mu^{(n)} E_{on} + ik_n k_n D^{n(n)}]}{k_m k_m \epsilon^{(m)} [\omega + k_n \mu^{(n)} E_{on} + ik_n k_n D^{n(n)}] + ik_n k_n \sigma^{(n)}} \qquad (2.35)$$

The equations in (2.17) written out in full become for this case.

$$[-\omega^2\rho + c_{11}\,k_1^2 + c_{66}\,k_2^2 + c_{44}\,k_3^2 + (e_{31}+e_{15})^2\,\chi\,k_1^2\,k_3^2\,]\,u_1$$

$$+\,[(c_{66}+c_{12})\,k_1k_2 + (e_{31}+e_{15})^2\,\chi\,k_1\,k_2\,k_3^2\,]\,u_2$$

$$+\,[(c_{44}+c_{13})\,k_1\,k_3 + (e_{31}+e_{15})(e_{15}\,(k_1^2+k_2^2) + e_{33}\,k_3^2)\,\chi\,k_1\,k_3]\,u_3$$

$$= 0 \qquad (2.36)$$

$$[(c_{12}+c_{66}) + (e_{31}+e_{15})^2\,\chi\,k_3^2\,]\,k_1\,k_2\,u_1$$

$$+\,[-\omega^2\rho + c_{66}\,k_1^2 + c_{22}\,k_2^2 + c_{44}\,k_3^2 + (e_{31}+e_{15})^2\,\chi\,k_2^2\,k_3^2\,]\,u_2$$

$$+\,[(c_{44}+c_{23}) + (e_{31}+e_{15})\,(e_{15}\,(k_1^2+k_2^2) + e_{33}\,k_3^2)\,\chi]\,k_2\,k_3\,u_3$$

$$= 0 \qquad (2.37)$$

$$[(c_{13}+c_{44}) + (e_{31}+e_{15})\,(e_{15}\,(k_1^2+k_2^2) + e_{33}\,k_3^2)\,\chi]\,k_1\,k_3\,u_1$$

$$+\,[(c_{23}+c_{44}) + (e_{31}+e_{15})\,(e_{15}\,(k_1^2+k_2^2) + e_{33}\,k_3^2\,)\,\chi\,]\,k_2\,k_3\,u_2$$

$$+\,[c_{44}\,(k_1^2+k_2^2) + c_{33}\,k_3^2 + (e_{15}\,(k_1^2+k_2^2) + e_{33}\,k_3^2)^2\,\chi]\,u_3$$

$$= 0 \qquad (2.38)$$

We see that throughout these equations, only two combinations of the elements of the piezoelectric tensor appear. These will be labelled

$$e_a = e_{31} + e_{15} \quad \text{and} \quad e_b = e_{15}\,(\alpha^2+\beta^2) + e_{33}\,\gamma^2$$

where $\alpha = k_1/k$, $\beta = k_2/k$, $\gamma = k_3/k$ (γ here should not be confused with γ used in the one-dimensional theory), are the direction cosines of the $\underline{k}$ vector. We shall find in the following that we can always write the dispersion relation in a form like $k^2 = \frac{\omega^2 \rho}{c''}$ where c'' is some effective combination of elastic constants involving the direction cosines of $\underline{k}$,k itself and the piezoelectric constants. Writing $k = k_r + ik_i$ where if the piezoelectric coupling is small $k_r >> k_i$ we have

$$k^2 = k_r^2 - k_i^2 + 2ik_r k_i = \frac{\omega^2 \rho}{|c''|^2} (\mathrm{Re}c'' - i\,\mathrm{Im}c'')$$

i.e. since $\mathrm{Re}c'' >> \mathrm{Im}c''$ we have

$$k_r^2 \simeq \omega^2 \rho / \mathrm{Re}c'' \quad \text{i.e.} \quad v_s' \simeq \frac{\omega}{k_r} = \sqrt{\frac{\mathrm{Re}c''}{\rho}} \tag{2.39}$$

where v_s' is the new velocity of sound, including piezoelectric coupling and

$$k_i \simeq -\frac{1}{2} \frac{\mathrm{Im}c'' \omega^2 \rho}{(\mathrm{Re}c'')^2 k_r} \simeq -\frac{1}{2} \frac{\omega}{\rho v_s^3} \mathrm{Im}c'' \tag{2.40}$$

where v_s is the velocity of sound in the absence of piezoelectric coupling.

We shall now apply this to acoustic wave propagation along various directions in a conducting piezoelectric 6 mm crystal in an applied d.c. electric field.

Propagation Parallel to the c-axis $\underline{k} = (0, 0, k_3)$, $\alpha = \beta = 0$, $\gamma = 1$

From (2.36) - (2.38) the secular equation is

$$\begin{vmatrix} -\omega^2\rho + c_{44} k_3^2 & 0 & 0 \\ 0 & -\omega^2\rho + c_{44} k_3^2 & 0 \\ 0 & 0 & -\omega^2\rho + c_{33} k_3^2 + e_3^2 k_3^4 \chi \end{vmatrix} = 0 \qquad (2.41)$$

For the 1st two roots we have

$$\frac{\omega}{k_r} = v_s = \sqrt{\frac{c_{44}}{\rho}} \quad \text{- shear wave pol. perp. to c-axis}$$

$$k_i = 0$$

For the last root we have

$$k_3^2 = \frac{\omega^2\rho}{c_{33} + e_3^2 k_3^2 \chi}. \quad \text{Hence we have from (2.27)-(2.28)}$$

$$v_s' = \sqrt{\frac{c_{33} + e_{33}^2 k_3^2 \, \mathrm{Re}\, \chi}{\rho}} \approx \sqrt{\frac{c_{33} + e_{33}^2 \frac{\omega^2\rho}{c_{33}} \mathrm{Re}\chi}{\rho}} \qquad (2.42)$$

and

$$k_i = -\frac{1}{2} \frac{\omega}{\rho v_s'^3} e_{33}^2 k_3^2 \, \mathrm{Im}\, (\chi(0, 0, k_3)) \qquad (2.43)$$

From (2.35) we have

$$\chi = \frac{[\omega + k_3 \mu_{33} E_{03} + ik_3^2 D_{33}^n]}{k_3^2 \epsilon_{33}[\omega + k_3\mu_{33}E_{03} + ik_3^2 D_{33}^n + i\sigma_{33}/\epsilon_{33}]} \tag{2.44}$$

i.e.

$$\text{Im } \chi = \frac{-\sigma_{33}/\epsilon_{33}\,(\omega + k_3 \mu_{33} E_{03})}{k_3^2 \epsilon_{33}\left[(\omega + k_3 \mu_{33} E_{03})^2 + (k_3^2 D_{33}^n + \frac{\sigma_{33}}{\epsilon_{33}})^2\right]} \tag{2.45}$$

Hence from (2.43)

$$k_i = \frac{1}{2}\left[\frac{e_{33}^2}{\sigma_{33}\epsilon_{33}}\right] \frac{\sigma_{33}/\epsilon_{33}}{v_s} \frac{(1 + \mu_{33} E_{03}/v_s)}{(1 + \mu_{33}E_{03}/v_s)^2 + \left(\frac{\omega D_{33}^n}{v_s^2} + \frac{\sigma_{33}}{\epsilon_{33}\omega}\right)^2} \tag{2.46}$$

We therefore see that the shear wave propagating parallel to the c-axis is unaffected by the piezoelectric coupling, while the longitudinal wave grows or decays with a decay constant k_i given by (2.46).

Propagation in the Basal Plane ($\underline{k} = (k_1, k_2, 0)$

Because of the hexagonal symmetry, it is found, (Appendix 2.3), that the elastic and piezoelectric tensors are invariant under rotations about the c-axis. Because of this, we may perform a rotation of axes such that in the new system $\underline{k} = (k_1', 0, 0)$. The secular equation then decouples. It is found that the longitudinal and shear waves polarised in the basal plane are unaffected by the piezoelectric coupling. For the shear wave

polarised parallel to the c-axis however we find the dispersion relation

$$k^2 = \frac{\omega^2 \rho}{c_{44} + e_{15}^2 k^2 \chi} \tag{2.47}$$

Using (2.35), (2.40) we thus obtain

$$k_i = \frac{1}{2}\left[\frac{e_{15}^2}{\epsilon_{11} c_{44}}\right] \frac{\sigma_{11}/\epsilon_{11}}{v_s} \left[\frac{1 + \frac{\mu_{11}\, \underline{k}\cdot\underline{E}_0}{\omega}}{\left(1 + \frac{\mu_{11}\underline{k}\cdot\underline{E}_0}{\omega}\right)^2 + \left(\frac{k^2 D_{11}}{\omega} + \frac{\sigma_{11}}{\epsilon_{11}\omega}\right)^2}\right] \tag{2.48}$$

Propagation in an Arbitrary Direction $\underline{k} = (k_1, k_2, k_3)$

Because of the rotational symmetry about the c-axis, this problem may again be reduced to propagation in the k_1', k_3 plane. After rotation through an angle α about the c-axis such that $\tan\alpha = k_2/k_1$ we have $k_2' = 0$, $k_1' = \sqrt{k_1^2 + k_2^2}$. The secular equation becomes in this case after rotation.

$$\begin{vmatrix} -\omega^2\rho + c_{11}k_1'^2 + c_{44}k_3^2 + e_a^2\chi k_1'^2 k_3^2 & 0 & [c_{44}+c_{13}+e_a e_b k^2\chi]k_1' k_3 \\ 0 & -\omega^2\rho + c_{66}k_1'^2 + c_{44}k_3^2 & 0 \\ [c_{44}+c_{13}+e_a e_b k^2\chi]k_1' k_3 & 0 & -\omega^2\rho + c_{44}k_1'^2 + c_{33}k_3^2 + e_b^2 k^4\chi \end{vmatrix} = 0 \tag{2.49}$$

Again, it is clear that the shear wave polarised perpendicular to the k_1', k_3 plane is decoupled and is unaffected by the piezoelectric coupling. For the other wave (2.49) yields

$$(-\omega^2\rho + c_{11}\, k_1'^2 + c_{44}\, k_3^2 + e_a^2\, \chi\, k_1'^2\, k_3^2)\,(-\omega^2\rho + c_{44}\, k_1'^2 + c_{33} k_3^2 + e_b^2\, k^4\chi)$$

$$- [c_{44} + c_{13} + e_a\, e_b\, k^2]^2 k_1'^2\, k_3^2 \;=\; 0 \qquad (2.50)$$

i.e.

$$\frac{\omega^2}{k^2} = \frac{1}{2\rho}\,[(c_{11} + c_{44})\,(\alpha^2 + \beta^2) + (c_{33} + c_{44})\,\gamma^2 +$$

$$k^2\chi\,(e_a^2\,(\alpha^2 + \beta^2)\,\gamma^2 + e_b^2) \pm [((c_{44} - c_{11})\,(\alpha^2 + \beta^2)$$

$$+ (c_{33} - c_{44})\,\gamma^2 + k^2\chi\,(e_b^2 - e_a^2\,(\alpha^2 + \beta^2)\,\gamma^2))^2 +$$

$$4\,(c_{44} + c_{13} + e_a\, e_b\, k^2\,\chi)^2\,(\alpha^2 + \beta^2)\,\gamma^2\,]^{\frac{1}{2}}\,] \qquad (2.51)$$

Since the piezoelectric coupling is weak, we may expand the square root term in (2.51) to first order in e^2. We then find:

$$\frac{\omega^2}{k^2} \approx \frac{1}{2\rho}\,[(c_{11} + c_{44})\,(\alpha^2 + \beta^2) + (c_{33} + c_{44})\,\gamma^2$$

$$\pm \sqrt{[(c_{44}-c_{11})(\alpha^2 + \beta^2) + (c_{33} - c_{44})\,\gamma^2]^2 + 4\,(c_{44} + c_{13})^2(\alpha^2+\beta^2)\gamma^2}$$

$$+\; k^2\,\chi\,(e_a^2\,(\alpha^2 + \beta^2)\,\gamma^2 + e_b^2) \pm$$

$$\frac{k^2\chi\,[(e_b^2 - e_a^2(\alpha^2+\beta^2)\gamma^2)\,((c_{44}-c_{11})(\alpha^2+\beta^2) + (c_{33}-c_{44})\gamma^2) + 4e_a e_b(\alpha^2+\beta^2)\gamma^2(c_{44}+c_{13})]}{\left|[(c_{44}-c_{11})(\alpha^2+\beta^2) + (c_{33}-c_{44})\cdot\gamma^2]^2 + 4\,(c_{44} + c_{13})^2\,(\alpha^2 + \beta^2)\,\gamma^2\right|^{\frac{1}{2}}}$$

$$(2.52)$$

Also, in this case we have from equation (2.35),

$$\chi = \frac{[\omega+k\,\mu_{11}(\alpha E_{01} + \beta E_{02}) + k\mu_{33}\,\gamma E_{03} + ik^2\,(D^n_{11}\,(\alpha^2+\beta^2) + D_{33}\,\gamma^2)]}{\left\{k^2((\alpha^2+\beta^2)\epsilon_{11}+\gamma^2\epsilon_{33})[\omega+k\mu_{11}(\alpha E_{01}+\beta E_{02})+ \mu_{33}k\,\gamma E_{03}+ik^2(D^n_{11}(\alpha^2+\beta^2)+D^n_{33}\gamma^2)]+\right.}$$

$$\left. + ik^2\,(\alpha^2+\beta^2)\,\sigma_{11} + \gamma^2\,\sigma_{33}\right\}$$

(2.53)

Combining equations (2.52) and (2.53) and using (2.40) we find for this case

$$k_i = \frac{K^2_{eff}(\alpha,\beta,\gamma)\;\omega_c^{eff}(\alpha,\beta,\gamma)\left(1 + \dfrac{\mu_{11}(\alpha E_{01}+\beta E_{02})+\mu_{33}\gamma E_{03}}{v_s(\alpha,\beta,\gamma)}\right)}{2v_s(\alpha,\beta,\gamma)\left(1+\dfrac{\mu_{11}(\alpha E_{01}+\beta E_{02}) + \mu_{33}\gamma E_{03}}{v_s(\alpha,\beta,\gamma)}\right)^2 + \left(\dfrac{\omega_c^{eff}}{\omega}(\alpha,\beta,\gamma) + \dfrac{\omega}{\omega_D^{eff}(\alpha,\beta,\gamma)}\right)^2}$$

(2.54)

where $v_s\,(\alpha,\beta,\gamma)$ is the sound velocity in the direction α, β, γ,

$$\omega_c^{eff}(\alpha\,\beta\,\gamma) = [(\alpha^2+\beta^2)\,\sigma_{11} + \gamma^2\sigma_{33}]/[(\alpha^2+\beta^2)\,\epsilon_{11} + \gamma^2\,\epsilon_{33}]$$

$$\omega_D^{eff}(\alpha,\beta,\gamma) = v_s^2\;(\alpha,\beta,\gamma) \,/\, [(\alpha^2+\beta^2)\,D^n_{11} + \gamma^2\,D^n_{33}] \qquad (2.55)$$

$$K^2_{\pm eff}\,(\alpha,\beta,\gamma)\,\frac{e^2_{\pm eff}\;(\alpha,\beta,\gamma)}{2((\alpha^2+\beta^2)\,\epsilon_{11} + \gamma^2\,\epsilon_{33})\;v_s^2} \qquad (2.56)$$

is the effective electromechanical coupling constant and

$$e^2_{\pm eff}(\alpha,\beta,\gamma) = e_a^2(\alpha^2+\beta^2)\gamma^2 + e_b^2 \pm$$

$$\frac{(e_b^2-e_a^2(\alpha^2+\beta^2)\gamma^2)((c_{44}-c_{11})(\alpha^2+\beta^2)+(c_{33}-c_{44})\gamma^2) + 4e_a e_b(\alpha^2+\beta^2)\gamma^2(c_{44}+c_{13})}{\left\{[(c_{44}-c_{11})(\alpha^2+\beta^2)+(c_{33}-c_{44})\gamma^2]^2 + 4(c_{44}+c_{13})^2(\alpha^2+\beta^2)\gamma^2\right\}^{\frac{1}{2}}}$$

(2.57)

Equation (2.54) together with (2.55)-(2.57) gives the decay or growth rate in an arbitrary direction in a 6 mm crystal due to piezoelectric coupling.

The results can be summarised as follows. The shear wave polarised perpendicular to the c-axis is unaffected by piezoelectric coupling and therefore plays no part in acoustoelectric phenomena. The quasi-shear and quasi longitudinal waves which are polarised in a plane containing the c-axis and $\underline{k}$ are affected by the piezoelectric coupling. Their decay (or growth) rates are given by (2.54). The results (2.46) and (2.48) and (2.54) should be compared with the one-dimensional formula (2.28). For CdS the values of the piezoelectric constants are given in Table 2.2 below[16]

Table 2.2

e_{15}	2.1×10^{-1} Coul/m^2
e_{31}	-2.6×10^{-1}
e_{33}	4.4×10^{-1}

The behaviour of $K^2_{eff\pm}(\alpha,\beta,\gamma)$ is indicated roughly below

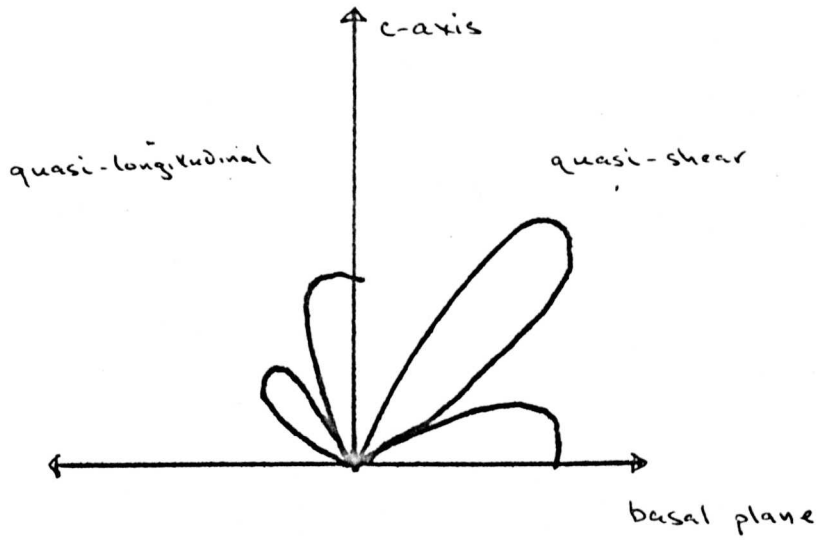

Finally, we note from (2.48) that the shear wave propagating in the basal plane polarised parallel to the c-axis has a growth (or decay) rate which is formally identical to the 1-dimensional result (2.28) except that effective piezoelectric constants etc. appear. In particular, the effective γ which appears is $1 - \frac{\mu_{11}\, \underline{k} \cdot \underline{E}_o}{\omega}$. Because of this, we see that at high d.c. applied fields, the waves which will have the largest amplification will be off-axis waves for which the effective γ is not too large $<\left(\frac{\omega_c^{eff}}{\omega} + \frac{\omega}{\omega_D^{eff}} \right)$, (c.f. diagram of k_i against γ in section 2.3).

References Chapter 2

1. Carleton, H.R., Kroger, H., and Prohofsky, E.W., (1965), Proc. IEEE, 10, 1452.
2. Pippard, A.B., (1963), Phil. Mag. 8, 161.
3. Yamashita, J., and Nakamura, K., (1968), Prog. Theor. Phys., (Japan) 39, 545.
4. Blatt, F.J. (1968), Physics of Electronic Conduction in Solids (McGraw Hill).
5. Landau, L.D., and Lifschitz, E.M., (1959), Theory of Elasticity (Pergamon).
6. Landau, L.D., and Lifschits, E.M., (1959), Fluid Mechanics (Pergamon).
7. Nye, J.F. (1957), Physical Properties of Crystals, (Clarendon Press, Oxford.)
8. See refs. (5) and (7).
9. See ref. (7).
10. Paige, E.G.S. Private Communication
11. Kyame, J.J., (1949), J. Acoust. Soc. Am. 21, 159.
12. Kyame, J.J., (1954), J. Acoust. Soc. Am. 26, 990.
13. White D.L., (1962), J. Appl. Phys. 33, 2547.
14. Adler, E.L., Farnell, G.W.(1965), McGill University Report - The Effect of Acoustoelectric Interactions on the Electrical Impedance of a CdS Bar.
15. Berlincourt, D., Jaffe, H., and Shiozawa, L.R., (1963), Phys. Rev. 129, 1009.
16. See ref. (15).
17. See ref. (5)
18. Hutson, A.R., and White, D.L., (1962), J. Appl. Phys. 33, 40.

Appendix 2.1

Lattice Loss

In discussing lattice loss we follow the treatment of Landau and Lifschitz[17]. We have mentioned that in the treatment of acoustic wave propagation given in Chapter 2, we neglected irreversible loss processes which dissipate energy from an acoustic wave. Dissipation may be represented phenomenologically by the introduction of dissipative frictional forces f_i which are linear functions of velocity. This linear dependence on velocity ensures that these forces change sign under time reversal and so describe irreversible effects. For a simple mechanical system, these frictional forces can be written as velocity derivatives of a certain quadratic function ψ of the velocities, called the dissipative function, i.e. $f_i = - \partial\psi/\partial\dot{q}_i$ where q_i is some generalised coordinate of the system. This relation is equivalent to $\delta\psi = - \sum_i f_i \delta\dot{q}_i$, where $\delta\psi$ is the increase in ψ due to an increase $\delta\dot{q}_i$ in the generalised velocities. For a continuous medium such a deformable elastic body, the state of the system is specified by the continuum of generalised coordinates $u_i(\underline{r})$ (i.e. the displacement vectors at each point in the body). In this case we have by analogy $\delta \int \psi dV = - \int f_i \delta\dot{u}_i \, dV$, where ψ and f_i are now per unit volume.

We may determine the general form of the function ψ for deformable bodies as follows. Clearly ψ must be zero if there is no internal motion, and in particular, if the body executes a macroscopic translatory or rotatory motion. This means that ψ depends on the spatial gradients of the velocity, and can only contain such combinations of the derivatives as vanish when $\dot{\underline{u}} = \underline{\Omega} \times \underline{r}$ where $\underline{\Omega}$ is some angular velocity. These are the sums $\partial\dot{u}_i/\partial x_k + \partial\dot{u}_k/\partial x_i$, i.e. the time derivatives of components of the strain tensor S_{ik}. Since f_i is linear in the velocities, it follows from

the above that the ψ must be quadratic in S_{ik}. The most general form for ψ is thus

$$\psi = \frac{1}{2} \eta_{ik\ell m} \dot{S}_{ik} \dot{S}_{\ell m} \tag{A1}$$

where $\eta_{ik\ell m}$ is called the viscosity tensor. $\eta_{ik\ell m}$ has the following obvious symmetry properties

$$\eta_{ik\ell m} = \eta_{\ell mik} = \eta_{ki\ell m} = \eta_{ikm\ell} \tag{A2}$$

The dissipative stress tensor is defined by $f_i = \partial T'_{ik}/\partial x_k$ hence

$$\int \delta\psi dv = \int \frac{\partial \psi}{\partial \dot{S}_{ik}} \delta \dot{S}_{ik} \, dv = - \int \frac{\partial T'_{ik}}{\partial x_k} \delta \dot{u}_i \, dv = \int T'_{ik} \delta \dot{S}_{ik} \, dv \tag{A3}$$

on integrating by parts

$$\text{i.e. } T'_{ik} = \partial\psi / \partial \dot{S}_{ik} = \eta_{ik\ell m} \dot{S}_{\ell m} \tag{A4}$$

The total stress in an elastic body is therefore given by

$$T_{ik} = c_{ik\ell m} S_{\ell m} + \eta_{ik\ell m} \dot{S}_{\ell m} \tag{A5}$$

i.e. in a travelling wave we have

$$T_{ik} = c''_{ik\ell m} S_{\ell m} \tag{A6}$$

$$\text{where } c''_{ik\ell m} = c_{ik\ell m} - i\omega \eta_{ik\ell m} \tag{A7}$$

is a modified complex elastic constant. Inserting a travelling wave form into the equation of motion (2.21) without piezoelectric coupling including lattice loss now yields the dispersion relation

$$k = \frac{\omega}{v_s}\left(1 + \frac{i\omega\eta}{2\rho v_s^2}\right) \tag{A8}$$

we therefore call $\omega^2\eta / 2\rho v_s^3 = \alpha_{lat}$ the lattice loss constant.

Appendix 2.2

Corrections to Dispersion Relation Owing to Transverse Electric Fields:

We follow here the derivation of Hutson and White[18]. The axes x_1, x_2, x_3 will be chosen such that x_1 lies along the direction of plane wave propagation. Derivatives with respect to x_2 and x_3 will therefore be zero. For plane waves it is convenient to define the strain as

$$S'_{ik} = \partial u'_k / \partial x_1 = iku'_k \qquad (B1)$$

The constitutive relations (2.2) and (2.9), (2.8) and (2.11) become

$$T'_{1i} = c_{1i1k} S'_{1k} - e_{k1i} E'_k \qquad (B2)$$

$$D'_k = e_{k1i} S'_{1i} + \epsilon_{ik} E'_i \qquad (B3)$$

$$B'_i = \mu^M H'_i \qquad (B4)$$

$$j'_i = \sigma_{ik}(E_{ok} + E'_k) + n'q\,\mu_{ik}E_{ok} + qD^n_{i1}\frac{\partial n'}{\partial x} \qquad (B5)$$

From the plane wave condition and the Maxwell equation $\nabla.\underline{B'} = 0$, together with (B4), we see that B'_1 and H'_1 are constant in space and time and $(\nabla \times H')1 = 0$. From the Maxwell equations (2.4) and (2.5), one can obtain equations for E'_2 and E'_3 from which $\underline{D'}$,$\underline{j'}$ and n' may be eliminated using (B3) and (B5) together with equation (2.7). We find

$$- \frac{\partial^2 E'_p}{\partial x_1^2} = i\omega\mu^M \left[\sigma_{pi} E'_i + (k^2 D^n_{p1} - ik\mu_{pk} E_{ok}) (\epsilon_{i1} E'_i + ie_{11i} k u'_i)\right.$$

$$\left. - i\omega (\epsilon_{ip} E'_i + ie_{p1i} k u'_i) \right] = k^2 E'_p . \qquad (B6)$$

$$= i\omega\mu^M [E'_q A_{pq} + E'_1 A_{p1} + u'_i B_{pi}]$$

for p, q = 2 or 3 only,

Where $A_{pq} = \sigma_{pq} + i\omega\epsilon_{pq} + \epsilon_{1q} (k^2 D^n_{p1} - ik\mu_{pk} E_{ok})$ (B7)

$$B_{pi} = ike_{11i} (k^2 D^n_{p1} - ik\mu_{pk} E_{ok}) - \omega e_{p1i} k$$

The other component gives

$$E'_1 = - \frac{E'_q A_{1q}}{A_{11}} - \frac{u'_i B_{1i}}{A_{11}} \qquad (B8)$$

where again p,q take only the values 2 and 3.

The wave equation (2.1) yields

$$- \omega^2 \rho u_i = - k^2 c_{1i1k} u_k - ie_{k1i} k E_k \qquad (B9)$$

Equation (B7) may be used to eliminate the longitudinal electric field E'_1 from (B6) and (B8) leaving 5 coupled equations in u_i and E_2, E_3. After some manipulation these become

$$\omega^2 \rho u_i' = k^2 \bar{c}_{1i1k} u_k' + ik \bar{e}_{p1i} E_p' \qquad (B10)$$

$$\text{and} \quad k^2 E_p' = i\omega\mu^M \left\{ E_q' \left[A_{pq} - \frac{A_{1q} A_{p1}}{A_{11}} \right] + u_i' \left[B_{pi} - \frac{B_{1i} A_{p1}}{A_{1i}} \right] \right\} \qquad (B11)$$

$$\text{where } \bar{c}_{1i1k} = c_{1i1k} + \frac{e_{11i} e_{11k} (k^2 D_{11}^n - ik \mu_{1k} E_{ok} - i\omega)}{(\sigma_{11} + (k^2 D_{11}^n - ik \sigma_{1k} E_{ok} - i\omega)\epsilon_{11})} \qquad (B12a)$$

and

$$\bar{e}_{p1i} = e_{p1i} - \frac{e_{11i} (\sigma_{1p} - (k^2 D_{11}^n - ik\mu_{1k} E_{ok} - i\omega) E_{1p}}{(\sigma_{11} + (k^2 D_{11}^n - ik\mu_{1k} E_{ok} - i\omega) \epsilon_{11})} \qquad (B12b)$$

It is not difficult to see from (B7) that the 2nd term in (B11) is proportional to the piezoelectric tensor e, in fact in the absence of diffusion and d.c. drift fields it is a multiple of $\bar{e}_{p1i}$.

The 5 x 5 secular determinant given by equations (B10) and (B11) may be manipulated until all elements have the dimensions of velocity squared. This may be done by introducing the average dielectric permittivity ϵ of the medium, and defining effective velocities (which can be complex) by $v = e'/(\epsilon\rho)^{\frac{1}{2}}$, where e' is any effective piezoelectric constant

The form of the secular determinant then becomes:

$$\begin{vmatrix} \left(\frac{c'_{1111}}{\rho} - \frac{\omega^2}{k^2}\right) & \frac{c'_{1112}}{\rho} & \frac{c'_{1113}}{\rho} & \frac{v'\omega}{k} & v'\frac{\omega}{k} \\ \frac{c'_{1211}}{\rho} & \left(\frac{c'_{1212}}{\rho} - \frac{\omega^2}{k^2}\right) & \frac{c_{1213}}{\rho} & \frac{v'\omega}{k} & v'\frac{\omega}{k} \\ \frac{c'_{1311}}{\rho} & \frac{c'_{1312}}{\rho} & \left(\frac{c'_{1313}}{\rho} - \frac{\omega^2}{k^2}\right) & \frac{v'\omega}{k} & v'\frac{\omega}{k} \\ v'\frac{\omega}{k} & v'\frac{\omega}{k} & v'\frac{\omega}{k} & \left(\frac{\omega^2}{k^2}\frac{\epsilon'}{\epsilon} - \frac{1}{\epsilon_\mu}^M\right) & \frac{\omega^2\epsilon'}{k^2\epsilon} \\ v\frac{\omega}{k} & v'\frac{\omega}{k} & v'\frac{\omega}{k} & \frac{\omega^2}{k^2}\frac{\epsilon'}{c} & \left(\frac{\omega^2}{k^2}\frac{\epsilon'}{\epsilon} - \frac{1}{\epsilon_\mu}^M\right) \end{vmatrix} = 0$$

(B13)

The v''s and ϵ''s in (B13) only indicate the form of the term and ϵ''s in different positions should not be read as being equal. It may be verified that the acoustic modes found in Chapter 2 using the approximation $\nabla \times \underline{E} = 0$, arise from (B13) by solving only the 3 x 3 upper left hand acoustic block in (B13). This gives corrections to the acoustic roots of order v'^2.

To demonstrate that the additional corrections obtained by solving (B13) exactly, are smaller by the square of the ratio of the sound velocity to the velocity of light, we proceed as follows. Suppose that the acoustic determinant has been solved giving $\frac{\omega}{k} = v_1, v_2, v_3$ and diagonalised by a suitable basis transformation. To find the correction δ^2 to v_1^2 resulting from the coupling to the electromagnetic wave, put $\frac{\omega}{k} = v_1$ in (B13). To order of magnitude (B13) becomes

$$\begin{vmatrix} \delta^2 & 0 & 0 & v'v_1 & v'v_1 \\ 0 & v_2^2-v_1^2+\delta^2 & 0 & v'v_1 & v'v_1 \\ 0 & 0 & v_3^2-v_1^2+\delta^2 & v'v_1 & v'v_1 \\ v'v_1 & v'v_1 & v'v_1 & v_1^2-c^2 & v_1^2 \\ v'v_1 & v'v_1 & v'v_1 & v_1^2 & v_1^2-c^2 \end{vmatrix} = 0 \qquad (B14)$$

Expanding (B14) gives

$$\delta^2 \simeq 2 \left(\frac{v_1}{c}\right)^2 v'^2 \qquad (B15)$$

which is required result.

Appendix 2.3

Contracted Notation and Symmetry Requirements on Elastic and Piezoelectric Constants

Because of the symmetry $e_{ijk} = e_{ikj}$ of the piezoelectric tensor, it is possible to reduce the number of independent components from 27 to 18. These 18 independent elements may be arranged in a 3 x 6 array as follow

$$\begin{bmatrix} e_{11} & e_{12} & e_{13} & e_{14} & e_{15} & e_{16} \\ e_{21} & e_{22} & e_{23} & e_{24} & e_{25} & e_{26} \\ e_{31} & e_{32} & e_{33} & e_{34} & e_{35} & e_{36} \end{bmatrix}$$

The first suffix in each element is the same as in the tensor e_{ijk}. The last suffix replaces the final pair of tensor suffices in e_{ijk} according to the following table

11	22	33	23,32	31,13	12,21
1	2	3	4	5	6

e.g. $e_{26} = e_{212} = e_{221}$.

Similarly for the elastic tensors which have 81 components. Because of the symmetry $c_{ijkl} = c_{jikl} = c_{ijlk}$, it is possible to reduce the number of independent components to 36. These may be arranged in a 6 x 6 array as follows

$$\begin{bmatrix} c_{11} & c_{12} & c_{13} & c_{14} & c_{15} & c_{16} \\ c_{21} & c_{22} & c_{23} & c_{24} & c_{25} & c_{26} \\ c_{31} & c_{32} & c_{33} & c_{34} & c_{35} & c_{36} \\ c_{41} & c_{42} & c_{43} & c_{44} & c_{45} & c_{46} \\ c_{51} & c_{52} & c_{53} & c_{54} & c_{55} & c_{56} \\ c_{61} & c_{62} & c_{63} & c_{64} & c_{65} & c_{66} \end{bmatrix}$$

In this case the first and last suffix in the table is to be replaced by a pair of elements according to the table above, e.g. $c_{36} = c_{3312} = c_{3321}$.

The requirements of hexagonal symmetry for a 6 mm crystal reduce the matrices to the following form.

$$\begin{bmatrix} o & o & o & o & e_{15} & o \\ o & o & o & e_{15} & o & o \\ e_{31} & e_{31} & e_{33} & o & o & o \end{bmatrix}$$

and

$$\begin{bmatrix} c_{11} & c_{12} & c_{13} & 0 & 0 & 0 \\ c_{12} & c_{11} & c_{13} & 0 & 0 & 0 \\ c_{13} & c_{13} & c_{33} & 0 & 0 & 0 \\ 0 & 0 & 0 & c_{44} & 0 & 0 \\ 0 & 0 & 0 & 0 & c_{44} & 0 \\ 0 & 0 & 0 & 0 & 0 & c_{66} \end{bmatrix}$$

where $c_{66} = \frac{1}{2}(c_{11} - c_{12})$.

A 6 mm crystal has the symmetry of the figure below

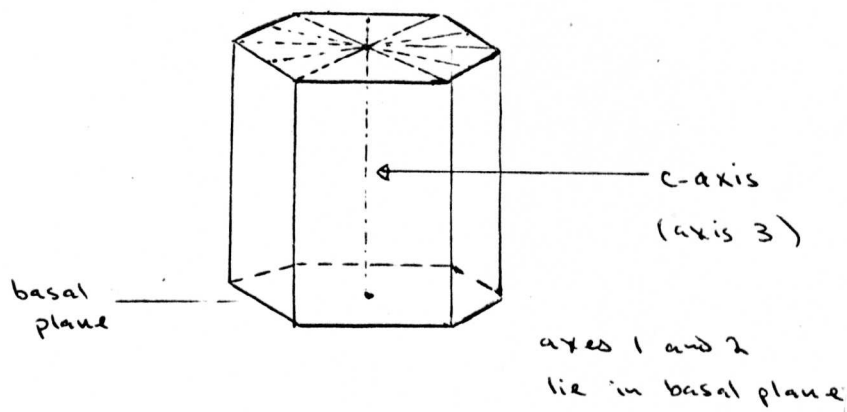

In addition we note that the hexagonal symmetry about the c-axis is such as to make the elastic and piezoelectric tensors invariant under rotations about the c-axis. This fact is used extensively in Chapter 2.

We note also, that all 2nd rank tensors must have the form under hexagonal symmetry

$$\begin{bmatrix} 11 & 0 & 0 \\ 0 & 11 & 0 \\ 0 & 0 & 33 \end{bmatrix}$$

Chapter 3

THE NON LINEAR THEORY OF ACOUSTOELECTRIC GAIN I - SPACE CHARGE DEPENDENT GAIN

3.1 Gain in the Non-Linear Regime

As we mentioned in chapter 1, there is at the present time a great deal of interest in non-linear acoustoelectric phenomena in piezoelectric semiconductors. Most of these phenomena were discussed in outline there. Several authors have attempted theoretical treatments of acoustoelectric effects in the large-signal regime using the results of White's linear theory (as given in Chapter 2), to provide a formula for acoustic gain. This approach is clearly unsatisfactory since the effects under discussion all arise in situations where acoustic wave amplitudes are large and non-linearities dominate. In the next three chapters of this work we shall develop a theory of acoustoelectric gain which takes explicit account of nonlinearities and accounts for some of the observed features of the behaviour of acoustic gain in the large signal regime[1].

While it is fairly clear what is meant by acoustic gain in the linear regime, this is not the case when non-linearities become of importance. When an acoustic wave is injected into an amplifying linear system, the wave which exits from the system will have the same form as the injected wave but will be of larger amplitude. For a nonlinear system things are quite different; when the wave enters the system, nonlinearities cause harmonic generation and frequency mixing, so that the shape of the wave changes as it propagates through the system. Thus, the wave which exits from a nonlinear system will have changed in form as well as in size. In addition, because in a non linear system acoustic gain will depend on the size and shape of the wave, and because these are changing from point to point, we are forced to consider the 'local' acoustic gain in the vicinity of a point. As we shall see later the concept of a 'local' gain must be defined as local in the sense of averaged over one wavelength of the acoustic wave. We shall not consider in the present work the average gain experienced by an acoustic wave after propagation through a finite sample of material. In principle there is no

difficulty in obtaining this from a knowledge of the local acoustic gain.

We have mentioned above that in the non-linear regime, in general, the acoustic gain will depend on the amplitude of the wave. This gives rise to a further complication. As we have seen in Chapter 2, when an acoustic wave propagates in a piezoelectric semiconductor, as well as containing a strain oscillation, the wave has accompanying it, a modulation in electric field and space charge, (as well as oscillations in stress, current etc). It is therefore somewhat ambiguous to refer to a dependence of the gain on the amplitude of the wave since there are several possible amplitudes one chould choose. As we shall see presently, the choice involved here is not a trivial one. The treatment of the dependence of the gain on the space charge differs radically from the treatment of its dependence on for example strain. In this Chapter we shall develop a non-linear theory of acoustoelectric gain based on a knowledge of the accompanying space charge modulation. The discussion of dependence of gain on electric field and strain will be postponed to Chapter 5.

In order to discuss non-linear gain, it is necessary to introduce the idea of gain at each harmonic component of the wave. These 'harmonic' gains will describe the growth of each individual harmonic of the wave and will include the effects of coupling to other harmonics via the non-linear interaction. When the growth of acoustic power is considered, it will be found expedient to introduce the concept of 'flux gain' or 'power gain'. We shall see that the flux gain is simply a weighted average of the various harmonic gains.

3.2 Harmonic Gain and Flux Gain

We shall be concerned only with a one dimensional theory of acoustic gain and we shall use the sign convention employed in Chapter 2. As we have seen in Chapter 2, at high d.c. electric field strengths, the acoustic gain in the direction of the applied field becomes small. The gain for off-axis waves travelling in other directions may however, remain large. In using a one-dimensional theory, we shall implicity neglect these off-axis waves. This limitation, which is probably fairly serious in certain circumstances, is necessary to obtain a tractable theory. The equation which determines the propagation of an acoustic wave is the wave equation (2.21). The lattice displacement u satisfies

$$\frac{\partial^2 u}{\partial t^2} - v_s^2 \frac{\partial^2 u}{\partial x^2} = \frac{e}{\rho} \frac{\partial E}{\partial x} \tag{3.1}$$

We define the instantaneous acoustic energy density W_{in} and instantaneous acoustic flux Φ_{in} by

$$W_{in} = \frac{1}{2} \rho \left(\frac{\partial u}{\partial t} \right)^2 + \frac{1}{2} c \left(\frac{\partial u}{\partial x} \right)^2 \tag{3.2}$$

$$\Phi_{in} = - c \frac{\partial u}{\partial x} \frac{\partial u}{\partial t} \tag{3.3}$$

where $c = \rho v_s^2$ is the appropriate elastic constant. W_{in} is simply the sum of the local kinetic and potential energy densities. Differentiating (3.2) with respect to time and using (3.1) together with (3.3) we find the energy conservation equation

$$\frac{\partial W_{in}}{\partial t} + \frac{\partial \Phi_{in}}{\partial x} = e \frac{\partial u}{\partial t} \frac{\partial E}{\partial x} \tag{3.4}$$

In the absence of piezoelectric coupling, ($e = 0$), (3.4) states that the rate of increase of energy density in some small volume of material is equal to the flux of energy flowing into the volume. The piezoelectric contribution on the right hand side of equation (3.4), represents an additional source of energy generation owing to the coupling of the acoustic waves to the conduction electrons.

We shall suppose that each of the field variables u, E etc. is a nearly periodic travelling wave with a fundamental frequency ω and a velocity close to the sound velocity v_s. To give expression to this assumption, it is convenient to introduce as an auxiliary coordinate, the phase $\theta = \omega (x/v_s - t)$. Then, any field variable f may be expressed as function of x, t, and θ which is slowly varying in x and t, periodic in θ and has the Fourier expansion

$$f(x, t, \theta) = \sum_{m=-\infty}^{\infty} f_m(x, t)\, e^{im\theta} \qquad (3.5)$$

where m takes all integral values from $-\infty$ to ∞ and $f_{-m} = f_m^*$ so that $f(x, t, \theta)$ is real, and the Fourier coefficient f_m is slowly varying in x and t compared with the exponential. The justification for this assumption depends on the fact that the electromechanical coupling constant K^2 is small compared to unity. It is this parameter which governs the rate of interchange of energy, both between the electrons and the sound wave, and between the various harmonic components of the sound wave. Because $K^2 \ll 1$ (~ 0.04 for CdS), this rate of energy interchange is slow in the sense that over a distance comparable to the wavelength of the acoustic wave or over a time comparable to the period of the acoustic wave, the change in amplitude of the various harmonic components of the sound wave will be small. The mathematical technique applicable to this sort of situation is known as the Bogoliubov-Krylov (B-K) technique or more commonly the method of slowly varying amplitude and phase.(2)

Taking the Fourier transform of equation (3.5) we see that the Fourier coefficients f_m are given by:

$$f_m(x, t) = \frac{1}{2\pi} \int_{-\pi}^{\pi} f(x, t, \theta)\ e^{-im\theta} d\theta$$

$$= \langle f(x, t, \theta)\ e^{-im\theta} \rangle \qquad (3.6)$$

In this equation and henceforth throughout the paper, we shall use angle brackets to denote a phase average.

For a nearly periodic lattice displacement, we define the average total energy density and average total flux by $W = \langle W_{in} \rangle$ and $\Phi = \langle \Phi_{in} \rangle$. If we neglect the variation of the Fourier coefficients f_m, then we have $\frac{\partial}{\partial t} = -\frac{\omega \partial}{\partial \theta}$ and $\frac{\partial}{\partial x} = \frac{\omega}{v_s} \frac{\partial}{\partial \theta}$. Working to this approximation and using the fact that the strain $S = \frac{\partial u}{\partial x} = \frac{\omega}{v_s} \frac{\partial \mathbf{a}}{\partial \theta}$ we have from (3.2) and (3.3) that

$$W = c \langle S^2 \rangle = \Phi / v_s \qquad (3.7)$$

Averaging the energy equation (3.4) and using (3.7) we find

$$\frac{\partial \Phi}{\partial t} + v_s \frac{\partial \Phi}{\partial x} = v_s \alpha \Phi \qquad (3.8)$$

where $\alpha = -\dfrac{\omega e \langle S \frac{\partial E}{\partial \theta} \rangle}{\Phi} = \dfrac{\langle E (\omega e \frac{\partial S}{\partial \theta}) \rangle}{\Phi}$ is (3.9)

the flux gain constant (by consideration of a stationary situation such that $\partial \Phi / \partial t = 0$ it is clear that α describes the spatial growth of the total

flux Φ). The final equality in equation (3.9) follows on integration by parts.

Corrections to (3.8) resulting from the variation of the Fourier coefficients may be verified to be of a higher order in the piezoelectric coupling constant.

Let us now turn to the harmonic gain α_m^c which determines the propagation of the m^{th} harmonic component of the strain. By substituting the Fourier expansions of the strain S and electric field E into the wave equation (3.1), and retaining only the first derivatives of the slowly varying coefficients, we obtain the equation governing the propagation of the m^{th} harmonic of the strain S. This is easily found to be

$$\frac{\partial S_m}{\partial t} + v_s \frac{\partial S_m}{\partial x} = v_s \alpha_m^c S_m \tag{3.10}$$

where $$\alpha_m^c = - \frac{2(-im\omega e S_m)^* E_m}{2 \Phi_m} \tag{3.11}$$

is the complex gain constant of the m^{th} harmonic of the strain and we shall write $\alpha_m^c = \alpha_m + i\Delta k_m$, where α_m is the real gain constant of $|S_m|$, and Δk_m is the corresponding change in the wave number of S_m produced by the piezoelectric coupling. α_m^c therefore automatically includes the dispersion of the acoustic wave as well as it growth. $\Phi_m = 2 c v_s |S_m|^2$ is the acoustic flux carried by the m^{th} harmonic of the strain S_m. The asterisk denotes complex conjugation and the right hand side of equation (3.11) has been written in a form which we shall use subsequently to relate the acoustic gain to power dissipation from the electron system.

It is not difficult to see from (3.7) that

$$\Phi = \sum_{m=1}^{\infty} \Phi_m \tag{3.12}$$

where the equality follows on using Parseval's theorem[3]. Hence, the total flux is just the sum of the fluxes carried by each harmonic. Also, from (3.9) it immediately follows on using (3.11) that

$$\alpha = \frac{1}{\Phi} \sum_{m=1}^{\infty} 2\,\alpha_m\,\Phi_m \tag{3.13}$$

We therefore see that the total flux gain which describes the growth of acoustic power in a material is just the average of the power gain coefficients of the individual harmonics each weighted in accordance with their contribution to the total flux.

From equations (3.9) and (3.11), we see that both α and α_m^c are determined when the electric field and strain distributions are known. Since we are attempting to find the dependence of acoustic gain on the space charge modulation which accompanies the acoustic wave, we must therefore relate the electric field and strain to the space charge distribution. We do this in the following section by using the space charge equations.

3.3 The Space Charge Equations and Relations Between Fourier Coefficients

The electric field E and the strain S are related to the electron density n by the space charge equations. These are the equation of current continuity, Poisson's equation, and the constitutive relation, which have already been introduced in Chapter 2. We have:

$$I(t) = nq\mu E - qD_n \frac{\partial n}{\partial x} + \frac{\partial D}{\partial t} \tag{3.14}$$

$$\frac{\partial D}{\partial x} = q\,(n-n_o) \tag{3.15}$$

$$D = \epsilon E - eS \tag{3.16}$$

Most of the notation has been defined in Chapter 2. In the present context however, the equation of current continuity will be used in its integrated form (3.14), which follows from (2.22) on integrating with respect to x and using (2.23). I(t), the constant of integration, is the total current density.

Because we shall use the expressions derived for E and S in the right hand sides of equations (3.8) and (3.10), we need only work to zeroth order here and drop all derivatives of slowly varying quantities. Owing to the smallness of the piezoelectric coupling constant on the right hand side of (3.8) and (3.10), the retention of derivatives of the Fourier amplitudes of E and S would lead to only small corrections to the results. In this approximation therefore we may use the relations $\frac{\partial}{\partial x} = \frac{\omega}{v_s} \frac{\partial}{\partial \theta}$, and $\frac{\partial}{\partial t} = -\omega \frac{\partial}{\partial \theta}$. When these relations are used in (3.14), we find that the electric displacement D can be eliminated with the aid of (3.15), to yield the following expression for E in terms of n.

$$E = E_s \left[1 - \left(1 - \frac{I}{I_S} \right) \frac{n_o}{n} + \frac{\omega}{\omega_D} \frac{\partial}{\partial \theta} \log \frac{n}{n_o} \right] \tag{3.17}$$

where $E_s = v_s/\mu$ is the synchronous field, $I_s = qn_o v_s$ is the synchronous current density, and $\omega_D = v_s^2 / D_n$ is the frequency characteristic of diffusion introduced in Chapter 2. We note that since the right hand side of (3.14) is a function of θ alone in the zeroth order approximation, I(t) must have a time independent value I.

The total current density I appears on the right hand side of (3.17) as an independent variable. It is more usual to employ the local d.c. electric field $E_o = \langle E \rangle$ as the independent variable instead of I. The relation between E_o and I is easily obtained by averaging (3.17) over θ and using the periodicity of n to obtain

$$E_o = E_s \left[1 - (1 - \frac{I}{I_s}) \left\langle \frac{n_o}{n} \right\rangle \right] \tag{3.18}$$

When this equation is solved for the total current density I, so that E_o appears as the independent variable, it takes on the physically more transparent form.

$$I = \sigma E_o (1-F) + F I_s \tag{3.19}$$

where $\sigma = n_o q \mu$ is the conductivity of the material and

$$F = 1 - \left\langle \frac{n_o}{n} \right\rangle^{-1} \tag{3.20}$$

The interpretation of the factor F is clear. The total current density I behaves as if a fraction F of the electrons were trapped at the sound velocity, while the rest exhibit the normal ohmic response to the local d.c. electric field. In this sense, we shall refer to F as the "trapping factor'. Such a factor has been introduced previously from a phenomenological standpoint[4]. We see here that F emerges naturally in the present analysis. The trapping factor F should not be confused with the trapping factor governing the removal of carriers from the conduction process by trapping into localised electronic states[5]. We shall discuss the properties of F presently.

When (3.18) or (3.19) is used to eliminate I from (3.17), we arrive at the required final expression for E in terms of n and E_o. We find

$$E = E_o + E' \tag{3.21}$$

where the a.c. electric field E' is given by

$$E' = E_s \left[\gamma \left(1 - \frac{n^{-1}}{\langle n^{-1} \rangle} \right) + \frac{\omega}{\omega_D} \frac{\partial}{\partial \theta} \log \frac{n}{n_o} \right] \tag{3.22}$$

where as before $\gamma = 1 - E_o/E_s$. By taking the Fourier transform of (3.22) we find that the Fourier coefficients of the a.c. electric field are

$$E_m = \langle E' e^{-im\theta} \rangle = \frac{E_s \omega_c}{\omega'_{cm}} \left(\gamma + \frac{im\omega}{\omega'_{Dm}} \right) \frac{n_m}{n_o} \tag{3.23}$$

$$m \geq 1$$

where $n_m = \langle n e^{-im\theta} \rangle$, $\omega_c = \sigma/\epsilon$ and

$$\omega'_{cm} = -\omega_c \frac{n_m}{n_o} \frac{\langle n^{-1} \rangle}{\langle n^{-1} \exp(-im\theta) \rangle} \tag{3.24}$$

$$\omega'_{Dm} = -\omega_D \frac{\langle n^{-1} \exp(-im\theta) \rangle}{\langle n^{-1} \rangle \langle \log(\frac{n}{n_o}) \exp(-im\theta) \rangle} \tag{3.25}$$

The frequencies ω'_{cm} and ω'_{Dm} (which are in general complex), have been defined in order to simplify the discussion of acoustic gain. Their significance will be discussed in due course. Equations (3.22) and (3.23) are the desired expressions giving the electric field in terms of the space charge n.

The expression of the strain S in terms of n is trivial in the same approximation. The d.c. component of strain must vanish if the lattice displacement is to be nearly periodic. Consequently, from (3.11) we have immediately that $D_o = \epsilon E_o$. This relation may be used to determine the arbitrary constant which arises when equation (3.15) is integrated to find D. By inserting the result of the integrating into the constitutive relation (5.16), we obtain the desired result for the strain:

$$S = \frac{\epsilon}{e}\left[E' - E_s \quad \frac{\omega_c}{\omega}(N - \langle N\rangle)\right] \tag{3.26}$$

where

$$N(x, t, \theta) = \int_o^{\theta}\left[\frac{n(x,t,\theta')}{n_o} - 1\right] d\theta' \tag{3.27}$$

is the integrated fractional excess electron density. It is easily seen that N is periodic since from (3.15)

$\langle n\rangle = n_o + \left\langle \frac{\partial D/\partial x}{q} \right\rangle = n_o$ and so from (3.27),

$$N(x,t,\theta + 2\pi) - N(x,t,\theta) = 2\pi\left(\frac{\langle n\rangle}{n_o} - 1\right) = 0.$$

From (3.26) it is also obvious that the d.c. component of the strain S is zero. The Fourier coefficients of the strain follows simply from (3.26) and (3.27) on integrating by parts. We find

$$S_m = \frac{\epsilon}{e}\left[E_m + \frac{iE_s\,\omega_c}{m\omega}\,\frac{n_m}{n_o}\right], \quad m \geq 1 \tag{3.28}$$

Finally, using (3.7) in conjunction with (3.26) and (3.22) we may relate the total acoustic flux Φ to the space charge distribution. We find

$$\Phi = \frac{v_s \epsilon E_s^2}{K^2}\left\langle\left[\gamma\left(1 - \frac{n^{-1}}{\langle n^{-1}\rangle}\right) + \frac{\omega}{\omega_D}\,\frac{\partial}{\partial\theta}\log\frac{n}{n_o}\right.\right.$$

$$\left.\left. + \frac{\omega_c}{\omega}\,(\langle N\rangle - N)\right]^2\right\rangle \tag{3.29}$$

where $K^2 = e^2/\epsilon c$ is the electromechanical coupling constant.

3.4 Acoustic Gain and Acoustoelectric Current

We are now in a position to evaluate the acoustic gain by combining the results of sections 3.2 and 3.3. The formula (3.11) for the complex gain α_m^c is written in a particularly transparent form. In the numerator we find $-im\omega eS_m$ which, by inspection of equation (3.14), is just the Fourier coefficient of the contribution to the total current density I from the piezoelectric part of the displacement current density $-e\partial S/\partial t$. Thus, the numerator in (3.11) is just the complex power dissipated by the m^{th} harmonic of the piezoelectric contribution to the total current. We also see from (3.14) that, since the dielectric part $\epsilon\partial E/\partial t$ of the displacement current density is in quadrature with E, and since the total a.c. current density is zero, the real part of the numerator in (3.11)

is just the real power dissipated by the m^{th} harmonic of the particle current density $j = nq\mu E - qD_n \partial n/\partial x$. The formula (3.9) may be similarly related to power dissipation by the electron system.

To obtain the desired final formula for α_m^c in terms of n, we need only substitute for S_m and E_m in (3.11) from (3.23) and (3.28). Thus we obtain

$$\alpha_m^c = \frac{-i K^2 m\omega \left(\gamma + \frac{im\omega}{\omega'_{Dm}}\right)}{2v_s \left[\gamma + i\left(\frac{\omega'_{cm}}{m\omega} + \frac{m\omega}{\omega'_{Dm}}\right)\right]} \tag{3.30}$$

We shall postpone a detailed discussion of this result until the next section.

Using equation (3.9) we may derive a formula for the total flux gain α in terms of the space charge density. Equations (3.15) and (3.16) may be employed to eliminate $\frac{\partial S}{\partial \theta}$ from (3.9) with the result that

$$\alpha = -\frac{qv_s}{\Phi} \left(\langle nE \rangle - n_o E_o\right) \tag{3.31}$$

From (3.14) and (3.19) this may be rewritten as

$$\alpha = -\frac{E_s}{\Phi} \left(I - \sigma E_o\right) = -\frac{E_s I_s \gamma F}{\Phi} \tag{3.32}$$

Equation (3.32) is the desired result, since the trapping factor F and the total flux Φ are given in terms of the electron density by equations (3.20) and (3.29).

The acoustoelectric current density is defined as the difference between the total current density and the ohmic current density

i.e.

$$I_{ae} = I - \sigma E_o \tag{3.33}$$

From (3.32) it follows immediately that

$$I_{ae} = I_s \gamma F \tag{3.34}$$

Consequently, the numerator in the right hand side of (3.32) has a formal interpretation as the power density dissipated by the acoustoelectric current in the synchronous field. We may also rewrite equation (3.32) in the form

$$I_{ae} = - \alpha \Phi / E_s \tag{3.35}$$

This is the Weinreich relation,[6] relating the acoustoelectric current to acoustic gain. Previous proofs[7] of this result have relied on the result of White's linear theory. The present analysis provides a rigorous justification of the relation for acoustic waves of arbitrary amplitude and harmonic content. We note here that the α appearing in (3.35) is the power gain of the total flux Φ. By use of (3.13) we may write

$$I_{ae} = - \sum_{m=1}^{\infty} \frac{2\alpha_m \Phi_m}{E_s} = \sum_{m=1}^{\infty} I_{ae}^m \tag{3.36}$$

i.e. the total acoustoelectric current is composed of the sum of the acoustoelectric currents produced by the individual harmonics.

3.5 Discussion

We must now consider the interpretation, significance and application of the results derived in the preceeding sections.

We consider first the expression (3.19) for the total current density in terms of the d.c. field E_0 and the trapping factor F defined by equation (3.20). First, it is easy to show that $0 \leq F \leq 1$. That $F \leq 1$ follows immediately from (3.20) since the electron density $n \geq 0$. Moreover, from Schwartz's inequality[8],

$$\langle n/n_0 \rangle \langle n_0/n \rangle \geq \langle (n/n_0)^{\frac{1}{2}} (n_0/n)^{\frac{1}{2}} \rangle^2 = 1 \qquad (3.32)$$

so that $\langle n_0/n \rangle \geq \langle n/n_0 \rangle^{-1}$. We have already seen that $\langle n \rangle = n_0$, so that we have $\langle n_0/n \rangle \geq 1$ and hence from (3.20), $F \geq 0$. These inequalities lend support to the formal interpretation of F as the effective fraction of electrons which are trapped at the sound velocity, which is suggested by (3.19). It is also clear from (3.20), that $F \to 0$ at small signal levels when $n \to n_0$, and that $F \to 1$ at large signal levels when the electrons are tightly 'bunched' with regions of nearly complete depletion between the bunches. This latter behaviour follows from an examination of the integral involved in (3.20). Also, as the electron distribution varies from the small signal regime to the tightly bunched regime, we see that the total current density changes progressively from the ohmic value σE_0 to the saturated value I_s. By inspection of the integrals involved in equation (3.29) for the total flux Φ, it is possible to deduce that as the electron distribution becomes more tightly bunched, the flux Φ increases. This will be made more obvious in the next chapter where we shall consider specific electron distributions. Because of this, we may conclude that as the amplitude of the acoustic wave increases, i.e. Φ increases, the electrons bunch more tightly leading to current saturation. We shall discuss this aspect further in Chapter 5.

The formula (3.30) for the complex gain α_m^c is identical to the usual small signal formula (Chap. 2), except that the amplitude dependent frequencies ω'_{cm} and ω'_{Dm} appear in place of the constant frequencies ω_c and ω_D respectively. It was to achieve this simple identification with the small signal formula that ω'_{cm} and ω'_{Dm} were defined by the rather complicated formulae (3.24) and (3.25). The behaviour of ω'_{cm} and ω'_{Dm} is easier to determine than these formidable expressions might suggest. In the small signal limit when $n = n_o + n'$ where $|n'/n_o| \ll 1$ and $\langle n' \rangle = 0$, we find immediately on expansion of n^{-1} in (3.24) and (3.25) that $\omega'_{cm} = \omega_c$ and $\omega'_{Dm} = \omega_D$, (unless $\langle n' e^{-im\theta} \rangle = 0$, when the formulae become indeterminate). At intermediate and large signal levels, ω'_{cm} and ω'_{Dm} are in general complex. However, provided an origin for θ can be found about which n is a symmetrical function of θ then a simplification occurs. We see from (3.24) and (3.25) that ω'_{cm} and ω'_{Dm} take on the real values

$$\omega'_{cm} = \frac{-\omega_c \langle n \cos m\theta \rangle \langle n^{-1} \rangle}{n_o \langle n^{-1} \cos m\theta \rangle} \tag{3.38}$$

$$\omega'_{Dm} = \frac{-\omega_D \langle n^{-1} \cos m\theta \rangle}{\langle n^{-1} \rangle \langle \log \left(\frac{n}{n_o}\right) \cos m\theta \rangle} \tag{3.39}$$

where the phase averages are now understood to be taken over the range $0 \leq \theta \leq \pi$.

Clearly, in the small signal limit the electron density distribution is symmetric. In the large signal regime this need not be the case. However, if in the large signal regime the d.c. electric field is smaller than the a.c. electric field, then the electrons will become trapped in regions of potential minima and will tend to distribute themselves in a nearly symmetrical fashion in these minima. This case of strong

trapping is the one of practical interest. We shall therefore confine our subsequent discussion to this case in view of its relative simplicity. The total mechanical potential is drawn schematically below

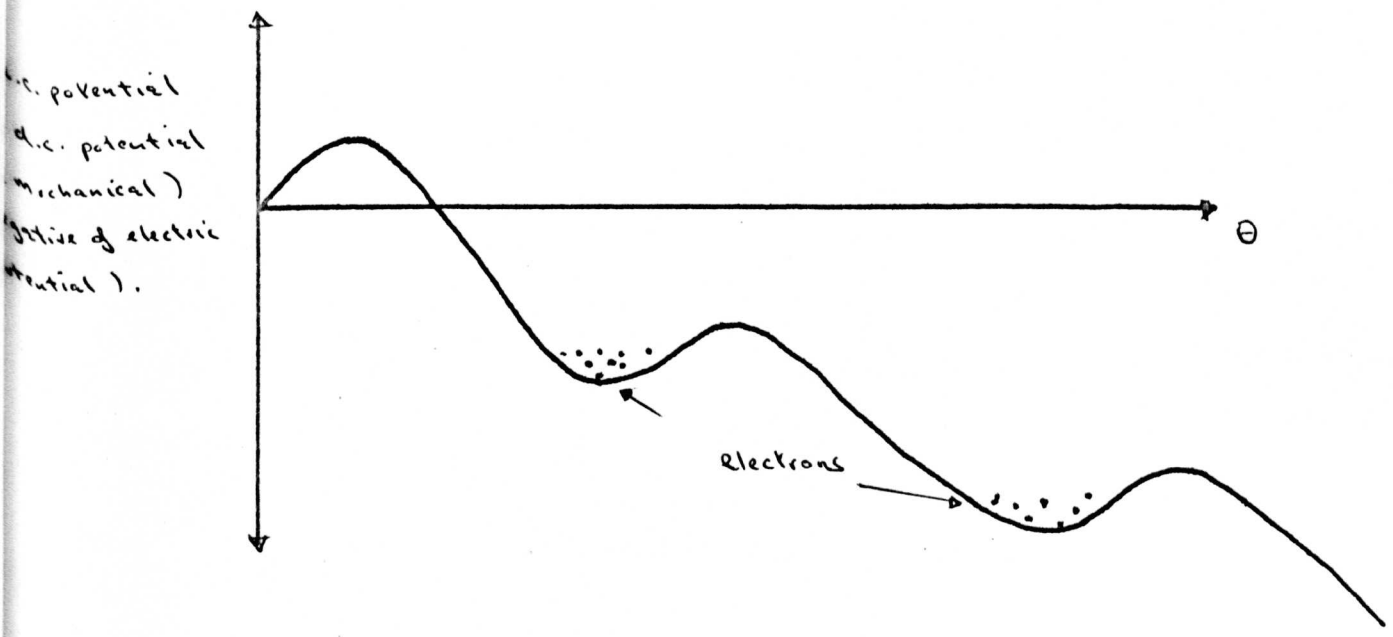

This 'staircase' model will be discussed further in Chapter 5 where we shall see the electron distribution to which it gives rise.

Since the electrons have a thermal energy which corresponds to an electric potential $k_B T/q$ where k_B is Boltzmann's constant and T is the absolute temperature, we should expect that the electrons will be trapped if $\phi_{ac} > \phi_{d.c} + k_B T/q$. In this case the electron distribution should be nearly symmetric.

From (3.30) we see that for a symmetrical space charge distribution since ω'_{cm} and ω'_{Dm} are real, the real gain and shift in wave vector at the m^{th} harmonic are given by

$$\alpha_m = \frac{-K^2 \omega'_{cm} \gamma}{2v_s \left[\gamma^2 + \left(\frac{\omega'_{cm}}{m\omega} + \frac{m\omega}{\omega'_{Dm}} \right)^2 \right]} \tag{3.40}$$

$$\Delta k_m = \frac{-K^2 m\omega \left(\gamma^2 + \frac{m\omega}{\omega'_{Dm}} \left(\frac{\omega'_{cm}}{m\omega} + \frac{m\omega}{\omega'_{Dm}} \right) \right)}{2 v_s \left[\gamma^2 + \left(\frac{\omega'_{cm}}{m\omega} + \frac{m\omega}{\omega'_{Dm}} \right)^2 \right]} \tag{3.41}$$

These formulae are seen to be identical with the small signal results found in Chapter 2 except for the appearance of ω'_{cm} and ω'_{Dm} in place of ω_c and ω_D respectively.

From (3.40) we see that for a given space charge distribution and d.c. field, the maximum gain at the m^{th} harmonic of the strain occurs at the frequency

$$\omega = (\omega'_{cm}\, \omega'_{Dm})^{\frac{1}{2}}/m = \frac{(\omega_c \omega_D)^{\frac{1}{2}}}{m} \left[\frac{\langle n \cos m\theta \rangle}{n_o \langle \log \frac{n}{n_o} \cos m\theta \rangle} \right]^{\frac{1}{2}} \tag{3.42}$$

The behaviour of ω'_{cm}, ω'_{Dm} and α_m may be obtained fairly easily in the limit of strong electron bunching. If the electron distribution has roughly the form indicated below, then we see that

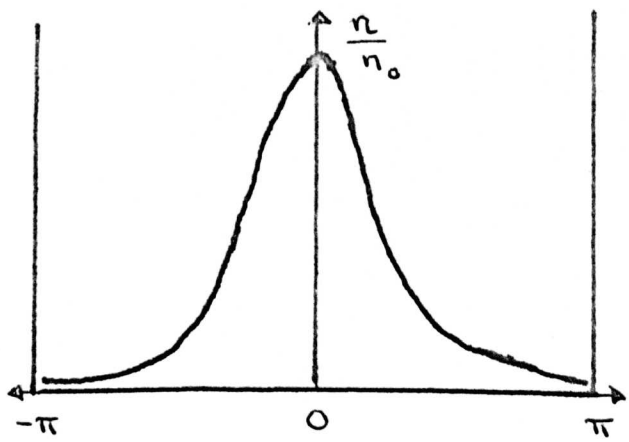

the most important contribution to the integral $\langle n \cos m\theta \rangle$ occurs at the origin, so that $\langle n \cos m\theta \rangle \simeq \langle n \rangle$. Similarly the most important contribution to $\langle n^{-1} \cos m\theta \rangle$ arises at $\theta = \pi$, so that $\langle n^{-1} \cos m\theta \rangle \simeq (-1)^m \langle n^{-1} \rangle$. In the same way because the logarithm varies most rapidly for small values of its argument we see that

$$\langle \log \frac{n}{n_o} \cos m\theta \rangle \simeq \langle \log \frac{n}{n_o} \rangle (-1)^m.$$

Hence approximately in the limit of strong bunching we have from (3.38) and (3.39) that $\omega'_{cm} \simeq \omega_c(-1)^{m-1}$ and $\omega'_{Dm} \simeq -\omega_D / \langle \log \frac{n}{n_o} \rangle \to 0$. Some care should be taken however in applying these arguments. Their validity depends on the rate at which the tails of the electron distribution reduce to zero. In some cases where the tails of distribution fall to zero slowly (an example is the exponential distribution to be dealt with in the next Chapter), the arguments used above break down and the results quoted are incorrect. However for a reasonably 'bunched' distribution they remain valid. Using the above results in (3.42) we find that for a tightly bunched distribution the peak of the m^{th} harmonic gain occurs at $\omega \simeq (\omega_c \omega_D)^{\frac{1}{2}} / (m \langle (-1)^m \log \frac{n}{n_o} \rangle^{\frac{1}{2}})$ which $\to 0$ for m odd as n bunches more strongly. Also from (3.40) we see that since $\omega'_{Dm} \to 0$, the bunching inceases, $\alpha_m \to 0$ i.e. the gain reduces. We therefore see that the two observed effects of non-linearities on acoustic gain i.e. gain reduction and shift in frequency of peak gain, are contained in the present theory.

Let us now consider the total flux gain α. From (3.32), we see that as the acoustic wave amplitude increases, so that Φ increases and the trapping factor $F \to 1$, $\alpha \to 0$. For a given space charge distribution, the peak of the total flux gain versus frequency curve in given by the solution of

$\left(\frac{\partial \alpha}{\partial \omega}\right)_n = 0$. From (3.32), this is identical with the solution of $\left(\frac{\partial \Phi}{\partial \omega}\right)_n = 0$ where the subscript n indicates that the differentiation is to be performed holding the electron distribution n fixed. From (3.29), we see that for a symmetric electron density distribution

$$\Phi = \frac{v_s \epsilon E_s^2}{K^2} \left[\gamma^2 \left(\frac{\langle n^{-2} \rangle}{\langle n^{-1} \rangle^2} - 1 \right) + \frac{\omega^2}{\omega_D^2} \left\langle \left(\frac{\partial}{\partial \theta} \log \frac{n}{n_o} \right)^2 \right\rangle \right.$$

$$\left. + \frac{\omega_c^2}{\omega^2} \langle N^2 \rangle + \frac{2\omega_c}{\omega_D} \left\langle (-N) \frac{\partial}{\partial \theta} \log \frac{n}{n_o} \right\rangle \right] \qquad (3.43)$$

where we have used the fact that for a symmetric distribution $\langle N \rangle = 0$. Differentiating (3.43) we find that the solution of $\left(\frac{\partial \Phi}{\partial \omega}\right)_n = 0$ is given by

$$\omega_{pk} = (\omega_c \omega_D)^{\frac{1}{2}} \left[\frac{\langle N^2 \rangle}{\left\langle \left(\frac{\partial \log \frac{n}{n_o}}{\partial \theta} \right)^2 \right\rangle} \right]^{\frac{1}{4}} \qquad (3.44)$$

We may similarly derive the peaks on the gain versus γ (or d.c. field) curve by differentiation of (3.43) for a given symmetric space charge distribution. We find

$$\gamma_{pk} = \pm \frac{\left[\frac{\omega_c^2}{\omega^2} \langle N^2 \rangle + \frac{\omega^2}{\omega_D^2} \left\langle \left(\frac{\partial \log \frac{n}{n_o}}{\partial \theta} \right)^2 \right\rangle + \frac{2\omega_c}{\omega_D} \left\langle (-N) \left(\frac{\partial \log \frac{n}{n_o}}{\partial \theta} \right) \right\rangle \right]^{\frac{1}{2}}}{\left(\frac{\langle n^{-2} \rangle}{\langle n^{-1} \rangle^2} - 1 \right)^{\frac{1}{2}}}$$

(3.45)

In the small signal limit, if $n = n_o + n'$ where $|n'/n_o| << 1$, (3.44) becomes

$$\omega_{pk} = (\omega_c \omega_D)^{\frac{1}{2}} \left[\frac{\left\langle \left(\int_o^\theta n'(\theta')\, d\theta' \right)^2 \right\rangle}{\left\langle \left(\frac{dn'}{d\theta} \right)^2 \right\rangle} \right]^{\frac{1}{4}} \qquad (3.46)$$

For $n' = n' \cos\theta$, (3.46) yields the expected result $\omega_{pk} = (\omega_c \omega_D)^{\frac{1}{2}}$. For other small signal distributions (3.46) yields results which may differ fractionally from $(\omega_c \omega_D)^{\frac{1}{2}}$. Similar results are obtained for the γ at which peak gain occurs. For $n'(\theta) = n' \cos\theta$ we find $\gamma_{pk} = \pm \left(\frac{\omega_c}{\omega} + \frac{\omega}{\omega_D} \right)$, with slight deviations from this for other distributions.

Although we have derived the above results for a given space charge distribution, the formulae remain the same if the total flux is given provided that the space charge distribution is specified by one parameter. In this case fixed space charge implies fixed flux and vice versa. We note here that a specification of the total flux alone does not allow the various gains to be determined. This is because a variety of space charge distributions can correspond to the same total flux. The various acoustic gains depend on the Fourier components of the space charge and these are not uniquely determined from a knowledge of the total flux. In this sense then, flux is a 'coarse' variable.

Finally, we note that in the non-linear regime, all the field variables do not have the same gain constants as is the case in the linear theory. This becomes clear when one considers a stationary situation where we have $\alpha_m^c = \frac{\partial S_m / \partial x}{S_m}$. If S_m is a linear function of say n_m then $\frac{\partial S_m / \partial x}{S_m}$ will equal $\frac{\partial n_m / \partial x}{n_m}$. However if S_m is

a nonlinear function of n_m this will no longer be true.

A physical interpretation of the gain reduction and frequency shift will be given in Chapter 6. In the next chapter, we shall apply the results developed here to specific electron distributions.

References Chapter 3

1. Butcher, P.N. and Ogg, N.R., (1969), Brit. J. Appl. Phys.

2. Minorsky, N., (1962), Nonlinear Oscillations (Van Nostrand).

3. Woodward, P.M., (1953), Probability and Information Theory with Applications to Radar, (Pergamon).

4. Hobson, G.S., and Paige, E.G.S., (1966), Proc. Int. Conf. Phys. of Semiconductors, Kyoto, 464.

5. White, D.L., (1962), J. Appl. Phys. 33, 2547.

6. Weinreich, G., (1956), Phys. Rev. 104, 321.

7. McFee, J.H. and Tien, P.K., (1966), J. Appl. Phys. 37, 2754.

8. Courant, R., (1957), Differential and Integral Calculus (Blackie).

Chapter 4

THE NON LINEAR THEORY OF ACOUSTOELECTRIC GAIN II - MODEL SPACE CHARGE DISTRIBUTIONS

4.1 Introduction

In this Chapter we shall examine and evaluate the results obtained in the general theory of non-linear acoustoelectric gain given in Chapter 3. We obtained there formulae for acoustic gain, acoustoelectric current etc. in terms of the electron density distribution accompanying the acoustic wave. In order to evaluate the formulae therefore, we require a knowledge of the electron density distribution. In the framework of the present theory, the electron density n is to be treated as an independent variable. This may seem inconsistent at first sight since one might imagine that the equations governing the growth of acoustic waves in a piezoelectric semiconductor should contain in them the information necessary to predict the electron density as well as the other variables. However, in a complete theory of acoustic gain, one would use these equations to describe the development of the field variables from some initial distribution subject to certain boundary conditions. Since the theory which has been developed is purely local, the requirement that the electron density distribution should be known is equivalent to the knowledge of initial conditions in a more complete theory. In order to use the theory, one must therefore guess at the form of the electron density distribution in the sort of situation which is under consideration. In a large amplitude acoustic wave one might expect that the electrons will tend to bunch in regions of minimum potential energy. One may therefore gain some insight into the behaviour of acoustic gain etc. for a large amplitude acoustic wave, by using a bunched form for the electron distribution in the formulae developed in Chapter 3. The actual detailed choice of the functional form of the electron density distribution is however, ultimately dictated by a compromise between the ease with which the integrals involved in the various formulae may be evaluated, and the realism of the distribution.

In the following sections of this Chapter, we shall consider three distributions, (a) the cosinusoidal distribution, (b) the exponential distribution, and (c) the Gaussian distribution. The cosinusoidal distribution (a) is of interest because it will be correct in the small signal limit, and has the advantage that all the integrals required may be performed analytically. The exponential distribution (b) also has this latter advantage and in addition gives one some insight into the strong bunching regime. The Gaussian distribution (c), as we shall see later, is the most realistic distribution in the large signal regime. Unfortunately, the integrals involved must now be performed numerically. However, the results for this case give considerable insight into the behaviour of the large signal acoustoelectric gain.

We collect below for easy reference the various formulae which we require to evaluate (for symmetric distributions).

$$F = 1 - \left\langle \frac{n_o}{n} \right\rangle^{-1} \tag{4.1}$$

$$\omega'_{cm} = \frac{-\omega_c \langle n \cos m\theta \rangle \langle n^{-1} \rangle}{n_o \langle n^{-1} \cos m\theta \rangle} \tag{4.2}$$

$$\omega'_{Dm} = \frac{-\omega_D \langle n^{-1} \cos m\theta \rangle}{\langle n^{-1} \rangle \langle \log \frac{n}{n_o} \cos m\theta \rangle} \tag{4.3}$$

$$\omega_{pk} = (\omega_c \omega_D)^{\frac{1}{2}} \left[\frac{\langle N^2 \rangle}{\left\langle \left(\frac{\partial \log \frac{n}{n_o}}{\partial \theta} \right)^2 \right\rangle} \right]^{\frac{1}{4}} \tag{4.4}$$

$$\gamma_{pk} = \pm \frac{\left[\frac{\omega_c^2}{\omega^2} \langle N^2 \rangle + \frac{\omega^2}{\omega_D^2} \left\langle \left(\frac{\partial \log \frac{n}{n_o}}{\partial \theta} \right)^2 \right\rangle \frac{2\omega_c}{\omega_D} \left\langle (-N) \frac{\partial \log \frac{n}{n_o}}{\partial \theta} \right\rangle \right]^{\frac{1}{2}}}{\left(\frac{\langle n^{-2} \rangle}{\langle n^{-1} \rangle^2} - 1 \right)^{\frac{1}{2}}} \qquad (4.5)$$

$$\alpha_m = \frac{- K^2 \omega'_{cm} \gamma}{2 v_s \left[\gamma^2 + \left(\frac{\omega'_{cm}}{m\omega} + \frac{m\omega}{\omega'_{Dm}} \right)^2 \right]} \qquad (4.6(a))$$

$$\alpha = \frac{-E_s I_s \gamma F}{\Phi} \qquad (4.6(b))$$

$$\Phi = \frac{v_s \epsilon E_s^2}{K^2} \left[\gamma^2 \left(\frac{\langle n^{-2} \rangle}{\langle n^{-1} \rangle^2} - 1 \right) + \frac{\omega^2}{\omega_D^2} \left\langle \left(\frac{\partial}{\partial \theta} \log \frac{n}{n_o} \right)^2 \right\rangle \right.$$

$$\left. + \frac{\omega_c^2}{\omega^2} \langle N^2 \rangle + 2 \frac{\omega_c}{\omega_D} \left\langle (-N) \frac{\partial}{\partial \theta} \log \frac{n}{n_o} \right\rangle \right] \qquad (4.7)$$

$$\text{where } N = \int_o^\theta \left(\frac{n(\theta')}{n_o} - 1 \right) d\theta' \qquad (4.8)$$

If γ_{pk} and Φ are evaluated at frequency $\omega = \omega_{pk}$ they become

$$\gamma_{pk} = \pm \frac{\left(2\frac{\omega_c}{\omega_D}\right)^{\frac{1}{2}} \left[\left(\langle N^2\rangle \langle(\frac{\partial}{\partial\theta} \log \frac{n}{n_o})^2\rangle\right)^{\frac{1}{2}} + \left\langle (-N)\frac{\partial}{\partial\theta} \log \frac{n}{n_o}\right\rangle\right]^{\frac{1}{2}}}{\left(\frac{\langle n^{-2}\rangle}{\langle n^{-1}\rangle^2} - 1\right)^{\frac{1}{2}}} \qquad (4.9)$$

and $$\Phi = \frac{v_s \epsilon E_s^2}{K^2} \left[\gamma^2 \left(\frac{\langle n^{-2}\rangle}{\langle n^{-1}\rangle^2} - 1\right) + \frac{2\omega_c}{\omega_D}\left(\left(\langle N^2\rangle \langle(\frac{\partial}{\partial\theta} \log \frac{n}{n_o})^2\rangle\right)^{\frac{1}{2}} + \langle(-N)\frac{\partial}{\partial\theta} \log \frac{n}{n_o}\rangle\right)\right] \qquad (4.10)$$

The various integrals required are:

$$\langle n^{-1}\rangle, \langle n \cos m\theta\rangle, \langle n^{-1} \cos m\theta\rangle, \langle \log \frac{n}{n_o} \cos m\theta\rangle,$$

$$N, \langle N^2\rangle, \langle(\frac{\partial}{\partial\theta} \log \frac{n}{n_o})^2\rangle, \langle(-N)\frac{\partial}{\partial\theta} \log \frac{n}{n_o}\rangle, \langle n^{-2}\rangle.$$

where $\langle \text{---} \rangle = \frac{1}{\pi} \int_o^{\pi} \text{---}\, d\theta$

4.2 The Cosinusoidal Distribution

In this section we shall consider the electron density distribution given by $\frac{n}{n_o} = 1 + a \cos\theta$. This is illustrated below

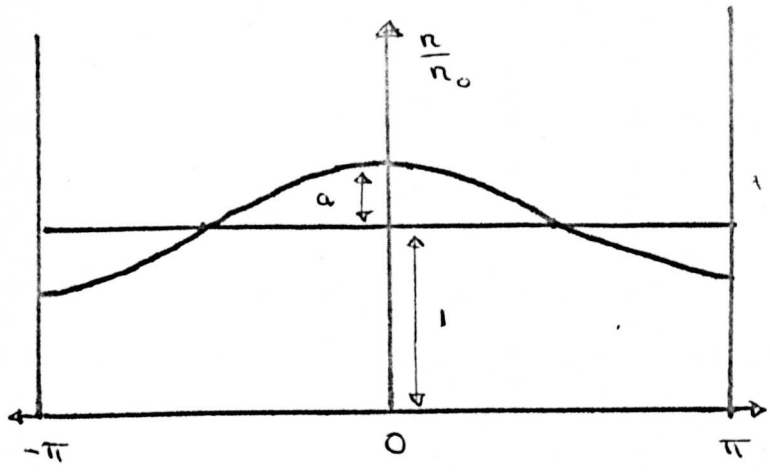

Clearly, if a = 1 this distribution will just reach complete depletion at $\theta = \pm \pi$. Also we see that $\left\langle \frac{n}{n_o} \right\rangle = 1$.

The various integrals listed above are given below for the cosinusoidal distribution. A detailed evaluation of some of the more troublesome integrals is given in Appendix 3.1.

$$\langle n^{-1} \rangle = \frac{1}{n_o \pi} \int_o^{\pi} \frac{d\theta}{1 + a \cos\theta} = \frac{1}{n_o \sqrt{1 - a^2}} \qquad (4.11)$$

$$\langle n \cos m\theta \rangle = \frac{n_o}{\pi} \int_o^{\pi} \cos m\theta \, (1 + a \cos\theta) \, d\theta = \frac{1}{2} a n_o \, \delta_{m,1} \qquad (4.12)$$

$$\langle n^{-1} \cos m\theta \rangle = \frac{1}{n_o \pi} \int_o^{\pi} \frac{\cos m\theta \, d\theta}{1 + a \cos\theta} = \frac{\left(\sqrt{1-a^2} - 1\right)^m}{n_o a^m \sqrt{1 - a^2}} \qquad (4.13)$$

$(m = 0, 1, 2, \ldots.)$

$$\left\langle \log \frac{n}{n_o} \cos m\theta \right\rangle = \frac{1}{\pi} \int_o^{\pi} \cos m\theta \log (1 + a \cos\theta) \, d\theta$$

$$= \frac{a}{m\pi} \int_o^{\pi} \frac{\sin\theta \sin m\theta \, d\theta}{1 + a \cos\theta}$$

$$= -\frac{1}{m a^m} \left[\sqrt{1 - a^2} - 1\right]^m \qquad (m = 1, 2, 3 \ldots..) \qquad (4.14)$$

$$N = a \sin\theta \tag{4.15}$$

$$\langle N^2 \rangle = a^2/2 \tag{4.16}$$

$$\left\langle \left(\frac{\partial}{\partial\theta} \log \frac{n}{n_o}\right)^2 \right\rangle = \frac{a^2}{\pi} \int_o^{\pi} \frac{\sin^2\theta \, d\theta}{(1 + a\cos\theta)^2} = \frac{1 - \sqrt{1-a^2}}{\sqrt{1 - a^2}} \tag{4.17}$$

$$\left\langle - N \frac{\partial}{\partial\theta} \log \frac{n}{n_o} \right\rangle = \frac{a^2}{\pi} \int_o^{\pi} \frac{\sin^2\theta \, d\theta}{1 + a\cos\theta} = 1 - \sqrt{1 - a^2} \tag{4.18}$$

$$\langle n^{-2} \rangle = \frac{1}{\pi n_o^2} \int_o^{\pi} \frac{d\theta}{(1 + a\cos\theta)^2} = \frac{1}{n_o^2 (1-a^2)^{3/2}} \tag{4.19}$$

We therefore have for this distribution, using these results in the formulae (4.1)-(4.8).

$$F = 1 - \sqrt{1 - a^2} \tag{4.20}$$

$$\omega'_{c_1} = \omega_c \left(1 - \tfrac{1}{2}F\right), \quad \omega'_{cm} = 0, \; m \neq 1 \tag{4.21}$$

$$\omega'_{Dm} = m\omega_D \tag{4.22}$$

$$\omega_{pk} = (\omega_c \omega_D)^{\frac{1}{2}} \left[\frac{a^2 \sqrt{1 - a^2}}{2(1 - \sqrt{1 - a^2}} \right]^{\frac{1}{4}} \tag{4.23}$$

$$\gamma_{pk} = \pm \left[\frac{\omega_c^2}{\omega^2} \frac{a^2 \sqrt{1-a^2}}{2(1-\sqrt{1-a^2})} + \frac{\omega^2}{\omega_D^2} + \frac{2\omega_c}{\omega_D} \sqrt{1 - a^2} \right]^{\frac{1}{2}} \tag{4.24}$$

$$\Phi = \frac{v_s \epsilon E_s^2}{K^2} \quad \frac{(1 - \sqrt{1-a^2})}{\sqrt{1 - a^2}} \left[\gamma^2 + \frac{\omega^2}{\omega_D^2} + \frac{\omega_c^2}{\omega^2} \frac{(1+\sqrt{1-a^2})\sqrt{1-a^2}}{2} + \frac{2\omega_c}{\omega_D}\sqrt{1-a^2} \right]$$

(4.25)

$$\alpha_1 = \frac{- K\gamma^2 \omega_c \left(1 - \frac{1}{2} F\right)}{2v_s \left[\gamma^2 + \left(\frac{\omega_c(1-\frac{1}{2}F)}{\omega} + \frac{\omega}{\omega_D} \right)^2 \right]} ; \quad \alpha_m = 0, \; m \neq 1 \qquad (4.26)$$

$$\alpha = -\frac{\omega_c \gamma K^2}{v_s} \quad \frac{\sqrt{1 - a^2}}{\left[\gamma^2 + \frac{\omega^2}{\omega_D^2} + \frac{(1 + \sqrt{1-a^2})\sqrt{1 - a^2}}{2} \frac{\omega_c^2}{\omega^2} + \frac{2\omega_c}{\omega_D}\sqrt{1-a^2} \right]}$$

(4.27)

The formulae (4.20)-(4.27) give the salient results for the cosinusoidal distribution. For $a \to 0$ the usual small signal results are recovered. For $a \to 1$ however the effects of nonlinearity make themselves felt. It is clear from (4.20) that as $a \to 1$, the trapping factor $F \to 1$, so that the total current density becomes equal to the synchronous current density in this limit. From (4.21) we see that $\omega'_{cm} = 0$ for $m \neq 1$. This means that there is no gain or loss at any harmonic other than the first. For $m = 1$, we see that as $a \to 1$, $\omega'_{c_1} \to \frac{1}{2}\omega_c$. Since $\omega_{D1} = \omega_D$ from (4.22) this means that in the limit $a = 1$ the frequency of peak fundamental gain is reduced to $(\omega_c\omega_D)^{\frac{1}{2}} / \sqrt{2}$. From (4.23) however,

we see that the frequency of peak total gain is reduced to zero as $a \to 1$. The magnitude of the fundamental gain also decreases as a increases provided $\left(\frac{\omega_c}{\omega}\right)^2 < \left(\frac{\omega}{\omega_D}\right)^2 + \gamma^2$. For the high d.c. field case, ($\gamma >> \frac{\omega_c}{\omega} + \frac{\omega}{\omega_D}$), the fundamental gain α_1 is proportional to ω'_{c1} and decreases by 50% as a increases from 0 to 1. From (4.27) we see that the total gain α decreases to zero as $a \to 1$. The apparent discrepancy between the behaviour of α_1 and α is resolved by noting that for this distribution from (3.13), $\alpha = 2\alpha_1 \Phi/\Phi$ so that α and α_1 need not have the same behaviour. As $a \to 1$ we also see that $\gamma_{pk} \to \pm \omega/\omega_D$.

Experiments[1],[2] have indicated that the reduction in the frequency of peak can be as much as a factor of 10. Simultaneous measurements of the d.c. electric field, acoustic flux and frequency of peak gain in an acoustic domain have been performed recently by Zucker, et al[3]. We shall use their estimates for comparison. Typical values of the various parameters used by these authors are collected below in table 4.1, although there seems to be some uncertainty in the accuracy of the measurements.

Table 4.1

v_s	ϵ	E_s	K^2	ω_c	ω_D	γ	Φ	$R^{-1} = \frac{\omega_{pk}}{(\omega_c \omega_D)^{\frac{1}{2}}}$
1.75×10^3 m/sec	8.8×10^{-11} farad/m	6×10^4 v/m	4×10^{-2}	1.6×10^{11} sec^{-1}	4.2×10^9 sec^{-1}	-5	~ a few Kwatt/cm^2	$\frac{1}{4}$

From (4.25) and (4.23) a reduction in the frequency of peak gain by a factor R occurs when the flux

$$\Phi = \frac{v_s \epsilon E_s^2}{K^2} \left[\frac{1}{2} \gamma^2 R^2 + \frac{\omega_c}{\omega_D} \right] R^2 . \qquad (4.28)$$

Using the parameter values given in table 4.1 we find that $\Phi \simeq 5 \times 10^7$ watt/m^2 = 5 kW/cm^2 which is about the order of magnitude observed according to table 4.1. From R = 4 we find from (4.23) that $a \simeq 1\text{-}2 \times 10^{-5}$.

4.3 The Exponential Distribution

We shall now consider the exponential electron density distribution given by $\frac{n}{n_o} = ae^{-b|\theta|}$. This is illustrated in the diagram below

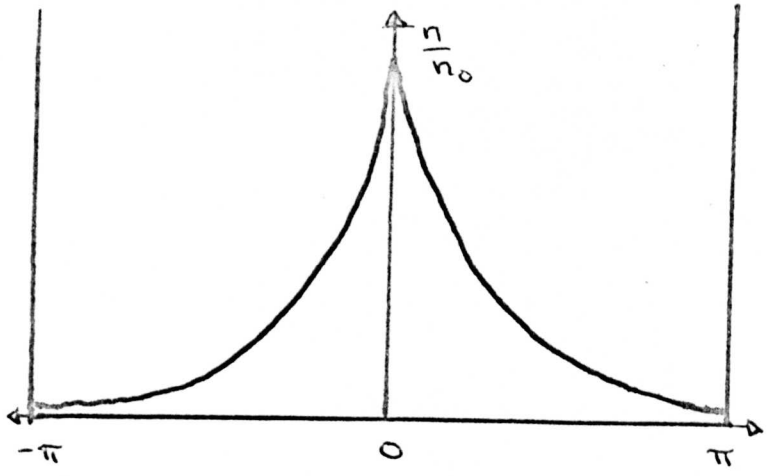

The condition $\left\langle \frac{n}{n_o} \right\rangle = 1$ yields $a = b\pi/(1-\exp(-b\pi))$. This distribution has the twofold advantage that the integrals involved may be performed analytically and at the same time the distribution approximates more closely than the cosinusoid to the 'strongly bunched' case. As the 'bunching' parameter b increases, the electrons bunch more tightly and the distribution becomes higher and narrower.

For this distribution then the various integrals required are listed below

$$\langle n^{-1} \rangle = \frac{1}{n_o a\pi} \int_o^{\pi} e^{b\theta} d\theta = \frac{1}{n_o a\pi b} (e^{b\pi} - 1) \qquad (4.29)$$

$$\langle n\cos m\theta \rangle = \frac{n_o a}{\pi} \int_o^{\pi} e^{-b\theta} \cos m\theta d\theta = \frac{n_o ab\,(1 + (-1)^{m-1} e^{-b\pi})}{\pi(b^2 + m^2)} \qquad (4.30)$$

$$\langle n^{-1} \cos m\theta \rangle = \frac{1}{n_o a\pi} \int_o^{\pi} e^{b\theta} \cos m\,\theta d\theta = - \frac{b(1 + (-1)^{m-1} e^{b\pi})}{n_o a\pi (b^2 + m^2)} \qquad (4.31)$$

$$\langle \log \frac{n}{n_o} \cos m\theta \rangle = - \frac{1}{\pi} \int_o^{\pi} b\theta \cos m\theta \, d\theta = \frac{b}{\pi m^2} [(-1)^{m-1} + 1] \qquad (4.32)$$

$$N = \frac{a}{b} (1 - e^{-b\theta}) - \theta \qquad (4.33)$$

$$\frac{\pi}{(1-e^{-b\pi})^2} (\pi + \frac{1}{b} [2e^{-b\pi} - \frac{1}{2} e^{-2b\pi} - \frac{3}{2}]) + \frac{\pi^2}{3}$$

$$- \frac{\pi^2}{(1-e^{-b\pi})} - \frac{2}{(1-e^{-b\pi})b} [e^{-b\pi} (\pi + \frac{1}{b}) - \frac{1}{b}] \qquad (4.34)$$

$$\langle (\frac{\partial}{\partial\theta} \log \frac{n}{n_o})^2 \rangle = b^2 \qquad (4.35)$$

$$\langle -N \frac{\partial}{\partial\theta} \log \frac{n}{n_o} \rangle = b\pi \left[\frac{1}{1 - e^{-b\pi}} - \frac{1}{2} \right] - 1 \qquad (4.36)$$

$$\langle n^{-2} \rangle = \frac{1}{2b\pi n_o^2 a^2} [e^{2b\pi} - 1] \qquad (4.37)$$

$$\left(a = \frac{b\pi}{1-e^{-b\pi}}\right)$$

Using these results in the formulae (4.1)-(4.8) we find for this distribution

$$F = 1 - \left[\frac{\frac{1}{2}\pi b}{\sinh \frac{1}{2}\pi b}\right]^2 \qquad (4.38)$$

$$\omega'_{cm} = (-1)^{m-1} \omega_c \qquad (4.39)$$

$$\omega'_{Dm} = \omega_D \frac{m^2}{m^2 + b^2} \left(\tfrac{1}{2}\pi b \coth \tfrac{1}{2}\pi b\right) \qquad \text{(m odd)}$$

$$= -\infty \qquad \text{(m even)} \qquad (4.40)$$

For the remaining formulae we shall only quote the results in the large b limit i.e. tight bunching ($b \gg 1$). The general results are easy to obtain from (4.29) - (4.37) but are rather complicated and would add little to our understanding. In addition, in the results quoted for γ_{pk}, Φ and α we shall take the frequency ω to equal ω_{pk} where from (4.4)

$$\omega_{pk} = (\omega_c \omega_D)^{\frac{1}{2}} \left(\frac{\pi}{\sqrt{3}\, b}\right)^{\frac{1}{2}} \qquad (4.41)$$

Then we find

$$\gamma_{pk} = \pm \left(\frac{2\omega_c}{\omega_D}\right)^{\frac{1}{2}} \left(\frac{2}{\sqrt{3}} + 1\right)^{\frac{1}{2}} \tag{4.42}$$

$$\Phi = \frac{v_s \epsilon E_s^2}{K^2} \left(\gamma^2 + \frac{2\omega_c}{\omega_D}\left(\frac{2}{\sqrt{3}} + 1\right)\right)\frac{\pi b}{2} \tag{4.43}$$

$$\alpha_m = \frac{K^2 \gamma \omega_c}{2v_s\left[\gamma^2 + \frac{\omega_c^2}{m^2\omega^2}\right]} \qquad \text{(m even)} \tag{4.44}$$

$$\alpha_m = \frac{-K^2 \gamma \omega_c}{2v_s\left[\gamma^2 + \left(\frac{\omega_c}{m\omega} + \frac{\omega}{\omega_D}\,\frac{(m^2 + b^2)}{\frac{1}{2}\pi bm}\right)^2\right]} \qquad \text{(m odd)} \tag{4.45}$$

$$\alpha = -\frac{2\omega_c \gamma K^2}{\pi b v_s\left(\gamma^2 + \frac{2\omega_c}{\omega_D}\left(\frac{2}{\sqrt{3}} + 1\right)\right)} \tag{4.46}$$

We see from (4.39) that as the degree of bunching increases i.e. b increases, the trapping factor $F \to 1$ as expected. From (4.39) and (4.40) together with (4.44) and (4.45) we see that for large applied d.c. fields, ($\gamma < 0$) only the odd harmonics are subject to gain, while the even harmonics suffer loss. This is a consequence of the exponential form of the distribution. The even Fourier components of this distribution place the electronsin regions where they are subject to a accelerative a.c. electric field and hence draw energy from the acoustic wave. For the odd harmonics the opposite is the case.

From (4.45) it is also clear that the gain at the odd harmonics decreases as b^{-2} for large b (for given ω; if $\omega = \omega_{pk}$ then α goes as b^{-1}). This is a consequence of the fact that for odd harmonics the parameter ω'_{Dm} decreases as b^{-1}. The frequency of peak gain on the harmonic gain versus frequency curve shifts to lower frequencies as b increases. The gain against frequency curve for even harmonics has no peak.

From (4.41) it is clear that the frequency of peak total gain $\to 0$ as b increases as does the total gain (from (4.46)). Equation (4.43) show that the total flux Φ for a fundamental frequency $\omega = \omega_{pk}$ increases as b for large b.

From (4.43) and (4.41) we see that the flux corresponding to a reduction in the frequency of peak gain by a factor R is given for this distribution by

$$\Phi = \frac{v_s \epsilon E_s^2}{K^2} \left[\gamma^2 + \frac{2\omega_c}{\omega_D} \left(\frac{2}{\sqrt{3}} + 1 \right) \right] \frac{\pi^2 R^2}{2\sqrt{3}} \qquad (4.47)$$

Using the values given in table 4.1 this gives $\Phi \simeq 8$ KW/cm^2. This is slightly higher than that found in the cosinusoidal case but still of the correct order of magnitude. From (4.47) we see that for a frequency reduction of R = 4 we have $b \simeq 30$.

Comparison of (4.47) and (4.28) shows that for larger frequency reductions R, the flux corresponding to the exponential distribution will be significantly lower than the flux corresponding to the cosinusoidal distribution. For R = 10 and $\gamma = 10$ we find for the cosinusoidal distribution $\Phi \simeq 10^3$ KW/cm^2 while for the exponential distribution we find $\Phi \simeq 10^2$ KW/cm^2. A flux of 10^2 KW/cm^2 is likely to be the more realistic estimate and this seems to be indicative of the fact that a highly bunched distribution like the exponential is more appropriate to a large signal situation.

4.4 The Gaussian Distribution

We have mentioned in section 4.1 that the Gaussian form of electron density distribution is probably the most realistic distribution we shall consider, and probably the one which will occur in practice in a large amplitude acoustic wave. This may be seen in the following manner.

From equation (3.22) we have for the a.c. electric field in an acoustic wave in terms of the space charge distribution

$$E' = E_s \left[\gamma \left(1 - \frac{n^{-1}}{\langle n^{-1} \rangle} \right) + \frac{\omega}{\omega_D} \frac{\partial}{\partial \theta} \log \frac{n}{n_o} \right] \qquad (4.48)$$

If the electrons are strongly bunched and we look near the peak of the distribution then $\frac{n^{-1}}{\langle n^{-1} \rangle} \rightarrow 0$. In this case (4.48) becomes

$$E - E_s = \frac{E_s \omega}{\omega_D} \frac{\partial}{\partial \theta} \log \frac{n}{n_o} \qquad (4.49)$$

where $E = E_o + E'$ is the total electric field.

Integrating (4.50) we find

$$\frac{n}{n_o} = A e^{\int_o^\theta \frac{\omega_D}{\omega} \left(\frac{E}{E_s} - 1 \right) d\theta} \qquad (4.50)$$

where the constant of integration A may be determined from the normalisation condition $\langle \frac{n}{n_o} \rangle = 1$. Writing $E' = \partial\phi/\partial x = \frac{\omega}{v_s} \frac{\partial \phi}{\partial \theta}$ where ϕ is the a.c. electrostatic potential, we find that (4.50) becomes

$$\frac{n}{n_o} = A' \exp \left[\frac{q\phi}{k_B T} - \frac{\omega_D}{\omega} \gamma \theta \right] \qquad (4.51)$$

where k_B is Boltzmann's constant and we have used the fact that $\omega_D / v_s E_s = q/k_B T$ and $A' = A e^{-q\phi(0)/k_B T}$.

The maximum electron density occurs (from 4.49) when $E(\theta_o) = E_s$. Let us take the solution of this equation θ_o as origin and expand the exponent in (4.51) about this point. The exponent becomes

$\frac{q}{kT}\ \phi''(\theta_o)\ \frac{\theta'^2}{2}$ + const, where the linear term vanishes due to the condition $E(\theta_o) = E_s$ and $\theta' = \theta - \theta_o$. Hence, using this in (4.51) the electron distribution in the vicinity of its maximum has the form

$$\frac{n}{n_o} = c\ e^{-b\theta^2} \qquad (4.52)$$

where $b = -q\phi''(0)/2k_BT$ and the constant c is determined by $\langle \frac{n}{n_o} \rangle = 1$. (4.52) is the Gaussian distribution.

It is clear that the equation $E = E_s$ determining the maximum of the n distribution will only have a solution (if E_o is large compared to E_s (as in a high field domain)), provided the a.c. field amplitude is comparable to the d.c. field amplitude. This merely restates the condition for a symmetric distribution mentioned earlier in chapter 3. The parameter b which occurs in (4.52) will again be referred to as the bunching parameter. It is clear that b is related to the curvature of the potential at the maximum of the electron density. For a sinusoidal potential well, this curvature is just equal to the well depth. The thermal potential k_BT/q emerges in (4.51) as the natural measure of potential well depths. We shall say more about this in Chapter 5.

We now go on to consider the various results of Chapter 3 applied to the Gaussian electron density distribution given by equation (4.52). Unfortunately, most of the integrals required for this distribution cannot be evaluated analytically. However, the arguments given in Chapter 3 for the behaviour of ω'_{cm} and ω'_{Dm} may be applied here in the strong bunching limit i.e. $b >> 1$. In this limit $\omega'_{cm} \to \omega_c(-1)^{m-1}$ and $\omega'_{Dm} \to 0$. For the parameters of most interest we have the following formulae.

$$c = \frac{\pi}{\int_0^{\pi} e^{-b\theta^2} d\theta} \tag{4.53}$$

$$F = 1 - \frac{\pi^2}{\int_0^{\pi} e^{-b\theta^2} d\theta \int_0^{\pi} e^{b\theta^2} d\theta} \tag{4.54}$$

$$\frac{\omega'_{cm}}{\omega_c} = - \frac{\int_0^{\pi} e^{-b\theta^2} \cos m\theta \, d\theta \int_0^{\pi} e^{b\theta^2} d\theta}{\int_0^{\pi} e^{-b\theta^2} d\theta \int_0^{\pi} e^{b\theta^2} \cos m\theta \, d\theta} \tag{4.55}$$

$$\frac{\omega'_{Dm}}{\omega_D} = \frac{(-1)^m m^2 \int_0^{\pi} e^{b\theta^2} \cos m\theta \, d\theta}{2b \int_0^{\pi} e^{b\theta^2} d\theta} \tag{4.56}$$

$$\frac{\omega_{pk}}{(\omega_c \omega_D)^{\frac{1}{2}}} = \left[\frac{\int_b^{\pi} \left[c^2 \left(\int_0^{\theta} e^{-b\theta'^2} d\theta' \right)^2 + \theta^2 - 2c\theta \int_0^{\theta} e^{-b\theta'^2} d\theta' \right] d\theta}{4 b^2 \pi^3/3} \right]^{\frac{1}{4}} \tag{4.57}$$

$$a_{pk} = - \left(\frac{\omega_D}{\omega_c} \right)^{\frac{1}{2}} \gamma_{pk} = \pm 2^{\frac{1}{2}} \left[\left[\frac{4b^2 \pi}{3} \int_0^{\pi} \left(c^2 \left(\int_0^{\theta} e^{-b\theta'^2} d\theta' \right)^2 + \theta^2 - 2c\theta \int_0^{\theta} e^{-b\theta'^2} d\theta' \right) d\theta \right]^{\frac{1}{2}} + \frac{2b}{\pi} \left(\int_0^{\pi} \theta \int_0^{\theta} e^{-b\theta^2} d\theta' d\theta - \frac{\pi^3}{3} \right) \right]^{\frac{1}{2}} \Bigg/ \left[\frac{\pi \int_0^{\pi} e^{2b\theta^2} d\theta}{\left(\int_0^{\pi} e^{b\theta^2} d\theta \right)^2} - 1 \right]^{\frac{1}{2}} \tag{4.58}$$

$$\frac{K^2 \Phi\, \omega_D}{v_s \epsilon E_s^2\, \omega_c} = a^2 \left(\frac{\pi \int_0^{\pi} e^{2b\theta^2}\, d\theta}{\left(\int_0^{\pi} e^{b\theta^2}\, d\theta \right)^2} - 1 \right) +$$

$$2 \left[\left[\frac{4b^2\pi}{3} \int_0^{\pi} \left(c^2 \left(\int_0^{\theta} e^{-b\theta'^2}\, d\theta' \right)^2 + \theta^2 - 2c\theta \int_0^{\theta} e^{-b\theta'^2}\, d\theta' \right) d\theta \right]^{\frac{1}{2}} \right.$$

$$\left. + \frac{2b}{\pi} \left(\int_0^{\pi} \int_0^{\theta} c e^{-b\theta'^2}\, d\theta'\, d\theta - \frac{\pi^3}{3} \right) \right] \qquad (4.59)$$

The formula (4.59) for Φ is for a frequency $\omega = \omega_{pk}$ where ω_{pk} is determined from equation (4.57). The results (4.53)-(4.59) have been evaluated numerically using the Royal Radar Establishment Computer (RREAC) and the results of the computation are displayed graphically in Figs. 1-6.

Fig. 1 shows the variation of the trapping factor F with the bunching parameter b. It is seen that for $b > 1$ trapping is essentially complete. Figs. 2 and 3 indicate the variation of ω'_{cm}/ω_c and ω'_{Dm}/ω_D respectively with b. The behaviour is fairly complicated but it is clear that as b becomes large $\omega'_{cm} \to (-1)^{m-1}\, \omega_c$ and $\omega'_{Dm} \to 0$ as we have already deduced. Because of this, the gain at each odd harmonic will tend to zero as b increases (Cf. equation (3.41)), while for even harmonics for $\gamma < 0$ there is loss which $\to 0$ as b increases. The frequency of peak gain on the gain versus frequency curves for the odd harmonics will also tend to zero as b increases since $\omega'_{Dm} \to 0$.

In Fig. 4 we display the variation of the ratio frequency of peak flux gain ω_{pk} to $(\omega_c\, \omega_D)^{\frac{1}{2}}$ with bunching parameter b. We see that ω_{pk} tends to zero as b increases.

A reduction in the frequency of peak flux gain by a factor R = 4 is found from Fig. 4 to occur for $b \simeq 7$. In Fig. 5 we display the variation of the flux Φ reduced to dimensionless form against b for $\omega = \omega_{pk}$ and for various values of the dimensionless parameter $a = -\left(\frac{\omega_D}{\omega_c}\right)^{\frac{1}{2}} \gamma$ (which specifies the d.c. electric field). We see from Fig. 5 that for $\gamma \simeq -5$ and $b \simeq 7, K^2 \Phi \omega_D / v_s \epsilon E_s^2 \omega_c \simeq 2 \times 10^2$ i.e. $\Phi \simeq 8$ kW/cm^2 where we have used the parameter values in table 4.1. For $\gamma = -10$ and R = 10 we find $\Phi \simeq 10^2$ kW/cm^2. We see that the results for the Gaussian distribution agree closely with the results for the exponential distribution. In Fig. 6 we plot the variation of $a_{pk} = -\left(\frac{\omega_D}{\omega_c}\right)^{\frac{1}{2}} \gamma_{pk}$ against b the bunching parameter. We note that for large b, a_{pk} reaches a constant value. This behaviour may be deduced from (4.58).

We therefore see that the exponential and Gaussian distributions both give fairly reasonable values for the acoustic power density when the frequency shift is about that observed in an acoustic domain. The sinusoidal distribution gives reasonable values for the flux for smaller frequency reductions.

In addition we may estimate the acoustic flux density required to produce a steady state as follows. In a steady state condition, the acoustic flux gain will be equal to the lattice loss. The lattice loss (for flux) is given approximately for CdS by $\alpha_{lat} \simeq 10^{-12} \omega^{3/2} m^{-1}$ (4). Using (3.32) we have for a steady state in the large signal case (since $F \simeq 1$)

$$\alpha = -\frac{E_s I_s \gamma}{\Phi} = \alpha_{lat} \simeq 10^{-12} \omega^{3/2}$$

Putting $\omega = \omega_{pk} = (\omega_c\ \omega_D)^{\frac{1}{2}}/4$ we have for a steady state

$$\Phi \propto -\frac{8 \times 10^{12}\ E_s I_s \gamma}{(\omega_c\ \omega_D)^{\frac{3}{4}}} \propto -2 \times 10^{12}\ \frac{\gamma\ \omega_c}{(\omega_c \omega_D)^{\frac{3}{4}}}$$

where we have used the parameter values given in table 4.1 i.e.

$$\Phi \propto 50\ \text{kW/cm}^2$$

This value is about an order of magnitude above that estimated experimentally (see table 4.1). This may be due to the uncertainty in the experimental estimates or to the fact that the theory is not directly applicable to the situation considered. There would seem to be some evidence to suggest that acoustic domains are not in a steady state (5).

Figure Captions Chapter 4

Fig. 1 Plot of the trapping factor F against the bunching parameter b for the Gaussian distribution.

Fig. 2 Plot of ω'_{cm}/ω_c against bunching parameter b for various harmonics m for the Gaussian distribution.

Fig. 3 Plot of ω'_{Dm}/ω_D against bunching parameter b for various harmonics m for the Gaussian distribution.

Fig. 4 Plot of the ratio of the frequency of peak flux gain to the small signal peak gain frequency against bunching parameter b for the Gaussian distribution.

Fig. 5 Plot of dimensionless flux ratio $\dfrac{K^2 \Phi \omega_D}{\epsilon v_s E_s^2 \omega_c}$ against bunching parameter b for various values of $a = -\left(\dfrac{\omega_D}{\omega_c}\right)^{\frac{1}{2}} \gamma$.

Fig. 6 Plot of $a_{pk} = -\left(\dfrac{\omega_D}{\omega_c}\right)^{\frac{1}{2}} \gamma_{pk}$ against bunching parameter b for the Gaussian distribution.

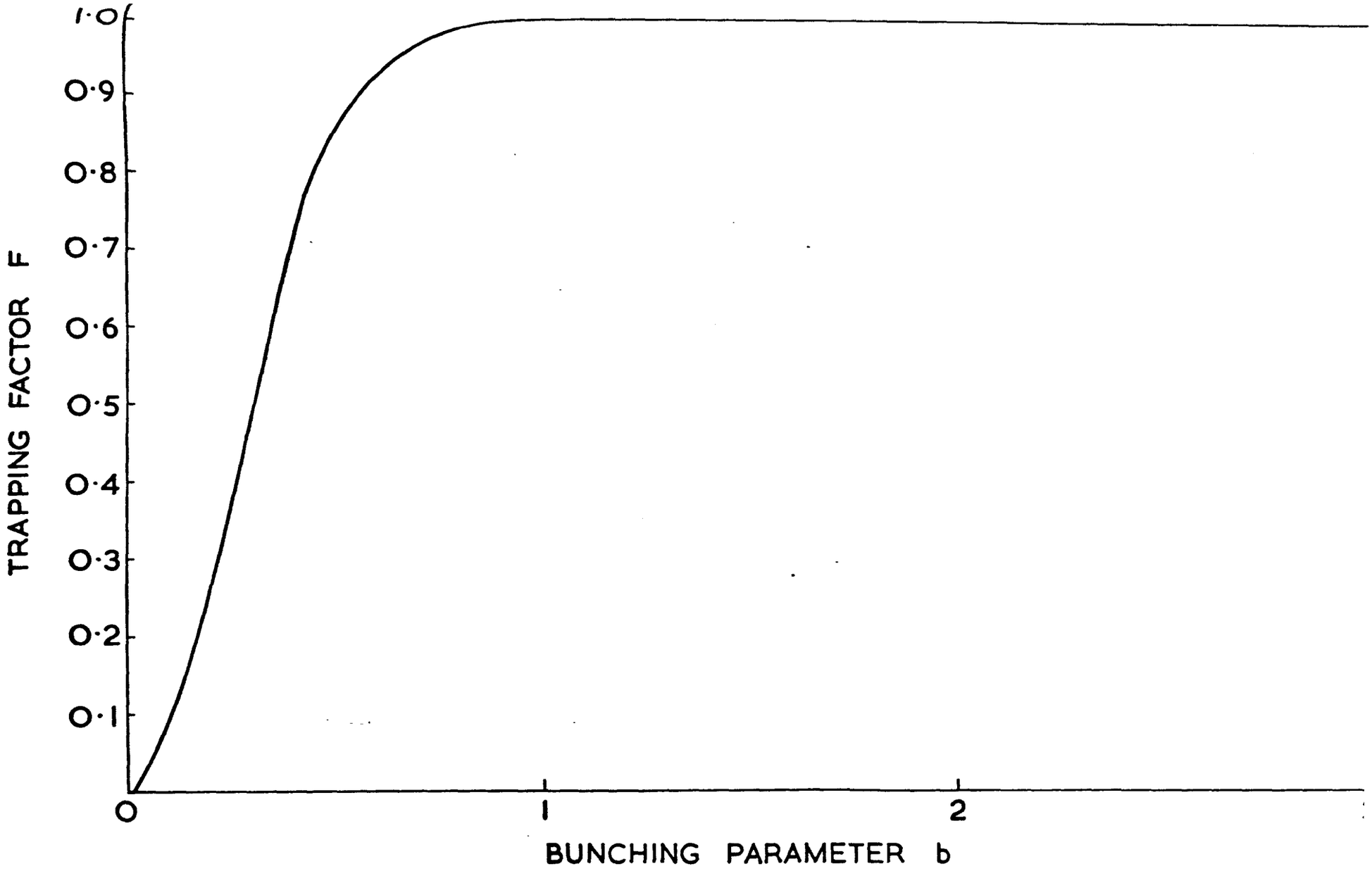
1·0
0·9
0·8
0·7
0·6
0·5
0·4
0·3
0·2
0·1
TRAPPING FACTOR F
0
1
2
BUNCHING PARAMETER b

FIG. 1

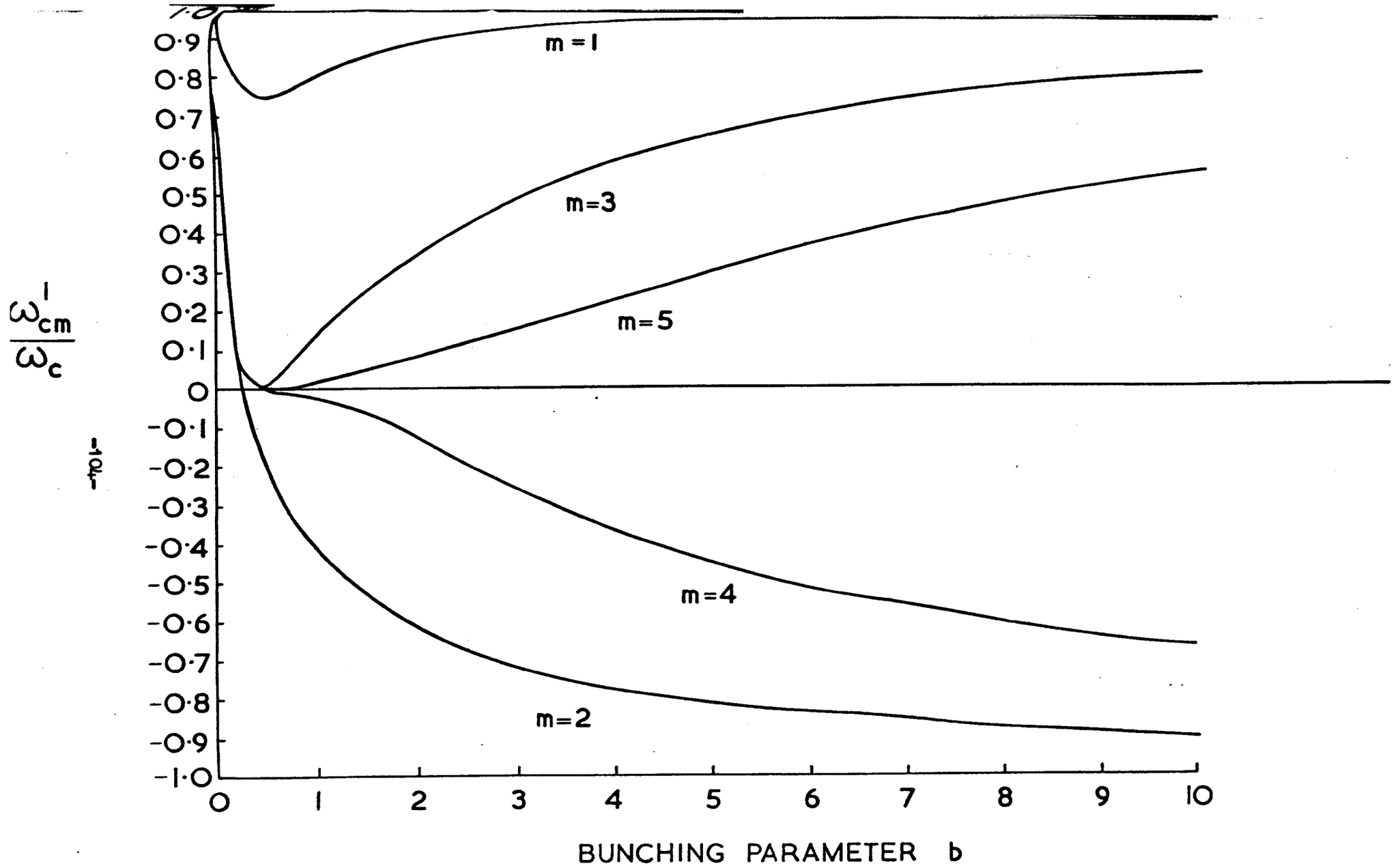

$\frac{\omega'_{cm}}{\omega_c}$

FIG. 2

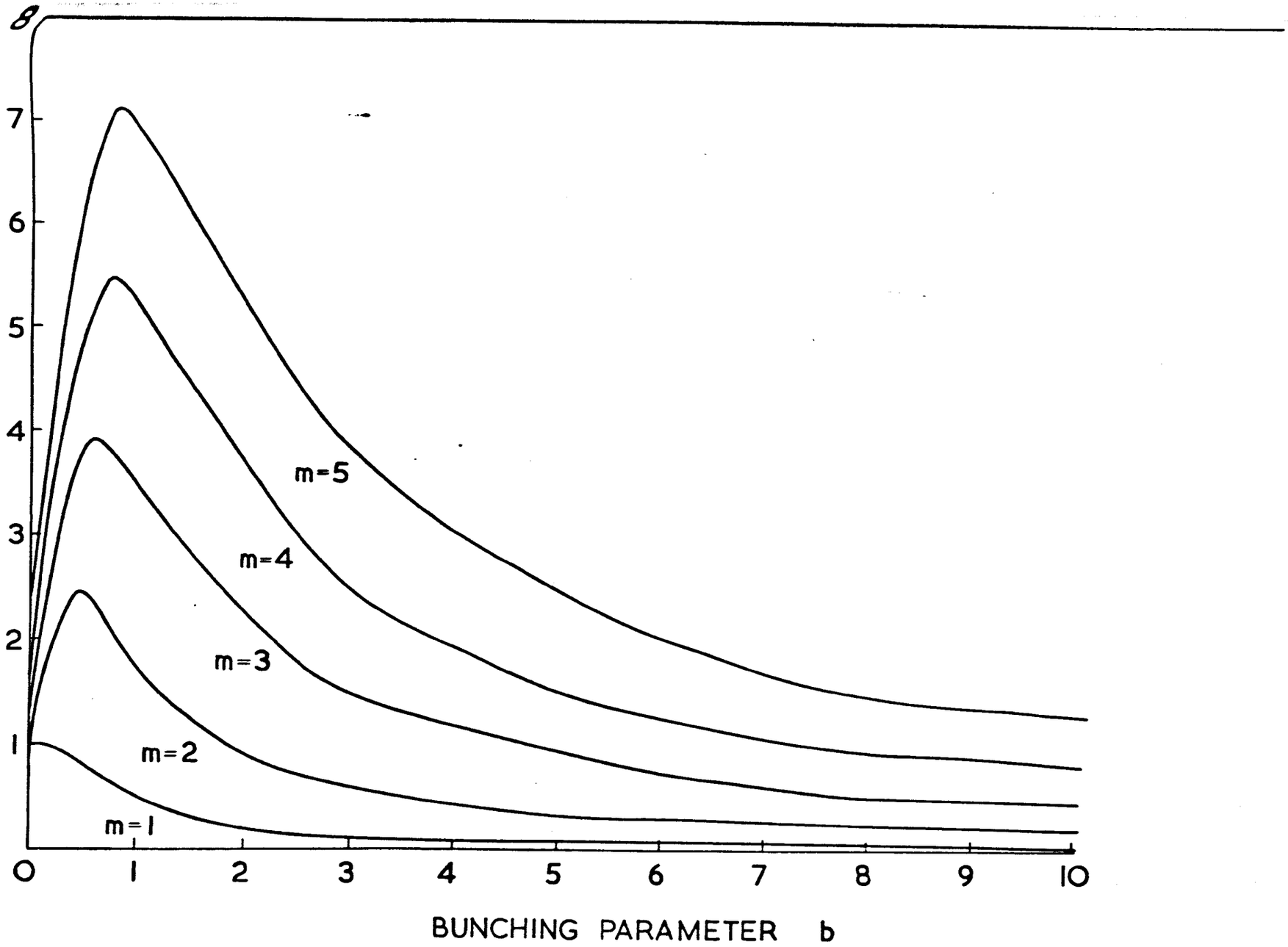

$\frac{\omega'_{Dm}}{\omega_D}$

FIG. 3

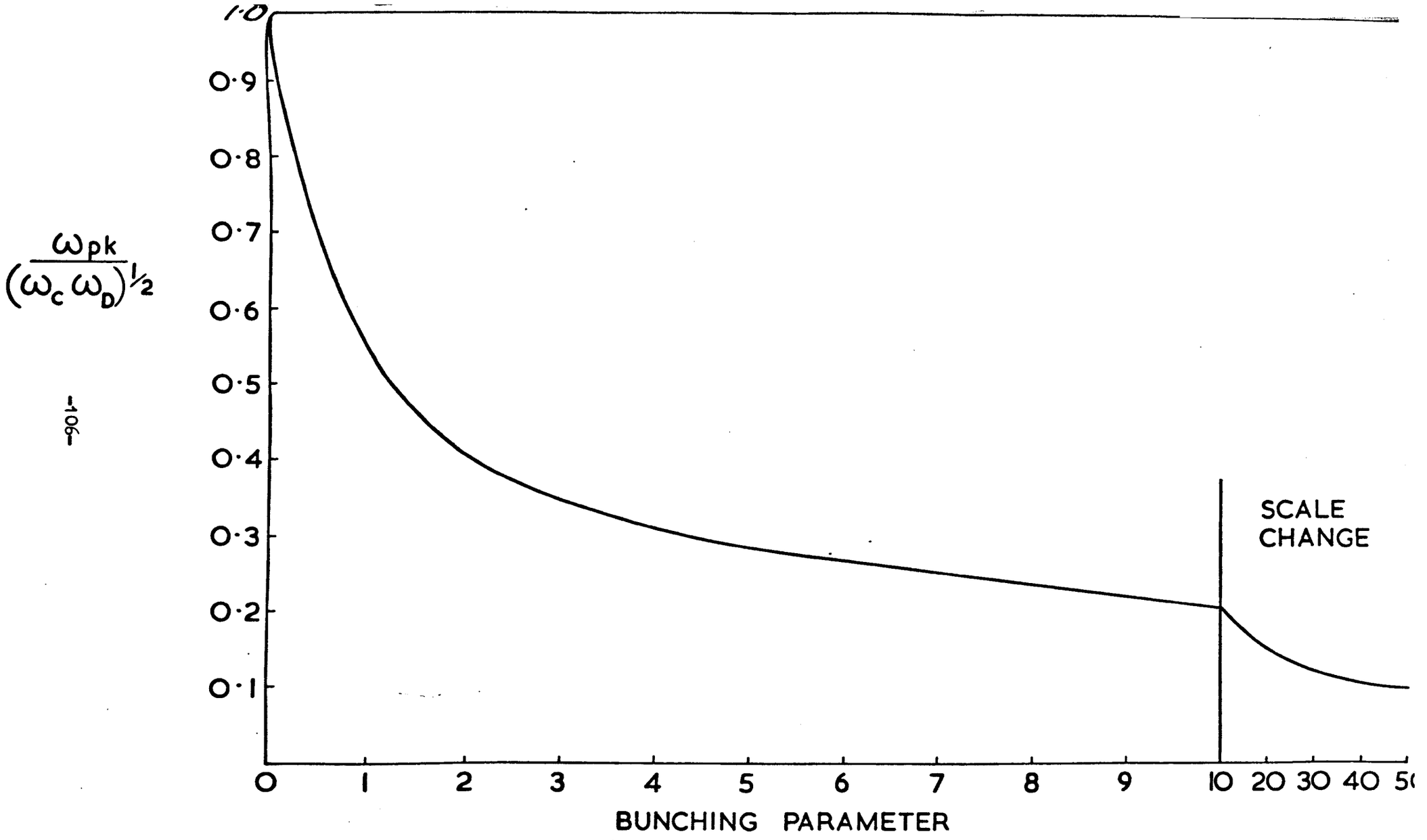
$\frac{\omega_{pk}}{(\omega_c \omega_D)^{1/2}}$
1·0
0·9
0·8
0·7
0·6
0·5
0·4
0·3
0·2
0·1
0
1
2
3
4
5
6
7
8
9
10
20
30
40
50
SCALE CHANGE
BUNCHING PARAMETER

FIG. 4

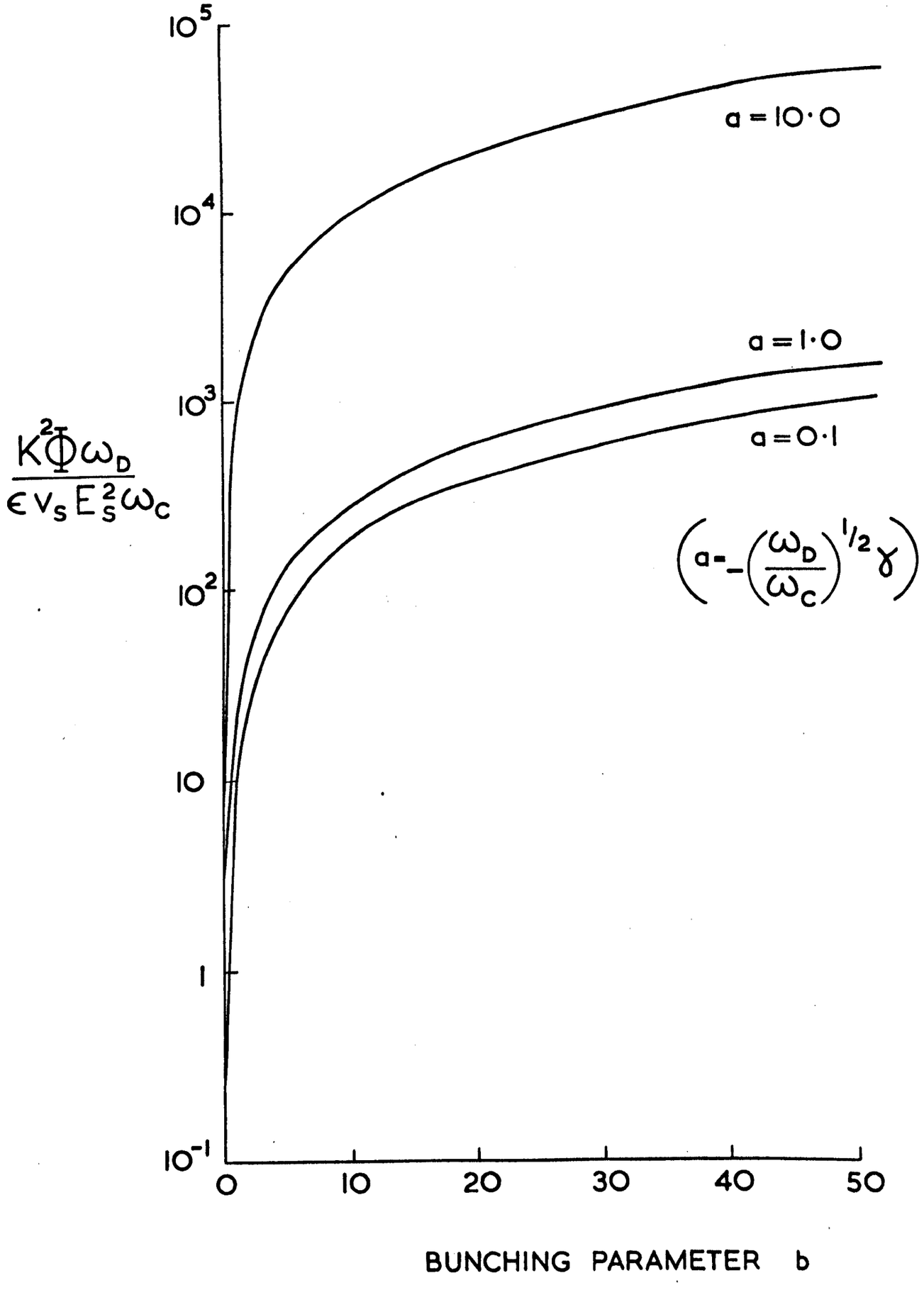
10^5
10^4
10^3
10^2
10
1
10^{-1}
0
10
20
30
40
50
a = 10·0
a = 1·0
a = 0·1
$\frac{K^2\Phi\omega_D}{\epsilon V_S E_S^2 \omega_C}$
$\left(a = \left(\frac{\omega_D}{\omega_C}\right)^{1/2}\gamma\right)$
BUNCHING PARAMETER b

FIG. 5

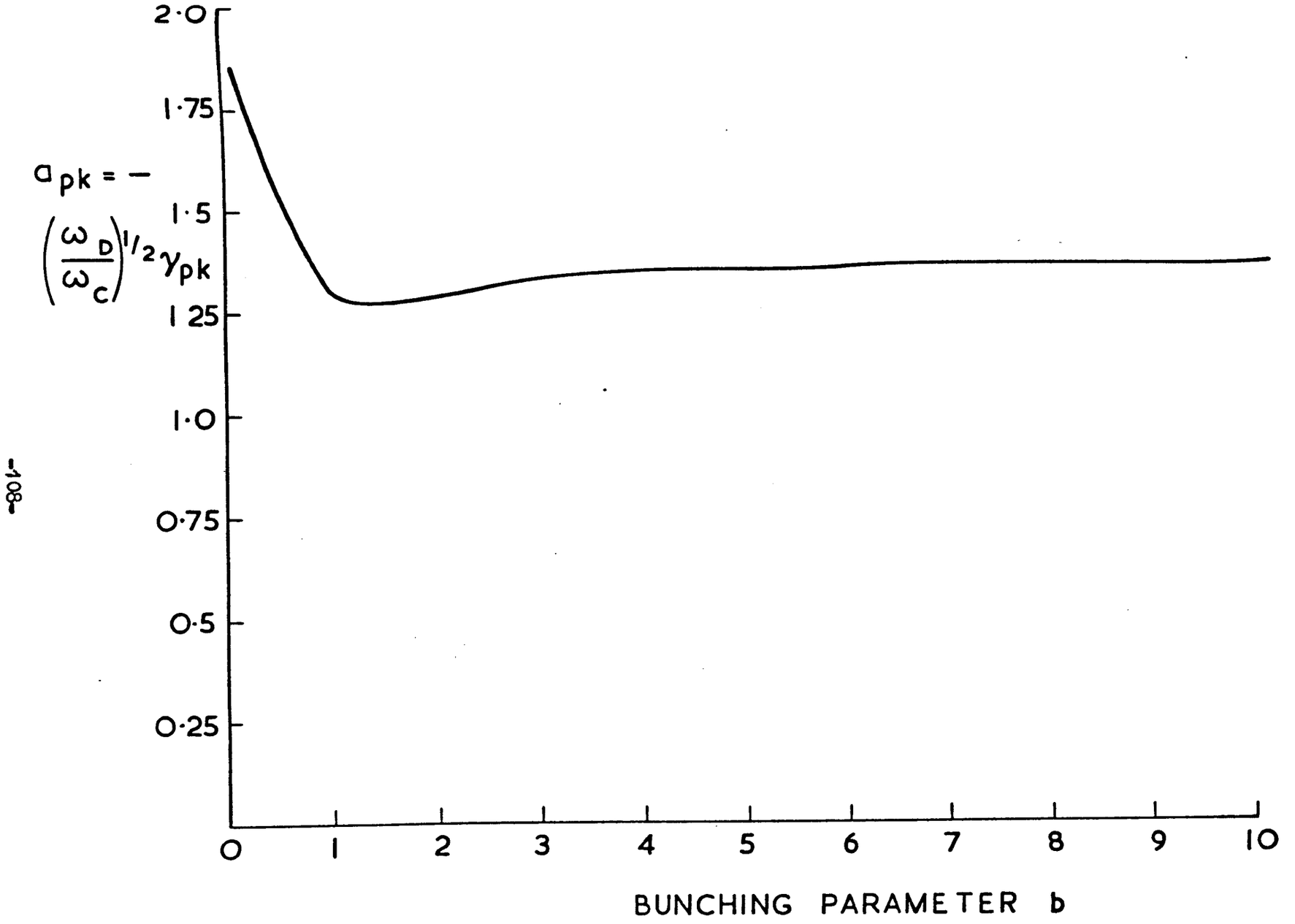
2·0
1·75
1·5
1 25
1·0
0·75
0·5
0·25
$a_{pk} = -\left(\frac{\omega_D}{\omega_c}\right)^{1/2} \gamma_{pk}$
0
1
2
3
4
5
6
7
8
9
10
BUNCHING PARAMETER b

FIG. 6

References Chapter 4

1. Zucker, J., and Zemon, S.A., (1966), Appl. Phys. Letts. 9, 398.

2. Zemon, S., Wasko, J.H., Hope, L.L., and Zucker, J. (1967), Appl. Phys. Letts., 11, 40.

3. Zucker, J., Zemon, S.A., and Wasko, J.H., (1968), Proc. Int. Conf. Phys. of Semiconductors, Moscow, 903.

4. Bateman, T.B. and McFee, J.H. (Unpublished) (see May, J.E. (1965) Proc. IEEE 54, 1465).

5. Butler, M.B.N. Private communication.

Appendix 4.1

Evaluation of Certain Integrals

$$\text{(i)} \quad I = \frac{1}{\pi}\int_0^{\pi} \frac{\cos m\theta \, d\theta}{1+a\cos\theta} = \frac{1}{2\pi} \operatorname{Re} \int_{-\pi}^{\pi} \frac{e^{im\theta} \, d\theta}{1+a\cos\theta}$$

Integrals of this type may be evaluated using the substitution $z = e^{i\theta}$ i.e. $dz = iz d\theta$, $\cos\theta = \frac{1}{2}(z + z^{-1})$ and the integral becomes a contour integral around the unit circle in the z-plane i.e.

$$I = \frac{1}{\pi a} \operatorname{Re} \oint \frac{z^m \, dz}{i(z^2 + \frac{2z}{a} + 1)} = \frac{1}{\pi a} \operatorname{Re} \oint \frac{z^m \, dz}{i(z-z_-)(z-z_+)}$$

where the poles of the integrand $z_{\pm} = -\frac{1}{a}\left[1 \pm \sqrt{1 - a^2}\right]$ are the roots of $z^2 + \frac{2z}{a} + 1 = 0$

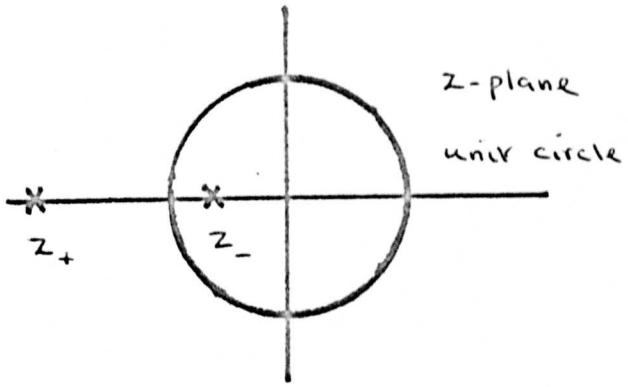

Clearly, since $z_+ z_- = 1$, we see that only z_- lies within the contour of integration. Using the residue theorem that $I = 2\pi i \, \Sigma$ residues we immediately find that

$$I = \frac{1}{\pi a} \operatorname{Re}\left[\frac{2\pi z_-^m}{z_- - z_+}\right] = \frac{\left(\sqrt{1 - a^2} - 1\right)^m}{a^m \sqrt{1 - a^2}}$$

$$\text{(ii)}\quad I = \frac{1}{\pi}\int_0^{\pi} \frac{\sin\theta \sin m\theta \, d\theta}{1 + a\cos\theta} = \frac{1}{2\pi} \operatorname{Im} \int_{-\pi}^{\pi} \frac{\sin\theta \, e^{im\theta} d\theta}{1 + a\cos\theta}$$

$$= -\frac{1}{2\pi a} \operatorname{Im} \oint \frac{(z - z^{-1}) z^m \, dz}{(z-z_-)(z-z_+)} = -\frac{1}{2\pi a} \operatorname{Im} 2\pi i \, \frac{(z_- - z_+) z_-^m}{z_- - z_+}$$

$$= -\frac{z_-^m}{a} = -\frac{1}{a^{m+1}} \left[\sqrt{1 - a^2} - 1\right]^m$$

$$\text{(iii)}\quad I = \frac{1}{\pi}\int_0^{\pi} \frac{\sin^2\theta}{(1 + a\cos\theta)^2} = \frac{1}{2\pi} \operatorname{Im} \int_{-\pi}^{\pi} \frac{\sin\theta e^{i\theta} d\theta}{(1+a\cos\theta)^2}$$

$$= \frac{1}{\pi a^2} \operatorname{Im} \oint \frac{(z^2 - 1) z \, dz}{(z-z_-)^2 (z-z_+)^2}$$

In this case the poles are of 2nd order. To find the residue at $z = z_-$ we must expand the integrand in a Laurent series about $z = z_-$ and determine the coefficient of $\frac{1}{z}$. The Laurent expansion of the integrand is

$$\frac{\left[(z - z_- + z_-)^2 - 1\right]\left[z - z_- + z_-\right]\left(1 + \dfrac{z - z_-}{z_- - z_+}\right)^{-2}}{(z-z_-)^2 (z_- - z_+)^2}$$

The coefficient of $(z-z_-)^{-1}$ is easily found to be $\dfrac{(z_-^2 - 1)}{(z_- - z_+)^2}$

$$\text{i.e. } I = -\frac{2(z_-^2 - 1)}{a^2(z_- - z_+)^2} = \frac{1 - \sqrt{1 - a^2}}{2\sqrt{1 - a^2}}$$

$$\text{(iv)} \quad \frac{1}{\pi}\int_0^{\pi} \frac{d\theta}{(1 + a\cos\theta)^2} = \frac{2}{\pi a^2 i}\oint \frac{z\,dz}{(z-z_-)^2\,(z-z_+)^2}$$

$$= \frac{1}{(1 - a^2)^{3/2}} \qquad \text{using a similar procedure to (iii)}$$

Chapter 5

THE NON LINEAR THEORY OF ACOUSTOELECTRIC GAIN III - ELECTRIC FIELD AND STRAIN DEPENDENT GAIN

5.1 Introduction

In the general discussion of acoustic gain in the non-linear regime given in section 3.1, we noted that the choice of the field variable on which the gain depended was at our disposal. We have seen in Chapters 3 and 4 how it is expedient to choose the electron density distribution n accompanying the acoustic wave, as the independent variable on which the gain and other quantities depend, in order to develop an analytical theory of the acousto-electric interaction in the non-linear regime. In this chapter, we shall turn to a consideration of acoustic gain as a function of a.c. electric field or strain.

The philosophy behind the method which we shall develop below is as follows. We have seen previously that in a large signal acoustic wave in a conducting piezoelectric semiconductor, the electrons will tend to become bunched in the troughs of minimum potential energy. For very large acoustic power densities, this will imply that the Fourier series for the electron density n will have a large harmonic content. In fact, in the limit of complete bunching, when the electron distribution becomes a periodic train of delta-functions, the amplitude at each harmonic becomes equal to that at the fundamental frequency of the wave. Because of this, in the large signal regime, the Fourier series for the electron distribution will be very slowly convergent. In any calculation of acoustic gain therefore, care must be taken to ensure that the strong harmonic content in n is adequately allowed for.

While the electron distribution in a large signal acoustic wave will contain many harmonics, it is plausible that this need not be the case for the electric field or strain in the wave. We shall therefore develop a theory which allows the calculation of acoustic gain when (a) the electric field distribution is taken to be sinusoidal, and when (b) the strain is taken to be sinusoidal.

The method we shall use is an extension of a technique used recently by Tien[1] to calculate acoustoelectric gain in the non-linear regime when the strain is sinusoidal. In Tien's calculation the fundamental frequency of

the acoustic wave ω is taken to be equal to $(\omega_c\,\omega_D)^{\frac{1}{2}}$, the small signal peak gain frequency. We shall remove this restriction and develop the theory for arbitrary frequencies. In doing so, we shall find that the method is applicable to all frequencies when the electric field distribution is taken as sinusoidal, but only to frequencies $\omega \geq (\omega_c\,\omega_D)^{\frac{1}{2}}$ when the strain is taken as sinusoidal. In fact, we shall see that for frequencies $\omega > (\omega_c\omega_D)^{\frac{1}{2}}$, the results of the sinusoidal field and strain calculations are practically identical.

Thoughout this chapter, we shall make similar assumptions to those employed in Chapter 3, i.e. the strain, electric field, electron density, etc. will be assumed to be made up of travelling waves moving close to the sound velocity with slowly varying amplitudes and phases.

5.2 Acoustoelectric Gain and Dimensionless Variables

In this section, we show how the acoustic gain may be calculated when the electric field or strain is given.

From equation (3.11), we see that the complex gain at the m^{th} harmonic of strain is given by

$$\alpha_m^c = \frac{-cE_m}{2\rho\, v_s^2\, u_m} \tag{5.1}$$

From Poisson's equation (3.15) and the constitutive relation (3.16) we have that

$$u_m = \frac{qn_m - imk\epsilon E_m}{m^2 k^2 e} \tag{5.2}$$

where $k = \omega/v_s$. Hence, combining (5.1) and (5.2) we have

$$\alpha_m^c = \frac{-ie^2 \phi_m m^3 k^3}{2\rho\, v_s^2 (qn_m + m^2 k^2 \epsilon \phi_m)} = \alpha_m + i\Delta k_m \tag{5.3}$$

where $\phi_m = E_m / imk$ is m^{th} Fourier component of the electrostatic potential. If we introduce the dimensionless variables

$$N_m = n_m/n_o, \quad P_m = q\,\phi_m/k_B T, \quad R = (\omega_c\,\omega_D)^{\frac{1}{2}}/\omega$$

then we find that (5.3) becomes

$$\frac{\alpha_m^c\ v_s}{K^2\,(\omega_c\,\omega_D)^{\frac{1}{2}}} = \frac{-i\,P_m\ m^3}{2R^3\,(N_m + \frac{m^2}{R^2}\,P_m)} \tag{5.4}$$

We see that P is the ratio of the a.c potential to the thermal potential $k_B T/q$, and R is the ratio of the frequency to the small signal peak gain frequency. Resolving (5.4) into real and imaginary parts we have

$$\frac{v_s\ \alpha_m}{K^2(\omega_c\omega_D)^{\frac{1}{2}}} = \frac{m^3\left[P_m''\,(N_m' + \frac{m^2}{R^2}\,P_m') - P_m'\,(N_m'' + \frac{m^2}{R^2}\,P_m'')\right]}{2R^3\left[(N_m' + \frac{m^2}{R^2}\,P_m')^2 + (N_m'' + \frac{m^2}{R^2}\,P_m'')^2\right]} \tag{5.5}$$

$$\frac{v_s\ \Delta k_m}{K^2(\omega_c\,\omega_D)^{\frac{1}{2}}} = -\frac{m^3\left[P_m'\,(N_m' + \frac{m^2}{R^2}P_m') + P_m''\,(N_m'' + \frac{m^2}{R^2}\,P_m'')\right]}{2R^3\left[(N_m' + \frac{m^2}{R^2}\,P_m')^2 + (N_m'' + \frac{m^2}{R^2}\,P_m'')^2\right]} \tag{5.6}$$

where the single and double primes refer to real and imaginary parts, respectively.

Expressed in the same dimensionless form, the formulae (2.28) and (2.27) for the small signal gain α_m^{ss} and wave vector shift Δk_m^{ss} are given by:

$$\frac{v_s \alpha_m^{s.s}}{K^2(\omega_c \omega_D)^{\frac{1}{2}}} = \frac{R^2 a}{2\left[R^2 a^2 + \frac{(R^2 + m^2)}{m^2}\right]^2} \tag{5.7}$$

$$\frac{v_s \Delta k_m^{s.s}}{K^2(\omega_c \omega_D)^{\frac{1}{2}}} = - \frac{m(R^2 a^2 + R^2 + m^2)}{2R\left[R^2 a^2 + \frac{(R^2 + m^2)}{m^2}\right]^2} \tag{5.8}$$

where we have introduced the dimensionless variable $a = -\left(\frac{\omega_D}{\omega_c}\right)^{\frac{1}{2}} \gamma$ used in section (4.4).

Equation (5.2) may be rewritten in dimensionless form as

$$\frac{e\omega_c\omega_D u_m}{q n_o v_s^2} = \frac{R^2}{m^2}\left(N_m + \frac{m^2}{R^2} P_m\right) \tag{5.9}$$

From (5.9) we easily find for the flux $\Phi_m = 2\rho v_s^3 m^2 k^2 |u_m|^2$ that

$$\frac{K^2 \omega_D \Phi_m}{\epsilon v_s \omega_c E_s^2} = \frac{2m^2}{R^2}\left|P_m + \frac{R^2}{m^2} N_m\right|^2 \tag{5.10}$$

We therefore see from equations (5.5) to (5.10) that if we are given $R = (\omega_c\omega_D)^{\frac{1}{2}}/\omega$, m, $a = -\left(\frac{\omega_D}{\omega_c}\right)^{\frac{1}{2}} \gamma$, $N_m = n_m/n_o$, $P_m = q\phi_m/k_B T$, (i.e. frequency, d.c. field, electron density and a.c. potential), then we may immediately calculate the acoustic gain together with the other quantities of interest. We shall see in the next section how the electron density is related to the a.c. potential.

5.3 The Non-Linear Equation for the Electron Density

In this section we shall show how the electron density distribution follows from a knowledge of the electric field in the acoustic wave.

The equation of current continuity (3.14) becomes on using Poisson's equation (3.15) and introducing the variable $\theta = kx - \omega t$ as in Chapter 3.

$$I = n_1 \mu E - I_s \left(\frac{n}{n_o} - 1\right) - I_s \frac{\omega}{\omega_D} \frac{d\left(\frac{n}{n_o}\right)}{d\theta} \qquad (5.11)$$

i.e.

$$\frac{d\left(\frac{n}{n_o}\right)}{d\theta} + \frac{\omega_D}{\omega}\left(1 - \frac{E}{E_s}\right)\frac{n}{n_o} + \frac{\omega_D}{\omega}\left(\frac{I}{I_s} - 1\right) = 0 \qquad (5.12)$$

Equation (5.12) is a linear inhomogeneous equation in $\frac{n}{n_o}$ with θ-dependent coefficients and may be integrated immediately on multiplication by the integrating factor[2]

$$\exp\left(\int_o^\theta \frac{\omega_D}{\omega}\left(1 - \frac{E}{E_s}\right) d\theta\right) = B \exp\frac{\omega_D}{\omega}\left(\gamma\theta - k\phi'(\theta)/E_s\right)$$

where $B = \exp\left(\frac{\omega_D}{\omega}\frac{k\phi'(0)}{E_s}\right)$ and ϕ' is the a.c. potential. The solution to (5.12) is found to be

$$\frac{n}{n_o} = e^{\frac{\omega_D}{\omega}\left(\gamma\theta - \frac{k\phi'(\theta)}{E_s}\right)}\left[\int_o^\theta \frac{\omega_D}{\omega}\left(1 - \frac{I}{I_s}\right) e^{\frac{\omega_D}{\omega}\left(\gamma\theta' - \frac{k\phi'(\theta')}{E_s}\right)} d\theta' - C\right] \qquad (5.13)$$

where C is a constant of integration. C may easily be found from the condition that we require n/n_o to be periodic i.e. $n(0) = n(2\pi)$. Using this in (5.13) to evaluate C and reinserting the result back in (5.13), we find on introducing the dimensionless variables used above that

$$\frac{n}{n_o} = \frac{\omega_D}{\omega}\left(\frac{I}{I_s} - 1\right) M(\theta) \tag{5.14}$$

where

$$M(\theta) = e^{Ra\theta + P(\theta)}\left[\frac{\int_o^{2\pi} e^{-Ra\theta' - P(\theta')}\, d\theta'}{1 - e^{-2\pi aR}}\right.$$

$$\left. + \int_o^{\theta} e^{-Ra\theta' - P(\theta')}\, d\theta'\right] \tag{5.15}$$

Averaging (5.14) and using $\left\langle \frac{n}{n_o} \right\rangle = 1$ we have finally

$$\frac{n(\theta)}{n_o} = \frac{M(\theta)}{\langle M(\theta)\rangle} \tag{5.16}$$

and

$$\frac{I}{I_s} - 1 = \frac{\omega}{\omega_D \langle M(\theta)\rangle} \tag{5.17}$$

Given the a.c. potential, the d.c. field and the frequency of the acoustic wave, equation (5.17) determines the total current, while 5.16 gives the electron distribution. Using the relation (3.19) $I = \sigma E_o (1-F) + FI_s$ in conjunction with (5.17) we find that the trapping factor F is given by

$$F = 1 - \frac{1}{< M(\theta) > \; Ra} \qquad (5.18)$$

The relations (5.16) and (5.17) were first derived by Beale[3] and Gurevich[4].

The results (5.16)-(5.18) together with the formulae derived in section (5.2) suffice to allow us to calculate acoustoelectric gain for given $\phi'(\theta)$, a, and R. Unfortunately, the calculation has to be done numerically. The necessary computations have been carried out using the RREAC computer and the plan of the calculation and the results are described in the next section.

5.4 Calculation of Acoustic Gain

We shall first outline the steps necessary to calculate the acoustic gain and other quantities of interest when we are given the electric field distribution, and then indicate the modifications necessary to do the calculation given the acoustic strain. The steps in the calculation are as follows:

(i) Using chosen values of $R = (\omega_c \omega_D)^{\frac{1}{2}}/\omega$, (determined by the acoustic wave frequency), and $a = -(\frac{\omega_D}{\omega_c})^{\frac{1}{2}} \gamma$, (determined by the d.c. field), together with a chosen a.c. electric potential ratio distribution i.e. $P(\theta)$, (which we shall take to be cosinusoidal), use equation (5.16) to determine $n(\theta)/n_o$ and (5.18) to determine F.

(ii) Fourier analyse $n(\theta)/n_o$ to obtain the N_m's for m = 1 , 2, --- up to some chosen limit.

(iii) Use these N_m's together with the given P_m's in equation (5.5) to determine $v_s \alpha_m / K^2 (\omega_c \omega_D)^{\frac{1}{2}}$ for required values of m, (we shall only be concerned with m = 1 since for a sinusoidal field, $P_m = 0$, $m > 1$), and (5.6) to determine $v_s \Delta k_m / K^2 (\omega_c \omega_D)^{\frac{1}{2}}$ if required.

(iv) Evaluate the dimensionless fluxes $K^2 \omega_D \Phi_m / \epsilon v_s E_s^2 \omega_c$ from equation (5.10) for the required range of m.

To modify this procedure if the strain is given as sinusoidal, we carry out steps (i), (ii) and (iii) as above for a sinusoidal electric field i.e. $P_m = P_1 \delta_{m,1}$. Then, since we require $S = \partial u/\partial x$ to be sinusoidal, we see from (5.9) that for $m \geq 2$, $P_m = -\frac{N_m R^2}{m^2}$. Using the results of step (ii) to evaluate P_m for $m \geq 2$, we then use these values as a new starting point in step (i) and proceed through steps (i), (ii) and (iii) again. This cycle of operations is repeated until the α_1 resulting from step (iii) has converged to within 1%. Since $u_m = 0$ for $m \geq 2$ we have $\alpha_m = 0$ for $m \geq 2$ as was the case for a sinusoidal field. The flux Φ is now given by $\Phi = \Phi_1 = 2 \rho v_s^3 |S_1|^2$.

For $R \leq 1$, i.e. $\omega \geq (\omega_c \omega_D)^{\frac{1}{2}}$, we find that the iterations described above are not really necessary. The reason for this becomes clear on noting that since $|N_m| \leq 1$, we have from above $|P_m| \leq \frac{R^2}{m^2}$ for $m \geq 2$. Hence for $R \leq 1$, $|P_m| << 1$ for $m \geq 2$. Since we shall be interested in $P_1 \geq 1$, the corrections to $P(\theta)$ produced by the iterations are small. For $R \geq 1$ however the reverse is the case. Again $|P_m| \leq R^2/m^2$ but now since $R \geq 1$ (i.e. $\omega < (\omega_c \omega_D)^{\frac{1}{2}}$), $|P_m|$ for $m \geq 2$ can be comparable or larger than P_1. Hence, the harmonics of the electric field produced by the iteration can be as large or larger then the fundamental. In this case, the iterative process produces large alterations in the acoustic gain, and in fact for R not too much bigger than 1, becomes non-convergent!

We therefore conclude that the method we have described is applicable for $\omega \geq (\omega_c \omega_D)^{\frac{1}{2}}$ to the calculation of acoustic gain under the constraint of sinusoidal electric field or strain, the results being nearly equal for the two cases. For $\omega < (\omega_c \omega_D)^{\frac{1}{2}}$ however, the method is only valid for the calculation of acoustic gain under the constraint of sinusoidal electric field.

Since we are primarily interested in producing shifts in the frequency of peak acoustic gain to frequencies below $(\omega_c \omega_D)^{\frac{1}{2}}$, it will be this latter case with which we shall be concerned.

The computations outlined in the steps (i) to (iv) above have been carried out using the Royal Radar Establishment Computer RREAC and the results are illustrated in Figs. 7-17.

Figs. 7 and 8 illustrate the electron concentration n/n_o as given by equation (5.16) for varying values of P_1 the ratio of the a.c. potential ϕ' to the thermal potential $k_B T/q$. We see that for $P_1 \leq 1$, the carrier concentration is nearly sinusoidal. As P_1 increases, n/n_o becomes a highly bunched Gaussian like pulse. Fig. 7 is for $aR = 0.1$ while Fig. 8 is for $aR = 10$. The effect of increasing a (i.e. increasing the d.c. field) or increasing R (i.e. decreasing the frequency), is seen to be a debunching and spreading out of the electron distribution. The physical reasons for this are easy to understand. The increased d.c. electric field acts to sweep the electrons out of the troughs of the potential wells (c.f. sec 3.5) while the reduced frequency aids dielectric relaxation. Regions of positive and negative a.c. electric field are also marked. The peak of the electron distribution is always seen to lie in the region of negative a.c. electric field. In this region the electrons undergo deceleration (taking account of our sign convention!), so that energy is transferred to the acoustic wave since the bulk of the electrons lie in negative a.c. electric fields. As the potential wave amplitude increases, we see from Figs 7 and 8 that the peak on the electron distribution shifts towards the boundary between the positive and negative field regions causing the acoustic gain to decrease. We note that the electron distribution is almost symmetric as we assumed in Chapter 3.

In Fig. 9 we plot 1-F against $\phi_1'/\phi_{th} = P_1$, for various values of the product aR. We see that for the smaller values of aR, (when the debunching effects mentioned above are small) F → 1 very rapidly i.e. current saturation occurs for potential well depths of a few times the thermal potential $\phi_{th} = k_B T/q$. For larger aR however, saturation does not occur until $P_1 > aR$, i.e. $E' > E_o - E_s$. This is understandable on the basis of the 'staircase' picture of the total electrostatic potential described earlier in Chapter 3.

It is of some interest to plot the amplitude of the various harmonics in the electron density distributions given in Figs. 7 and 8. This is done for the first five harmonics in Figs. 10 and 11. As the amplitude of the a.c. potential well is increased, the harmonic content in n becomes very significant. Ultimately as $P_1 \to \infty$, the electron concentration will approach a delta-function-like form, and in this limit the magnitude of each harmonic component will reach unity. This behaviour reflects the slow convergence of the Fourier series for the carrier concentration referred to previously, and illustrates the use of the present technique in dealing with this difficulty. It is clear that the fundamental component of the electric field alone can give rise to a large harmonic content in the electron density distribution via equation (5.17). Plots similar to Eqs. 7-11 have been given previously for the case R = 1 (i.e. $\omega = (\omega_c \omega_D)^{\frac{1}{2}}$, by Tien[1].

In Figs. 12 and 13, the ratio of the 1st harmonic gain α_1 to the small signal gain α_1^{ss} is plotted against $\phi_1'/\phi_{th} = P_1$ for various values of a and for two values of R. It is clear that the gain reduces as the potential ratio P_1 increases. This is a consequence of the movement of electron distribution peak mentioned above. In Figs 14 and 15 we illustrate the frequency dependence of the first harmonic gain. The quantity

$$\alpha_{1d} = \frac{v_s \alpha_1}{K^2 (\omega_c \omega_D)^{\frac{1}{2}}}$$ is plotted against R for various values of $\phi_1'/\phi_m = P_1$

and for two values of a. It is clear that the two effects desired are

present i.e. the gain reduces as the potential amplitude is increased (or flux increased) and the frequency of peak gain shifts to lower frequencies (higher R).

The plot of the frequency ratio of peak gain R_{pk} against the potential amplitude ratio P_1 is given in Fig. 18. For the range of parameters over which calculations have been carried out, the curve has been found to be more or less independent of a. The frequency of peak gain has shifted by a factor of R = 5 when the potential amplitude ratio $\simeq$ 50. Computation has proved troublesome for larger potential ratios.

In Fig. 17 and 18 we plot the flux at the first harmonic $\frac{K^2\Phi_1\omega_D}{\epsilon v_s E_s^2 \omega_c}$ against the potential ratio P_1 for $R = R_{pk}$. The curve was again found to be fairly insensitive to variation of a over the range of values used ($0.1 \leq a \leq 1.0$). The shift in frequency of peak gain by a factor of 5 is found at a flux of about 7 kW/cm^2, where we have used the parameter values given in table 4.1. Again this value is in reasonable agreement with the experimental data given in Chapter 4.

It is not difficult to compare the results obtained in this Chapter with the results obtained in Chapter 4 for the Gaussian electron density distribution. We see that a given a.c. electric potential ratio, value of d.c. field, and frequency, specify the electron density distribution. For large potential ratios, we have seen from figures 7 and 8 that the electron distribution is approximately Gaussian. The bunching parameter b used in Chapter 4 may be measured from Figs 7 and 8 and a direct comparison of results can then be made. Good agreement is found.

Figure Captions Chapter 5

Fig. 7 Plots of fractional electron density in a potential wave against $\theta = kx - \omega t$ for various potential ratios $P_1 = \phi_1' / \phi_{th}$ for $aR = - \frac{\omega_D}{\omega} \gamma = 0.1$. Regions of positive and negative a.c. electric field E' are marked.

Fig. 8 Plots of fractional electron density in a potential wave against $\theta = kx - \omega t$ for various potential ratios $P_1 = \phi_1' / \phi_{th}$ for $aR = - \frac{\omega_D}{\omega} \gamma = 10.0$. Regions of positive and negative a.c. electric field E' are marked.

Fig. 9 Plot of 1-F (F trapping factor) against the potential ratio $P_1 = \phi_1' / \phi_{th}$ in an acoustic wave for various values of $aR = - \omega_D \gamma / \omega$.

Fig. 10 Plot of harmonic content in the electron distribution for various harmonics m against the potential ratio P_1 for $aR = - \frac{\omega_D}{\omega} \gamma = 0.1$.

Fig. 11 Plot of harmonic content in the electron distribution for various harmonics m against potential ratio P_1 for $aR = - \omega_D \gamma / \omega = 10.0$.

Fig. 12 Plots of the ratio of the fundamental gain α_1 to its small signal value α_1^{ss} against potential ratio P_1 for 2 values of $a = - \left(\frac{\omega_D}{\omega_c} \right)^{\frac{1}{2}} \gamma$ and $R = \frac{(\omega_c \omega_D)^{\frac{1}{2}}}{\omega} = 1$.

Fig. 13 Plots of the ratio of the fundamental gain α_1 to its small signal value against potential ratio P_1 for 3 values of $a = - (\omega_D / \omega_c)^{\frac{1}{2}} \gamma$ and $R = (\omega_c \omega_D)^{\frac{1}{2}} / \omega = 10$.

Fig. 14 Plots of the dimensionless fundamental gain $\alpha_{1d} \times 10^2 = \frac{v_s \alpha_1}{K^2(\omega_o \omega_D)^{\frac{1}{2}}} \times 10^2$ against frequency ratio $R = (\omega_o\ \omega_D)^{\frac{1}{2}}/\omega$ for various potential ratios P_1 for $a = -(\omega_D/\omega_o)^{\frac{1}{2}}\gamma = 0.1$.

Fig. 15 Plots of the dimensionless fundamental gain $\alpha_{1d} \times 10 = \frac{v_s \alpha_1}{K^2(\omega_o \omega_D)^{\frac{1}{2}}} \times 10$ against frequency ratio $R = (\omega_o\ \omega_D)^{\frac{1}{2}}/\omega$ for various potential ratios P_1 for $a = -(\omega_D/\omega_o)^{\frac{1}{2}}\gamma = 1.0$

Fig. 16 Plot of R_{pk} the ratio of the frequency of small signal peak fundamental gain to the frequency of peak gain against potential ratio P_1.

Fig. 17 Plot of dimensionless fundamental flux $K^2 \varphi_1' \omega_D / \epsilon v_s E_s^2\ \omega_o$ against potential ratio P.

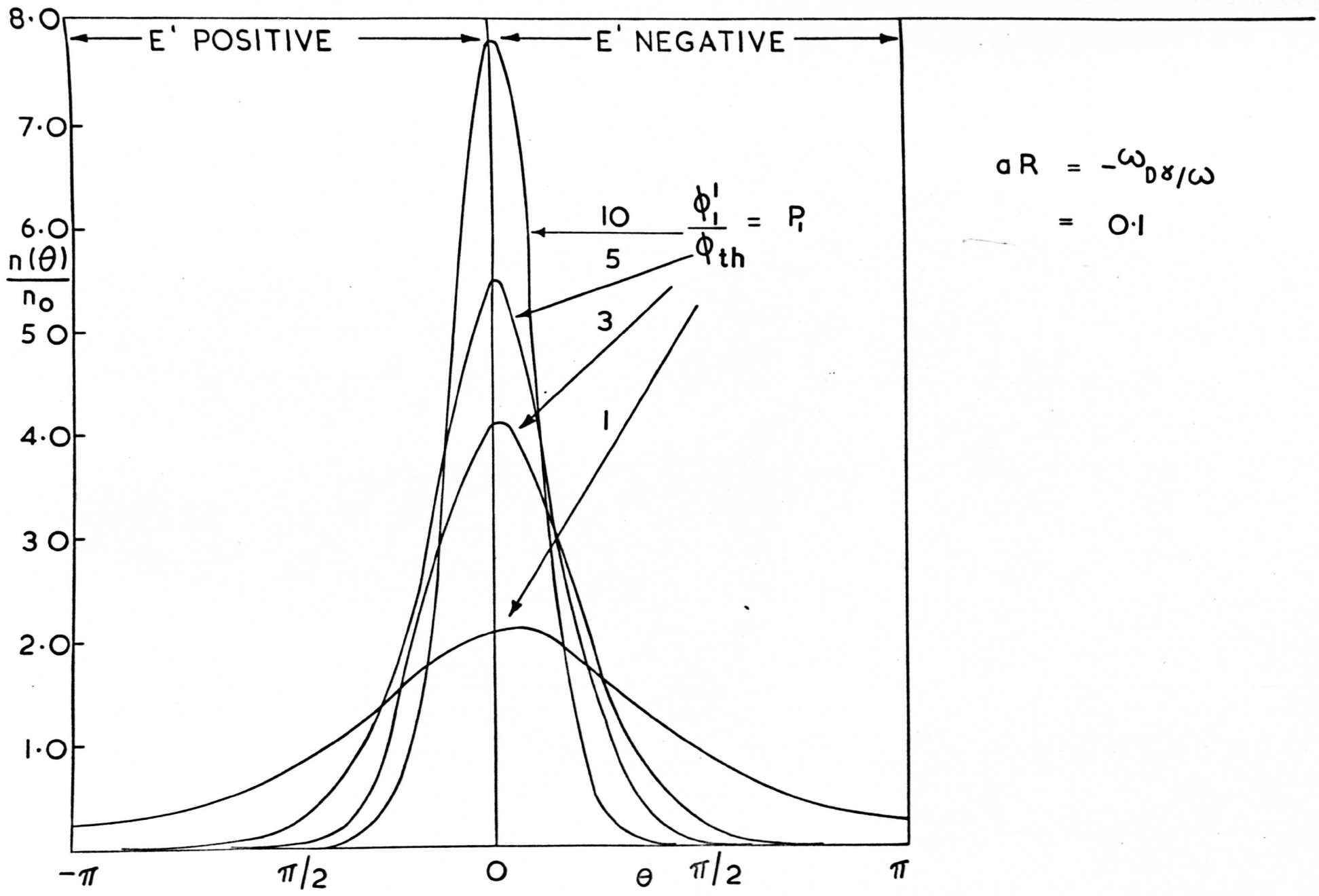
E' POSITIVE
E' NEGATIVE
8·0
7·0
6·0
5 0
4·0
3 0
2·0
1·0
n(θ)/n₀
10
5
3
1
φ'₁/φ_th = P_i
-π
π/2
0
θ
π/2
π
aR = -ω_Dγ/ω
= 0·1

FIG. 7.

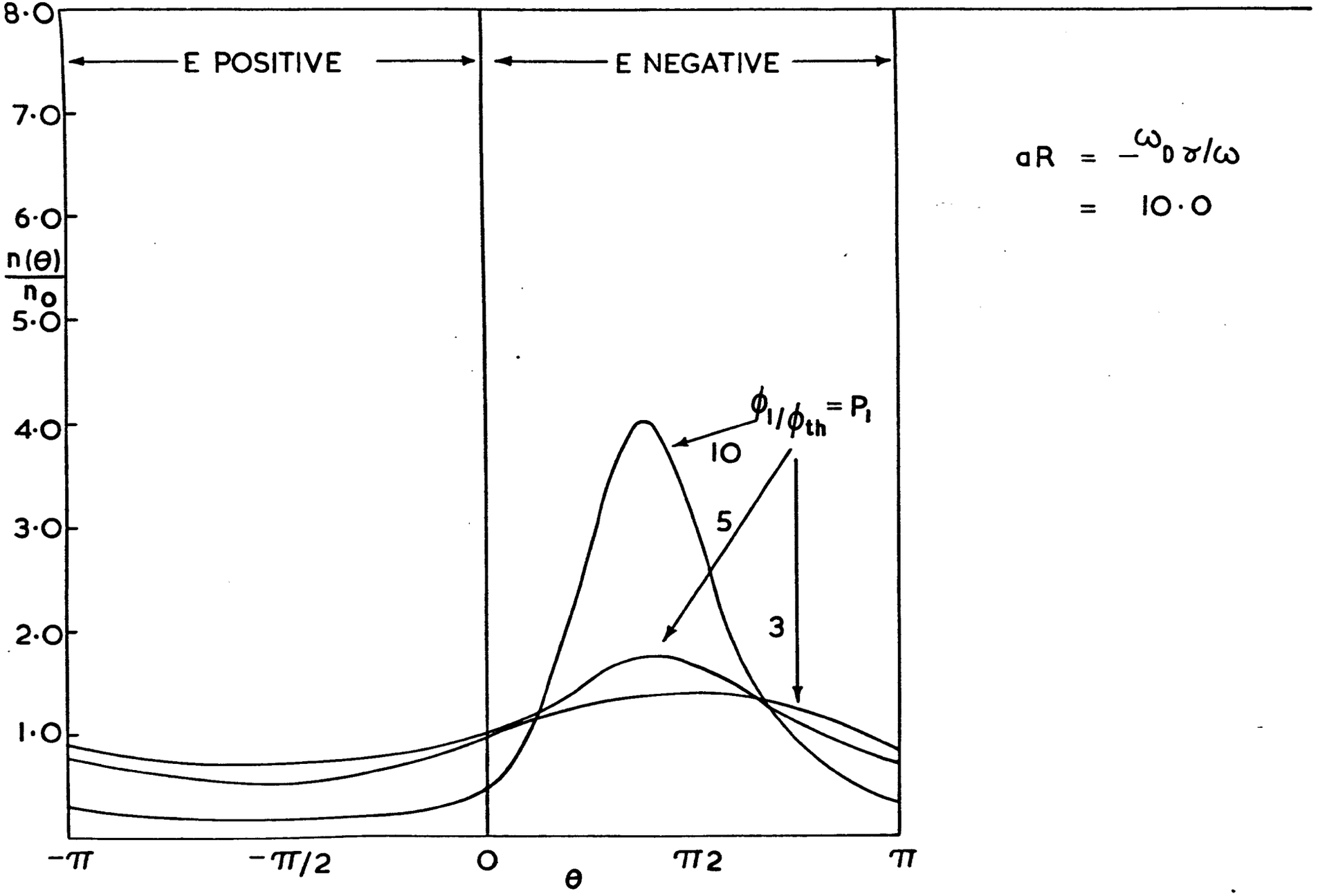
8·0
7·0
6·0
n(θ)/n₀
5·0
4·0
3·0
2·0
1·0
E POSITIVE
E NEGATIVE
$\phi_I/\phi_{th} = P_I$
10
5
3
−π
−π/2
0
π2
π
θ
aR = $-\omega_0 \gamma/\omega$
= 10·0

FIG. 8.

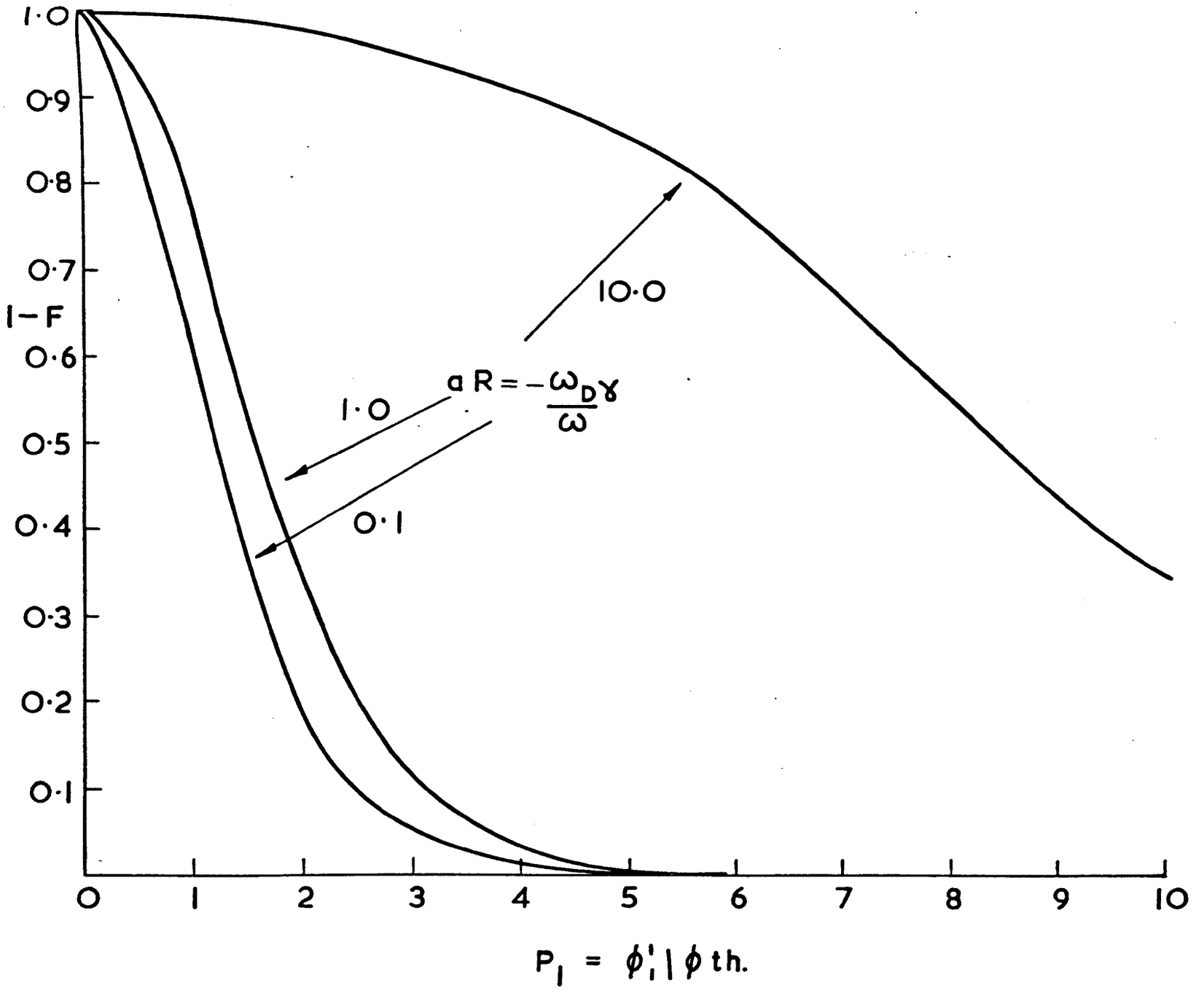
1·0
0·9
0·8
0·7
1−F
0·6
0·5
0·4
0·3
0·2
0·1
0
1
2
3
4
5
6
7
8
9
10
10·0
1·0
0·1
a R = −ω_D γ / ω
P_1 = φ'_1 | φ th.

FIG. 9

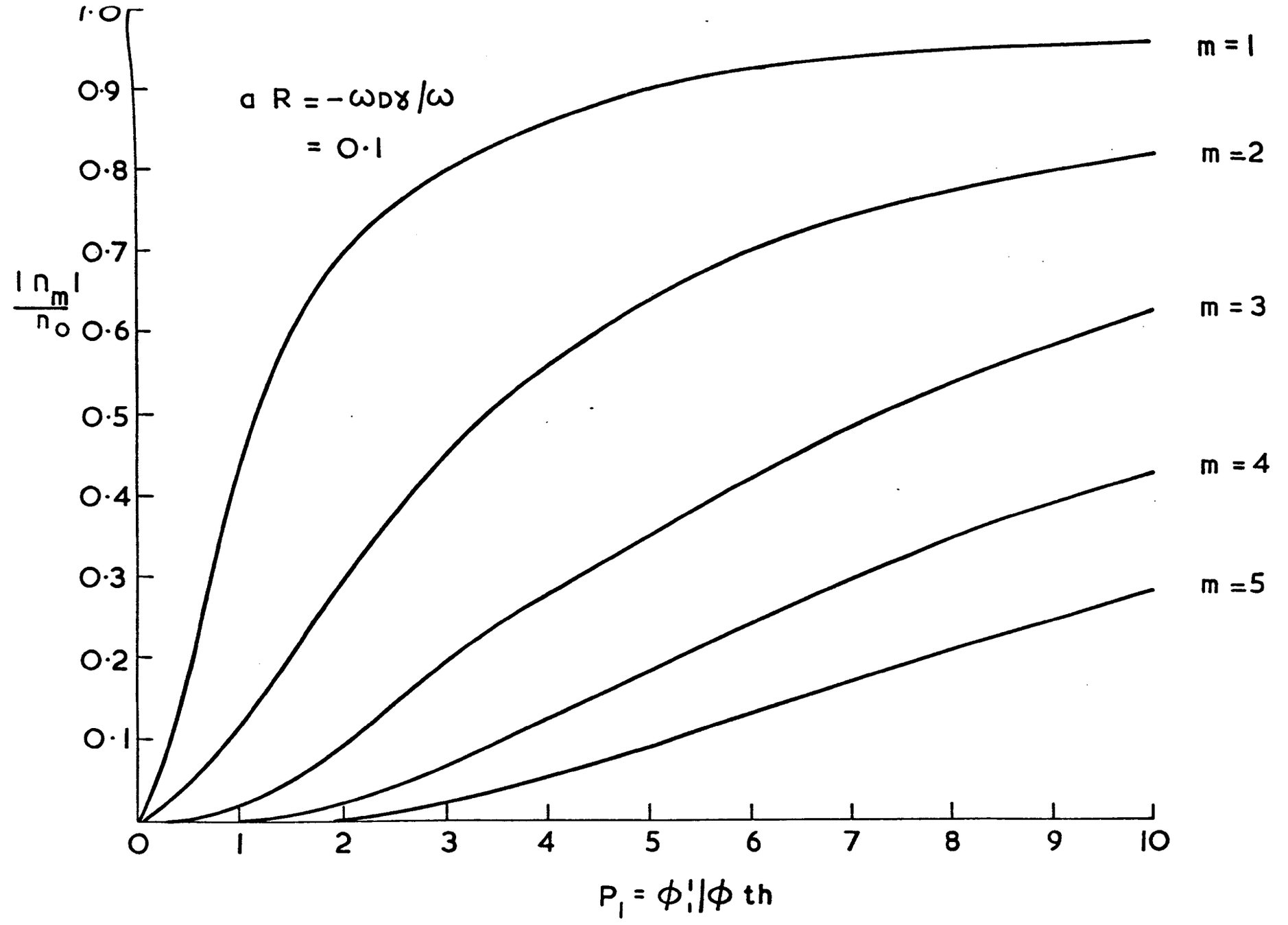
1·0
0·9
0·8
0·7
0·6
0·5
0·4
0·3
0·2
0·1
$\frac{|n_m|}{n_o}$
a R = $-\omega_D\gamma/\omega$
= 0·1
m = 1
m = 2
m = 3
m = 4
m = 5
0
1
2
3
4
5
6
7
8
9
10
$P_1 = \phi_1'/\phi$ th

FIG. 10

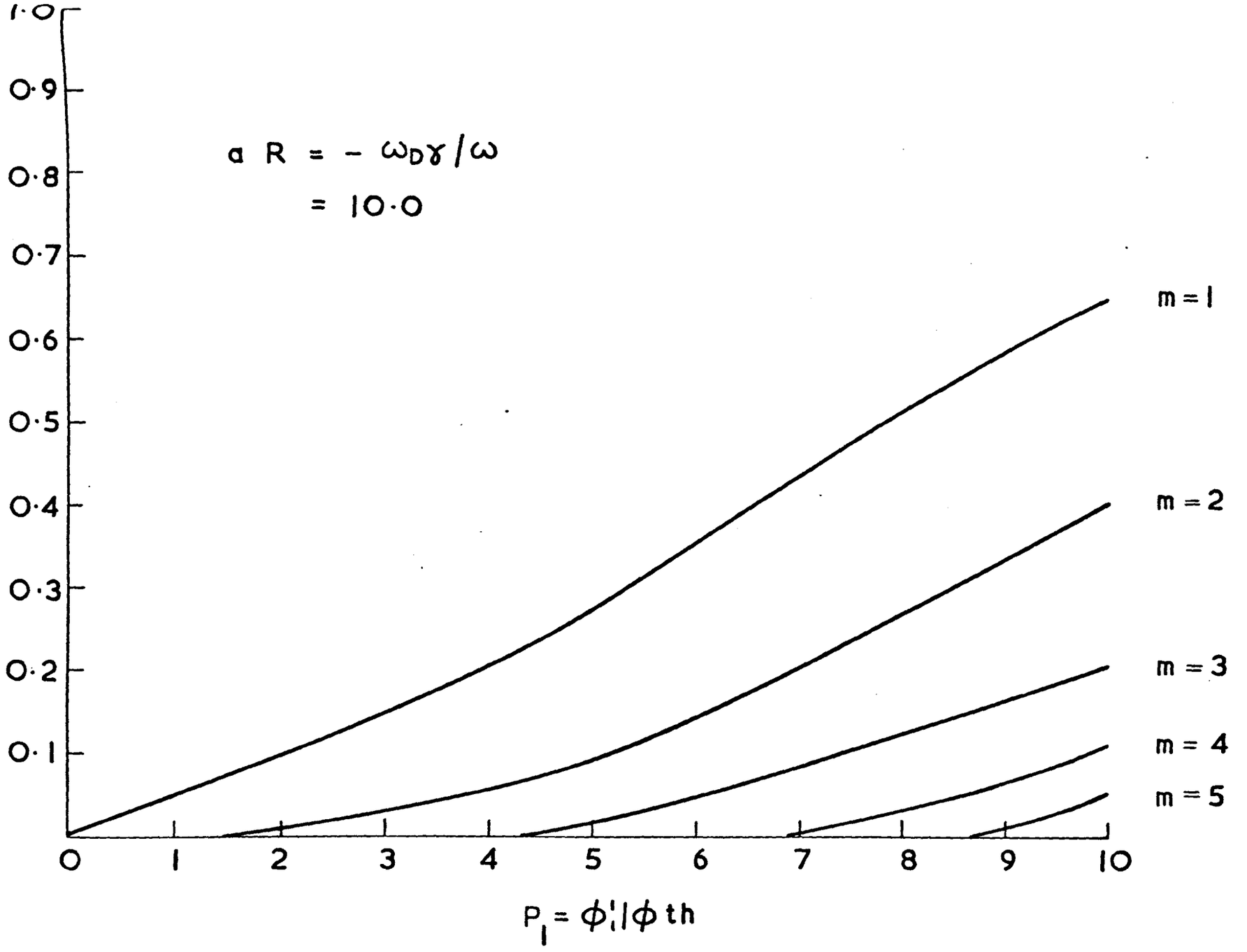
a R = − ωDγ/ω
= 10·0
1·0
0·9
0·8
0·7
0·6
0·5
0·4
0·3
0·2
0·1
m = 1
m = 2
m = 3
m = 4
m = 5
0
1
2
3
4
5
6
7
8
9
10
P1 = φ'1/φ th

FIG. 11

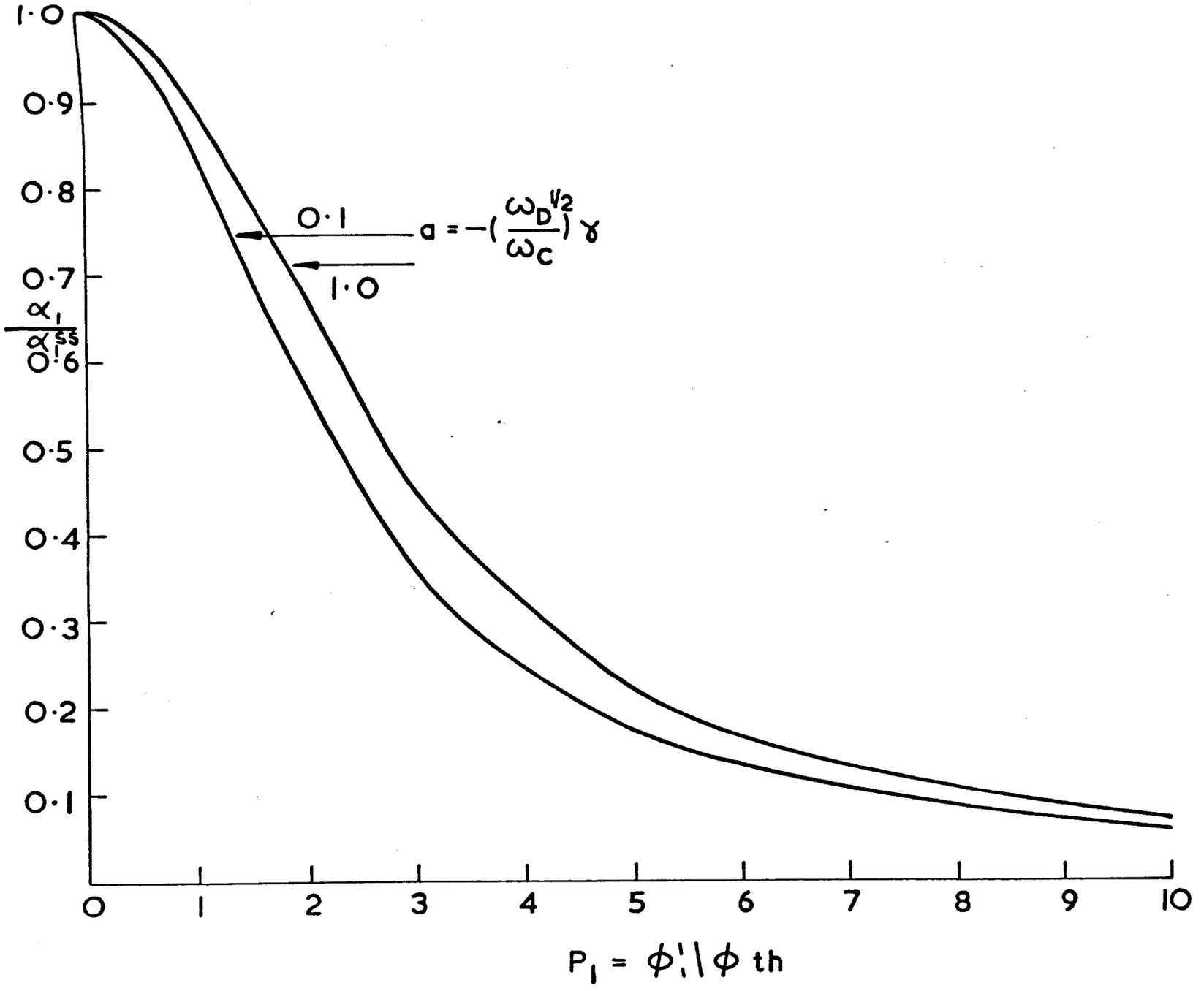
1·0
0·9
0·8
0·7
0·6
0·5
0·4
0·3
0·2
0·1
$\frac{\alpha_1}{\alpha_1^{ss}}$
0·1
1·0
$a = -\left(\frac{\omega_D}{\omega_c}\right)^{1/2} \gamma$
0
1
2
3
4
5
6
7
8
9
10
$P_1 = \phi_1' / \phi$ th

FIG. 12

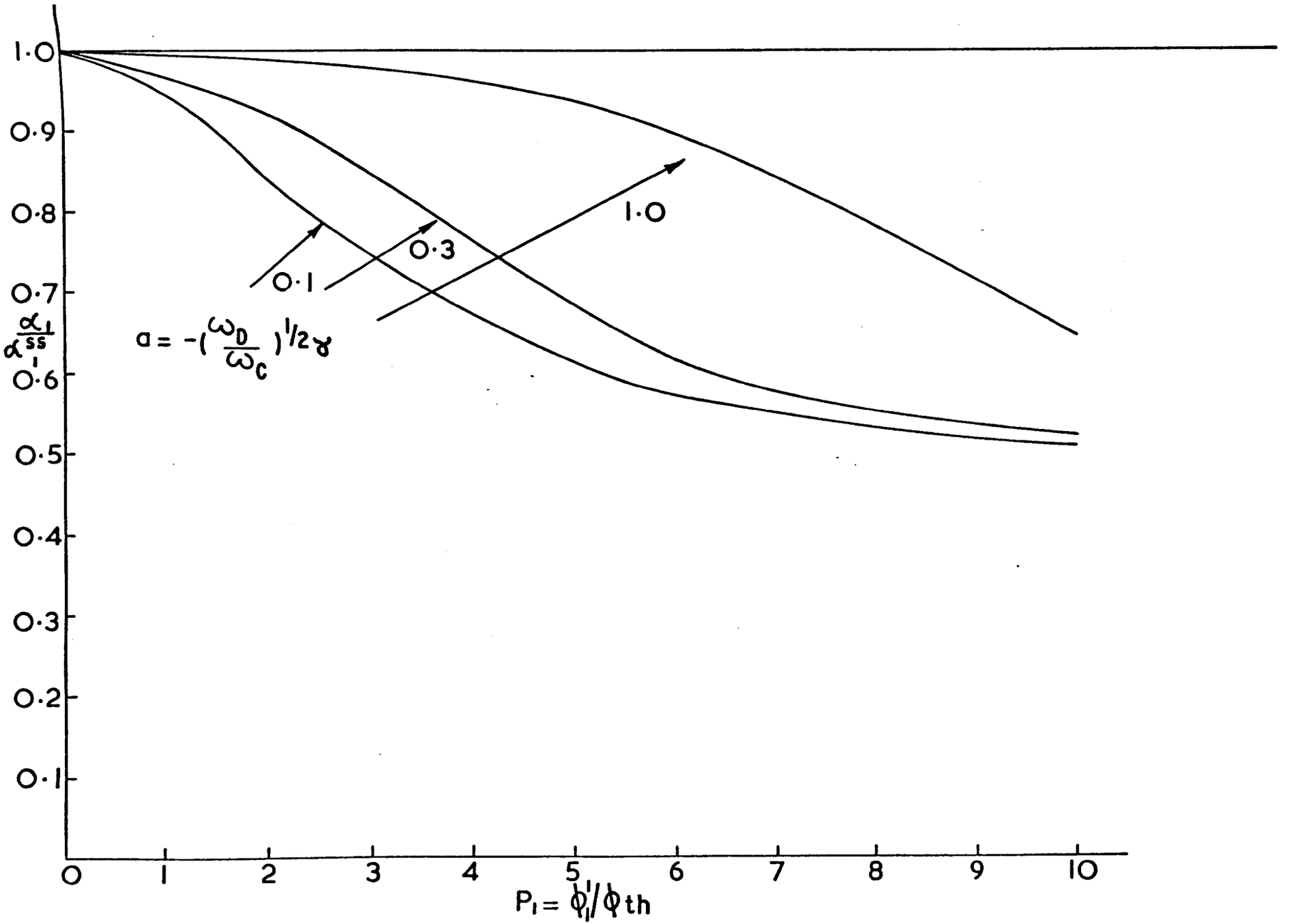
1·0
0·9
0·8
0·7
0·6
0·5
0·4
0·3
0·2
0·1
$\frac{\alpha_1}{\alpha_1^{ss}}$
$a = -(\frac{\omega_D}{\omega_c})^{1/2}\gamma$
0·1
0·3
1·0
0
1
2
3
4
5
6
7
8
9
10
$P_1 = \phi_1'/\phi th$

FIG. 13.

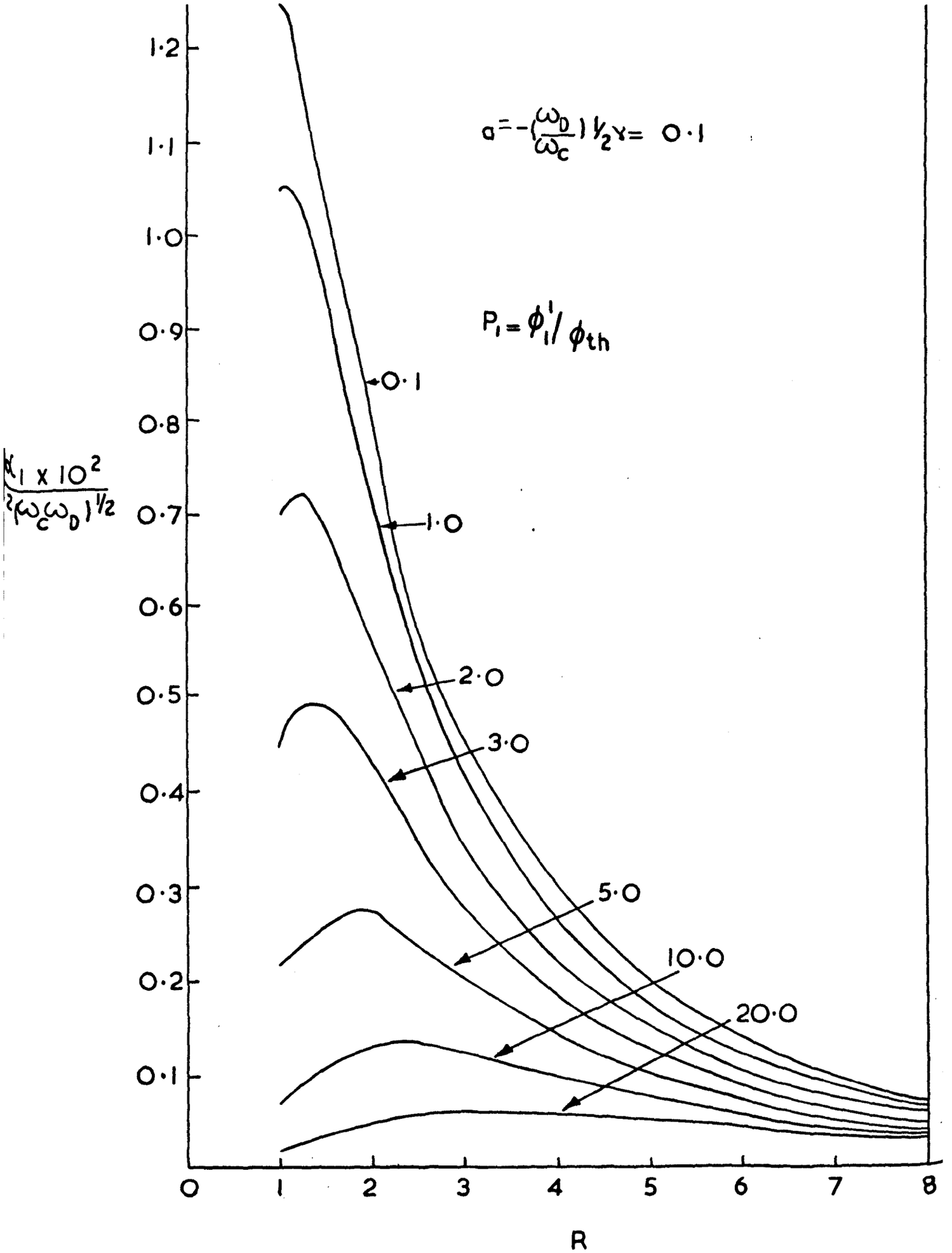
$a = -(\frac{\omega_D}{\omega_c})^{1/2}\gamma = 0.1$
$P_1 = \phi_1' / \phi_{th}$
0·1
1·0
2·0
3·0
5·0
10·0
20·0
$\frac{\alpha_1 \times 10^2}{(\omega_c\omega_D)^{1/2}}$
1·2
1·1
1·0
0·9
0·8
0·7
0·6
0·5
0·4
0·3
0·2
0·1
0
1
2
3
4
5
6
7
8
R

FIG. 14.

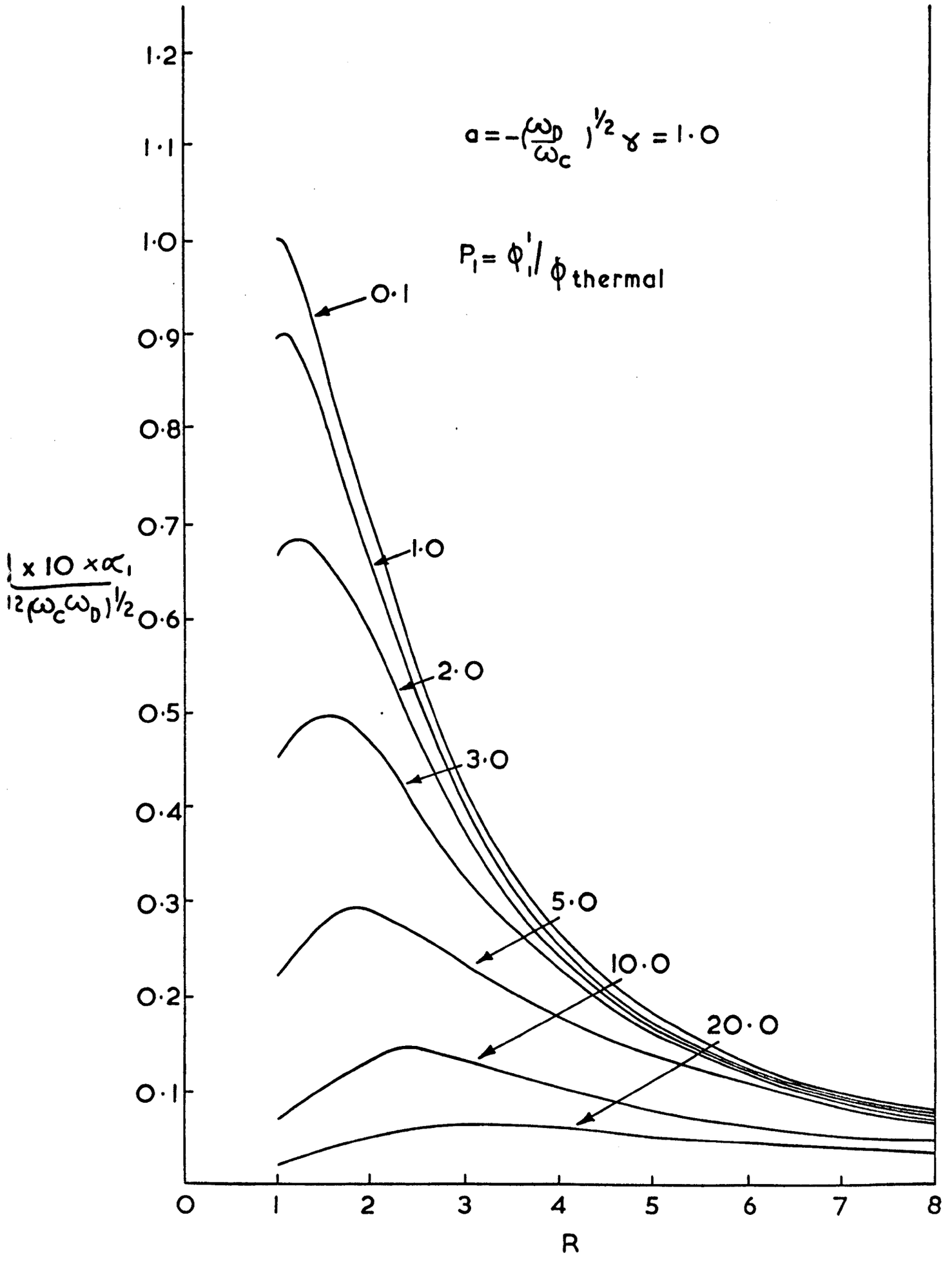
$a = -\left(\frac{\omega_D}{\omega_c}\right)^{1/2}$ $\gamma = 1.0$
$P_1 = \phi_1' / \phi_{thermal}$
0·1
1·0
2·0
3·0
5·0
10·0
20·0
$\frac{I \times 10 \times \alpha_1}{12(\omega_c \omega_D)^{1/2}}$
1·2
1·1
1·0
0·9
0·8
0·7
0·6
0·5
0·4
0·3
0·2
0·1
0
1
2
3
4
5
6
7
8
R

FIG. 15.

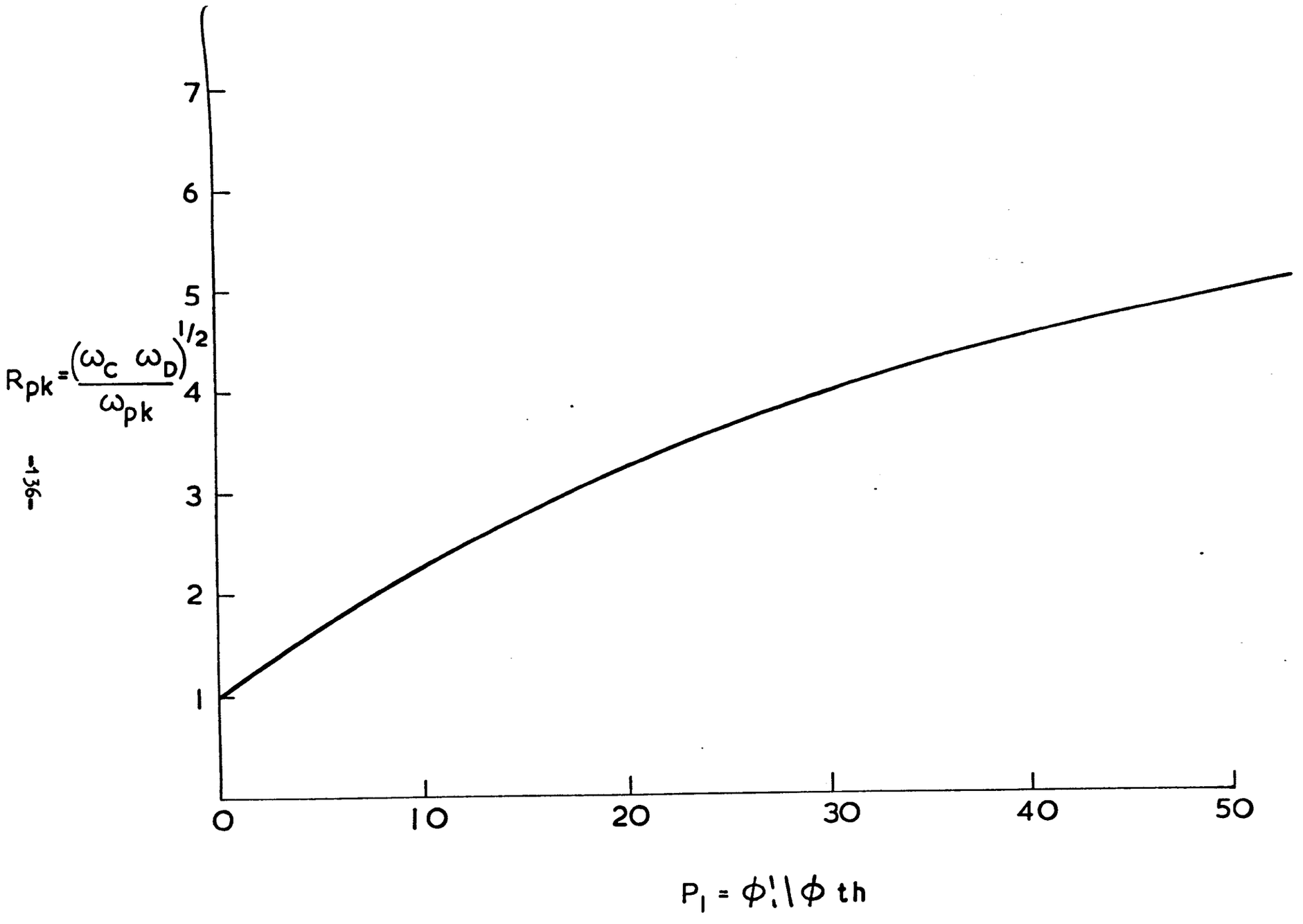
$R_{pk} = \frac{(\omega_c \omega_D)^{1/2}}{\omega_{pk}}$
7
6
5
4
3
2
1
0
10
20
30
40
50
$P_1 = \phi'_1 / \phi$ th

FIG. 16

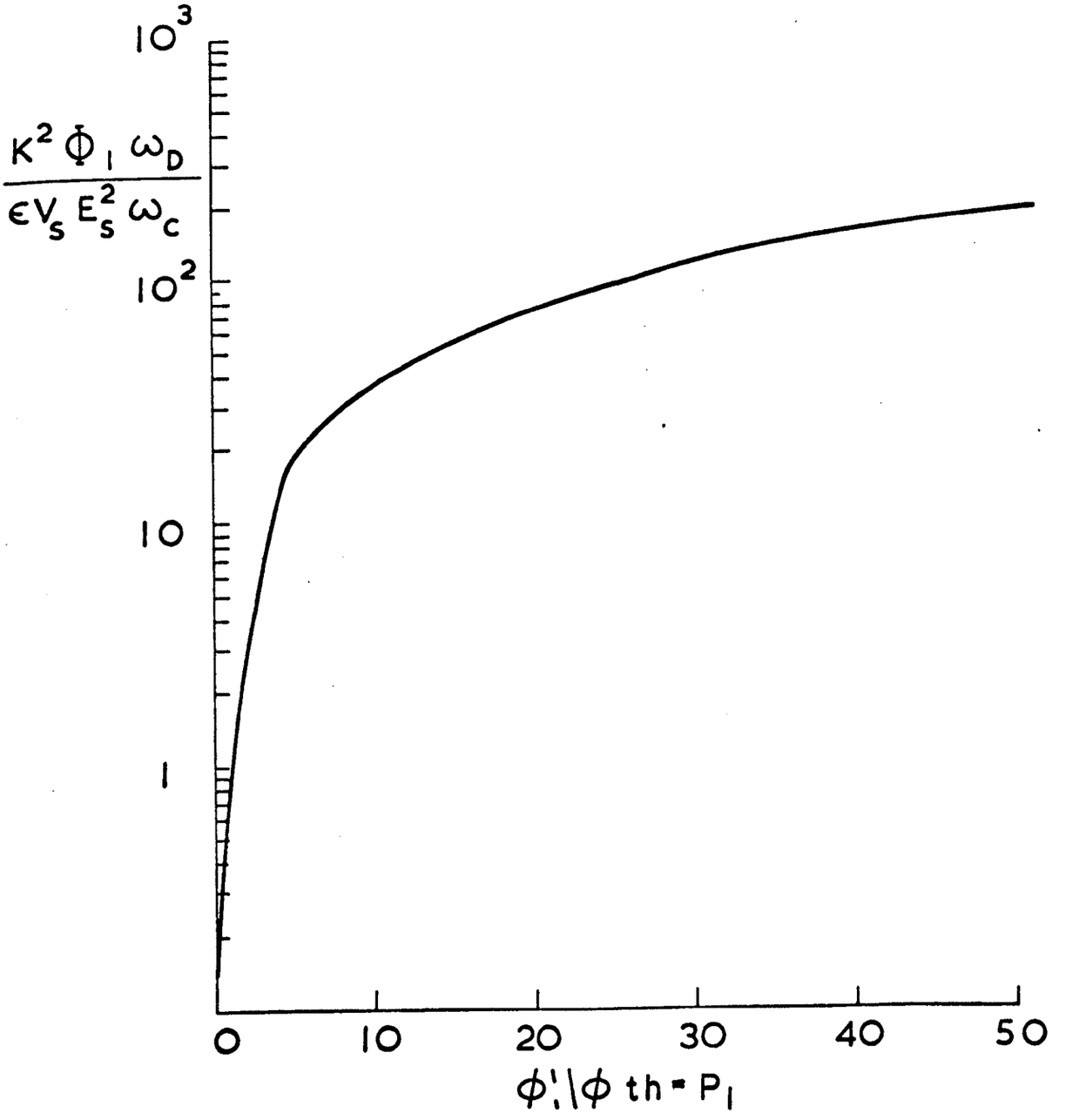
10^3
$\frac{K^2 \Phi_1 \omega_D}{\epsilon V_s E_s^2 \omega_c}$
10^2
10
1
0
10
20
30
40
50
$\phi_1' \backslash \phi$ th = P_1

FIG. 17

References Chapter 5

1. Tien, P.K. (1968), Phys. Rev. 171, 970

2. Piaggio, H.T.H., (1958), Differential Equations (Bell, London).

3. Beale, J.R., (1964), Phys. Rev. 135, 1761.

4. Gurevich, V.L. (1963), Sov. Phys. Solid State, 5, 888.

Chapter 6

DISCUSSION AND CONCLUSION

6.1 Discussion

We have seen in the previous Chapters that the non-linear theory of acoustoelectric gain which we have developed, contains the major features of gain in the large signal regime which have been observed experimentally. These are, (i) the reduction of the acoustic gain with increasing acoustic flux, (ii) the shift in the frequency of peak gain towards lower frequencies with increasing acoustic flux, and (iii) the saturation in the total current through the material as the acoustic flux increases. The physical explanation of these three effects would seem to be as follows.

We have seen in Chapter 5 that as the amplitude of the acoustic flux or the depth of the accompanying electric potential well is increased the tendency is for the electrons to bunch themselves more and more closely to the minimum of the mechanical potential energy well. (or maximum of the electric potential well). Because of this, the number of electrons in regions of positive a.c. electric field tends to become equal to the number of electrons in regions of negative a.c. electric field. It is the imbalance between the numbers of electrons in the positive and negative a.c. electric field regions which produces acoustoelectric gain (or loss). When the numbers become nearly equal therefore, as is the tendency in a large amplitude acoustic wave, the gain reduces in magnitude.

Current saturation is of similar origin. We have seen that in a large amplitude acoustic wave the electrons become bunched in regions of minimum potential energy. This means that they become 'trapped' at the velocity of sound so that the current carried by them will exhibit saturation at about the synchronous current I_s.

The shift in the frequency of peak gain towards lower frequencies with increasing acoustic wave amplitude is slightly more complex. In the small signal regime, the fact that the frequency of peak gain is $\omega_{pk} = (\omega_c \omega_D)^{\frac{1}{2}}$ may be argued as follows. In order for the acoustic

gain to be large, it is necessary that the accompanying electron density modulation is large and that most electrons travel in regions of a.c. field which decelerate them. The size of the electron density modulation that will accompany a given amplitude of acoustic strain is determined by a balance between the rate at which electron density modulations are produced by the a.c. electric fields accompanying the acoustic wave, and the rate at which electron density modulations decay due to debunching mechanisms. These debunching mechanisms are dielectric relaxation and diffusion. Dielectric relaxation is characterised by the frequency ω_c. If the acoustic wave frequency ω is greater than ω_c then significant debunching due to dielectric relaxation will not occur in a period of the acoustic wave. In a period of the acoustic wave electrons will diffuse a distance $\sim \sqrt{D_n/\omega}$. If this is less than a wavelength $\lambda = 2\pi v_s/\omega$ then significant debunching will not occur. This yields the criterion $\omega < \omega_D$. Hence for no significant debunching, the frequency ω must lie in the range $\omega_c \lesssim \omega \lesssim \omega_D$. For negative γ when we have acoustic gain, the majority of the electrons lie in regions of decelerating (negative) field. Increasing the diffusion current (by current continuity), tends to move the electron distribution peak towards the region of crossover between positive and negative fields. For optimum positioning of the electron distribution we therefore require that diffusion effects are small i.e. $\omega < \omega_D$. Combining these requirements then, it is reasonable that the peak acoustic gain should occur when $\omega = (\omega_c\ \omega_D)^{\frac{1}{2}}$. In the nonlinear large signal regime when the electrons are tightly bunched we may argue in a similar fashion. However, in this case the electrons must not diffuse more than the width of the bunch in a period of the wave i.e. $\sqrt{D_n/\omega} < \frac{\lambda}{w}$ where w is a parameter which specifies the bunch width as a fraction of a wavelength. This yields $\omega < \omega_D/w^2$. We still require $\omega > \omega_c$. In addition, in order that the electrons should lie in the correct part of the electric field wave, we require that effects producing phase shifting of n' relative to E' should be small. Examination of

equation (3.22) indicates that the term involving $\frac{\omega}{\omega_D} \frac{\partial}{\partial\theta} \log \frac{n}{n_o}$ has a phase shifting effect. We should therefore require that this term be small i.e. $\omega < \frac{\omega_D}{x}$ where x denotes $\frac{\partial}{\partial\theta} \log \frac{n}{n_o}$ and represents a parameter which determines the phase shifting of the electrons due to diffusion into regions of acoustic loss. Putting the various requirements together one has $\omega_o \lesssim \omega \lesssim \omega_D/y$ where y is either w^2 or x depending on which effect is the most important. One might then argue in analogy with the small signal case that the frequency of peak gain will be given by $\omega_{pk} \approx (\omega_o \omega_D/y)^{\frac{1}{2}}$.

An examination of the results obtained in Chapter 4 for ω_{pk} show that this interpretation seems to be borne out. For the exponential and Gaussian distributions it is clear from (4.39) and (4.47) that a parameter relating to the bunch width appears in the denominator of the formula for ω_{pk}. For the cosinusoid however since the bunch width will be just the wavelength λ, the parameter appearing on the right hand side of (4.21) must relate to a phase shifting effect.

6.2 Conclusion

We have developed a theory of acoustoelectric gain in the non-linear regime. In its present form the theory has several limitations. First, the theory only takes account of acoustic gain in one direction. In practice, the amplification of off-axis waves mentioned in Chapter 2 is probably considerable in many experimental situations. Second, the theory is a local one. While this is not a fundamental limitation, the difficulties involved in studying the propagation of an acoustic wave through an extended region are formidable, especially for the theory based on a knowledge of the space charge density. Thirdly, the theory is strictly only applicable to the amplification of acoustic waves in an

infinite medium. Because of this, the theory may not be directly applied to the acoustoelectric oscillator. It is not clear how the theory should be generalised in order to take into account situations where backward going as well forward going waves are present.

However, even with the limitations outlined above, the theory contains the essential features of acoustoelectric gain in the non-linear regime. The reduction of the acoustic gain, the shift in the frequency of peak gain towards lower frequencies, and current saturation all emerge from the theory which we have developed. The quantitative comparisons of the results with available experimental data indicate agreement to within an order of magnitude for the acoustic flux which produces a given frequency shift. In view of the fact that the theory does not describe in detail any specific experimental situation this degree of agreement is encouraging.

Finally, therefore, we conclude that the non-linear theory of acoustic gain which has been developed provides a useful guide to the qualitative behaviour of acoustic gain in the large signal regime. It is hoped that ultimately the theory will provide a starting point for more detailed theories of specific experimental situations.

Notation

Most of the notation used is summarised below

k	$= k_r + ik_i$ acoustic wave vector
ω	acoustic frequency
ℓ	electron mean free path
τ	electron relaxation time
v_s	sound velocity
v_{th}	thermal velocity
T	stress
ρ	density
u	mechanical displacement
κ	thermal conductivity
λ	acoustic wavelength
c	elastic constant
S	strain
e	piezoelectric constant
E	electric field
B	magnetic induction
H	magnetic field
j	particle current density
D	electric displacement
q	magnitude of electron charge
n	electron density
n_o	equilibrium electron density
μ^M	magnetic permeability
ϵ	dielectric constant
μ	mobility
D_n	diffusion constant

σ conductivity

ϕ electrostatic potential

$\omega_c = \sigma/\epsilon$ inverse dielectric relaxation time

$K^2 = \frac{e^2}{\epsilon c}$ electromechanical coupling constant

$E_s = v_s/\mu$ synchronous field

E_o d.c. electric field

$\gamma = 1 - E_o/E_s$

$\omega_D = v_s^2/D_n$

Ψ dissipative function

η viscosity tensor

α_{lat} lattice loss

Φ acoustic flux

W acoustic energy density

$\theta = kx - \omega t$ phase

α acoustic gain

I total current density

$I_s = qn_o v_s$ synchronous current density

F trapping factor

N integrated fractional excess electron density

I_{ae} acoustoelectric current density

k_B Boltzmann's constant

T absolute temperature

$\phi_{th} = k_B T/q$ thermal potential

$P = \phi/\phi_{th}$ potential ratio

$R = (\omega_c \omega_D)^{\frac{1}{2}}/\omega$ frequency ratio

Where the notation conflicts with that listed above the definition is given in the context.